MONTHLY NOTICES

OF THE

ROYAL ASTRONOMICAL SOCIETY

Vol. 108 No. 6

ADDITIONAL MEETING OF 1948 OCTOBER 29

in the rooms of the Royal Society of Edinburgh

Professor W. M. H. Greaves, President, in the Chair

The President announced that this meeting was the first in the history of the Society to be held outside London. He expressed the thanks of the Society to the Royal Society of Edinburgh for their hospitality on this occasion. He welcomed also the guests from the University of Edinburgh and those representing other Societies. The meeting had been arranged in cooperation with the Astronomical Society of Edinburgh and the President invited Mr R. W. Wrigley, President of the Astronomical Society of Edinburgh, to address the meeting.

A number of Fellows signed the Admission Book. Several papers communicated to the Society were read by their authors, and Dr E. H. Linfoot spoke on the Schmidt–Cassegrain telescope under construction at the University Observatory, St. Andrews.

On the afternoon of 1948 October 28, Thursday, the Rt. Hon. Lord Provost Andrew H. A. Murray, accompanied by the Lady Provost, Miss Rodney Murray, received Fellows of the Society, and members of the Astronomical Society of Edinburgh, in the Edinburgh City Chambers.

On the evening of 1948 October 28, Fellows were invited to attend the Lorimer Lecture of the Astronomical Society of Edinburgh, and were subsequently entertained by the President and Council of that Society.

On the morning of 1948 October 29, Fellows visited the Royal Observatory on the invitation of the Astronomer Royal for Scotland (Professor W. M. H. Greaves).

On 1948 October 30, Fellows visited the University Observatory, St. Andrews, on the invitation of the Director (Dr E. Finlay–Freundlich) and were entertained to luncheon by the Court of the University of St. Andrews.

MEETING OF 1948 NOVEMBER 12

Professor W. M. H. Greaves, President, in the Chair

The election by the Council of the following Fellows was duly confirmed:—

A. Coward, Gainsborough Cottage, Church Street, Pinchbeck, Lincolnshire (proposed by F. Tyler);

Andrew McKellar, Ph.D., Dominion Astrophysical Observatory, British Columbia, Canada (proposed by C. S. Beals);

Thomas Hay O'Beirne, M.A., 16 Avenue Elmers, Surbiton, Surrey (proposed by D. H. Sadler);

Eric William Turner, 130 Orford Road, Walthamstow, London (proposed by H. P. Wilkins); and

Anne Barbara Underhill, Ph.D., The Observatory, Copenhagen (proposed by S. Chandrasekhar).

The election by the Council of the following Junior Members was duly confirmed:—

John Michael Anthony Danby, Christ Church, Oxford (proposed by G. Merton);

Edward Gerard Docherty, 66 Raglan Street, St. Helens, Lancashire (proposed by H. P. Wilkins);

Phillip John David Gething, 62 Carlton Crescent, Luton, Bedfordshire (proposed by H. H. Plaskett); and

Bryan Summers, 365 New King's Road, Fulham, London (proposed by H. S. W. Massey).

One hundred and one presents were announced as having been received since the last meeting, including:—

J. G. Porter, *The Night Sky* (presented by the author);

The Chemical Society, *A Record of the Centenary Celebrations*, 1947 (presented by the Chemical Society); and

Photograph in colour showing mosaic grating for the Schmidt camera at Mount Palomar (presented by Professor R. W. Wood).

MEETING OF 1948 DECEMBER 10

Professor W. M. H. Greaves, President, in the Chair

The election by the Council of the following Fellows was duly confirmed:—

Leason H. Adams, Ph.D., Geophysical Laboratory, Washington, D.C., U.S.A. (proposed by H. Jeffreys);

Francis Birch, Ph.D., Dunbar Laboratory, Harvard University, Cambridge, Mass., U.S.A. (proposed by H. Jeffreys);

Ronald Henry Brockman, Optical Works, Ltd., Ealing, London (proposed by C. C. L. Gregory);

John McGarva Bruckshaw, Ph.D., 24 Newton Wood Road, Ashstead, Surrey (proposed by S. Chapman);

Stanley Horace Carter, 29 Ennismore Mews, London, S.W. 7 (proposed by I. E. Roberts);

William Chipchase Dowell, 119 Watford Road, North Wembley, Middlesex (proposed by M. W. Ovenden);

Harry Alfred Wynsor Futcher, 44 Boswall Avenue, Edinburgh (proposed by W. D. Oliphant);

Thomas Gold, M.A., Trinity College, Cambridge (proposed by H. Jeffreys);

Henry William Headland, B.Sc., Elmhurst, Heath Road, Weston, Runcorn (proposed by A. T. Doodson);

Harold Edmund Howle, Norton House, 23 Nicholls Street, West Bromwich, Staffordshire (proposed by E. L. Hawke);

Nita Elise Knaggs, Ph.D., New Barn, Micheldever Station, Winchester, Hants (proposed by D. W. Millar);

John George Lloyd, 78 High Street, Frodsham, Cheshire (proposed by A. T. Doodson);

Alexander Charles Menzies, D.Sc., 98 St. Pancras Way, London, N.W. 1 (proposed by W. M. H. Greaves);

Guido Munch, Ph.D., Yerkes Observatory, Williams Bay, Wisconsin, U.S.A. (proposed by S. Chandrasekhar);

William Henderson Ramsey, Ph.D., Physical Laboratories, The University, Manchester (proposed by P. M. S. Blackett);

Cyril Francis Trigg, B.Sc., 14 Erw-Wen, Rhibina, Cardiff (proposed by A. Buxton);

Alexander George Undery, 28 Irish Town, Gibraltar (proposed by W. C. Aubrey-Rees);

Peter James Waters, 41 Littleover Avenue, Hall Green, Birmingham (proposed by T. J. Harding); and

Roy Vivian Whitlock, 21 Boundary Road, Chatham, Kent (proposed by J. G. Porter).

Eighty presents were announced as having been received since the last meeting, including :—

E. A. Milne, *Kinematic Relativity*, presented by the author.

ON THE THEORY OF THE ZONAL FOUCAULT TEST

E. H. Linfoot

(Received 1948 September 30)

Summary

The aim of the paper is to provide a theory of the zonal Foucault test which permits a discussion of its systematic errors and of its limiting accuracy. In Sections 2 and 3 it is shown that ray theory is inadequate for this purpose and that the analysis must be based on diffraction theory. In Sections 4 and 5 the diffraction theory of the test is developed and it is shown that, provided certain precautions are observed, the zonal readings for a true spherical mirror are not disturbed by the coherence-asymmetry which may be present in the illumination. In Section 6 it is shown that, in the zonal testing of astronomical paraboloids with $f/300$ zonal apertures and with a pinhole or slit of width not much exceeding 0·001 inch, the zonal readings are not sensibly disturbed by the diffraction phenomena and the Foucault shadows on the two members of a pair of zonal apertures show the same sequence of changes as the knife-edge is brought across. It follows that, used in this way, the test is free from appreciable systematic errors and its accuracy is in practice limited only by the observer's limited power of brightness-discrimination.

1. *Introduction.*—Because of its simplicity, the zonal Foucault test seems likely to remain one of the most widely used methods of testing the figures of medium-sized astronomical mirrors, although for large mirrors the "caustic" method of Platzeck and Gaviola is probably superior in accuracy. In an interesting account of their method, published nine years ago in the *Journal of the Optical Society of America*, Platzeck and Gaviola tried to estimate the limits of accuracy of the zonal Foucault test, of two other "longitudinal aberration methods" (in which the knife-edge is replaced by a thin wire and a slit respectively, while the mirror is unmasked), and of their own method of testing on the caustic. Their estimates were made by means of calculations based on the predictions of ray theory; in the last case they were supported by some experimental results.

In none of these tests can ray theory be said to provide an adequate basis for such a discussion, but in the zonal Foucault test its predictions show less resemblance to what is actually observed than in the others, and its inadequacy is therefore more evident. Not until a diffraction theory of each of these tests is available will a reliable theoretical estimation be possible of their limits of accuracy and of their systematic errors.

In the present paper a discussion based on diffraction theory is made of the properties of the zonal Foucault test, and some results are established which bear on these two questions. In Section 2 a brief account is given of the method of carrying out the test and the appearances seen in practice on the zonal apertures are described. In Section 3 the geometrical theory of the test as applied to a paraboloid is set out, the predictions of geometrical optics are shown to differ widely from the appearances seen in practice, and the inference is drawn that, in order to be of practical value, the analysis must be based on diffraction theory.

In Section 4 the diffraction theory of the test is discussed and a generalized form of the reduction theorem is established, according to which the appearances seen along any line running perpendicular to the knife-edge in the plane of the zonal screen depend only on the figure of the exposed parts of the mirror immediately behind that line.

In Section 5 the question is considered whether diffraction phenomena can cause disturbances of the zonal readings in the practically important case where a pair of zonal apertures is uniformly lit but the coherence of the lighting is unsymmetrical. It is shown that, although the appearances seen will in general be altered by diffraction effects which depend on the coherence, the zonal readings are not disturbed in the case of a true spherical mirror tested with a pinhole or slit of width small compared with the lateral resolution of a single zonal aperture.

In Section 6 it is shown that when a paraboloid is zonally tested at its centre of curvature, the two members of any pair of zonal apertures will appear to darken similarly when the knife-edge is moved across at the correct zonal focus, and that when the test is done with a fine pinhole or slit its systematic errors are inappreciable in a practical case. It follows that in practice the accuracy of the test is limited only by the observer's power of visual discrimination in comparing the total brightness of the two members of each pair of zonal apertures.

2. *The zonal knife-edge test.*—In setting up the zonal test, the mirror surface is divided into narrow concentric zones, and two cardboard screens, of the same diameter as the mirror and provided with bases which can rest on the mirror-stand, are pierced with zonal apertures ranged symmetrically along the horizontal diameter of the mirror surface, as shown in Fig. 1. Placed close in front of the mirror, one screen enables the odd-numbered zones to be tested with a vertical

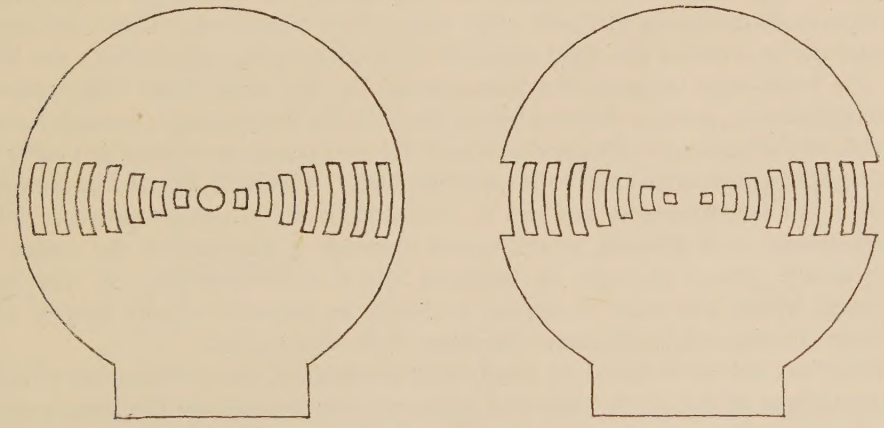

FIG. 1.—*Pair of zonal screens.*

knife-edge and the other the even-numbered zones. If the top and bottom edges of each zonal aperture are cut horizontally instead of radially, the "bright edge" effect there is reduced and the apertures can be compared more critically under the test. Only one zone is tested at a time; small cardboard slips, passing behind horizontal tapes sewn to the screens above and below the line of apertures, provide a convenient means of closing all except the pair of apertures belonging to this zone. Fig. 2 represents the two "zonal sectors" of the mirror surface

exposed by a pair of apertures. R′S′ and RS, lying in the mirror surface, are the "zonal segments" cut off by these sectors on the principal diameter LM.

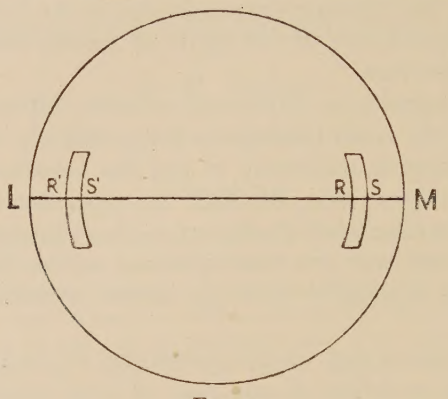

FIG. 2.

We suppose that the light source, an illuminated pinhole or a narrow vertical slit, moves with the knife-edge and can be regarded as optically coincident with it. In practice, the light source and knife-edge are usually given a small relative lateral displacement to bring the image into an accessible position clear of the pinhole mounting. The only error of appreciable amount which this displacement introduces into the pencils under test is an astigmatism which has one of its principal directions parallel to the knife-edge, and this does not interfere with the test.*

To carry out the test, the eye is placed close behind the knife-edge and focused on the screen, the knife-edge is moved to and fro across the axis of the mirror, near to its mean centre of curvature, and the manner in which the two exposed zonal apertures darken as the knife-edge advances is compared. If the left-hand aperture darkens before the right when the knife-edge is brought in from the left, then the knife-edge is inside the focal setting for the zone under observation; if the right-hand aperture darkens before the left, the knife-edge is outside focus. By trial, a focal setting is obtained at which the two apertures darken as nearly as possible at the same time and in the same manner. That is to say, the darkening, which is not instantaneous but can be followed as a continuous process while the knife-edge and pinhole are advanced through a distance of the order of 0·003 inch †, passes through its different stages simultaneously on the two apertures, which are made to appear as nearly as possible equally bright, and similarly illuminated, in all lateral positions of the knife-edge.

When the mirror is a true or nearly true paraboloid, the distribution of light is not uniform in the partly darkened apertures, nor (except on the inner zones) does it appear symmetrical as between left and right-hand sides of a single aperture.

* See (3). From equation (2.4) of that paper it follows that the only effect of the astigmatism on the test is to cause a small change in the adopted focal settings of the knife-edge. The amount of this change (which is of the order of $\frac{1}{100}$ inch in practice) is the same for all the pairs of zonal apertures; consequently its only practical effect is to change, by an amount of the order of $\frac{1}{100}$ inch, the adopted zero-point of the zonal readings.

† With zonal apertures of width $\frac{1}{300}$ of the focal distance, illuminated from a pinhole 0·001 inch in diameter, the central bright region of the diffraction image formed by each zonal sector is 0·012 inch wide. Its "visible" width is about half this, and another factor $\frac{1}{2}$ enters because light source and knife-edge move together.

Each aperture appears darker on the side towards the knife-edge, as shown in Figs. 6 and 7. If the darkening process is carefully watched, undulatory fluctuations of intensity can be seen on each aperture during its earliest stages. The most noticeable of these fluctuations is the appearance and subsequent disappearance of a broad central dark band, easily distinguished, by its softer appearance and by its different behaviour as the knife-edge is moved sideways, from the diffraction fringes seen when the eye is malfocused on the zonal aperture. At a suitable focal setting of the knife-edge the fluctuations take place simultaneously on the two apertures, and the intensities at corresponding points remain equal as the apertures darken.

A focal setting is determined in this way for each pair of zonal apertures and the corresponding micrometer reading noted. The setting for the central zone is taken as that for which its circular aperture darkens as symmetrically as possible. The differences between the micrometer readings are regarded as measuring the variation of zonal focus between the different zones of the mirror surface.

Horizontal halo bands appear to the right and left of each aperture as the knife-edge is brought in; they are brightest when the knife-edge bisects the diffraction image. If the two zonal apertures are well separated, their halos do not visibly overlap; in testing the inmost zones, however, a continuous band of light can be seen extending across from one aperture to the other, and it is not clear without investigation whether this diffraction phenomenon will or will not affect the determination of the focal setting for the zone when the mirror is lit by means of a fine pinhole or slit, and not by a point source.

3. *Zonal testing of paraboloids: geometrical theory.*—Fig. 3 shows an arc of the parabola $Y^2=4aX$ of vertex A, paraxial centre of curvature $C_0=(2a, 0)$

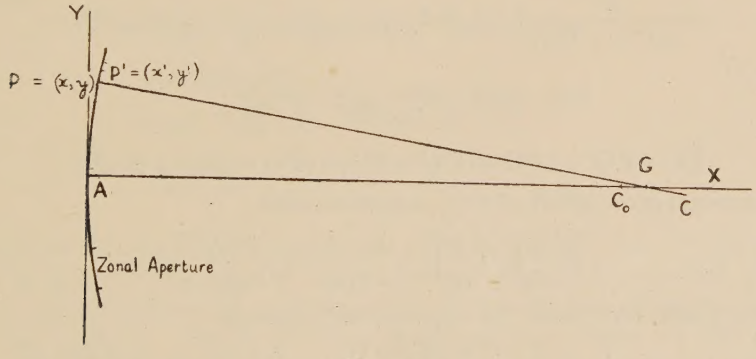

FIG. 3.

and paraxial radius of curvature $\rho_0=2a$. An arbitrary point on the arc may be denoted by $P=(x, y)=(at^2, 2at)$, where t is a parameter.

The normal at P then has the equation

$$Xt+Y=2at+at^3; \tag{1}$$

it cuts the axis AC_0 in the point $G=(2a+at^2, 0)$. Thus

$$PG=2a(1+t^2)^{\frac{1}{2}}. \tag{2}$$

The centre of curvature C corresponding to P is the point $(2a+3at^2, -2at^3)$ and the radius of curvature

$$PC=2a(1+t^2)^{\frac{3}{2}}. \tag{3}$$

Evidently

$$C_0G = AG - AC_0 = at^2 = y^2/2\rho_0; \tag{4}$$

this quantity therefore measures the longitudinal aberration of the zone of radius y on a paraboloid of paraxial radius of curvature ρ_0, tested with knife-edge and light source moving together.

Now let $P' = (at'^2, 2at')$ be a point on the arc near P. Then

$$\begin{aligned} P'G^2 - PG^2 &= [2a + a(t^2 - t'^2)]^2 + (2at')^2 - (2a)^2 - (2at)^2 \\ &= a^2(t'^2 - t^2); \end{aligned}$$

$$P'G - PG = \frac{a^2}{P'G + PG}(t' - t)^2[2t + (t' - t)]^2. \tag{5}$$

To discuss the geometrical properties of a zone of mean radius y and width d (both measured perpendicular to the axis of the mirror) we take

$$P = (x, y) = (at^2, 2at)$$

to lie midway on the zone and let $P' = (x', y') = (at'^2, 2at')$ run from side to side of the zone. Thus $y' = 2at'$ runs from $y - \frac{1}{2}d$ to $y + \frac{1}{2}d$. Let

$$u = \frac{2}{d}(y' - y) = \frac{4a}{d}(t' - t); \tag{6}$$

then u runs from -1 to 1,

$$t' - t = \frac{ud}{4a}, \qquad t = \frac{y}{t_0}$$

and (5) can be written

$$\begin{aligned} P'G - PG &= \frac{\rho_0^2}{4(P'G + PG)}\left(\frac{ud}{2\rho_0}\right)^2\left(\frac{2y}{\rho_0} + \frac{ud}{2\rho_0}\right)^2 \\ &= \frac{d^2}{4(P'G + PG)}[(y/\rho_0)^2u^2 + \tfrac{1}{2}(y/\rho_0)(d/\rho_0)u^3 + \tfrac{1}{16}(d/\rho_0 u^4)^2]. \end{aligned} \tag{7}$$

Now by (2)

$$PG = 2a(1 + t^2)^{\frac{1}{2}} = \rho_0(1 + y^2/\rho_0^2)^{\frac{1}{2}};$$

hence

$$PG + PG' = 2PG + (P'G - PG) \simeq 2PG = 2\rho_0(1 + y^2/\rho_0^2)^{\frac{1}{2}},$$

with a fractional error which, by (7), never exceeds

$$\tfrac{1}{8}\left(\frac{d}{\rho_0}\right)^2\left[\left(\frac{y}{\rho_0}\right)^2 + \frac{1}{2}\frac{y}{\rho_0}\frac{d}{\rho_0} + \frac{1}{16}\left(\frac{d}{\rho_0}\right)^2\right].$$

Equation (7) therefore yields the approximate formula

$$P'G - PG = \tfrac{1}{8}\rho_0\left(1 + \frac{y^2}{\rho_0^2}\right)^{-\frac{1}{2}}\left(\frac{d}{\rho_0}\right)^2\left[\left(\frac{y}{\rho_0}\right)^2u^2 + \frac{1}{2}\frac{y}{\rho_0}\frac{d}{\rho_0}u^3 + \frac{1}{16}\left(\frac{d}{\rho_0}\right)^2u^4\right], \tag{8}$$

with an error which nowhere exceeds

$$\rho_0\left\{\tfrac{1}{8}\left(\frac{d}{\rho_0}\right)^2\left[\left(\frac{y}{\rho_0}\right)^2 + \frac{1}{2}\frac{y}{\rho_0}\frac{d}{\rho_0} + \frac{1}{16}\left(\frac{d}{\rho_0}\right)^2\right]\right\}^2.$$

For a mirror of aperture not exceeding 200 inches and focal ratio not shorter than $f/3$, tested in zones of width $\frac{1}{300}\rho_0$ or less, this quantity is always less than $1{\cdot}2 \times 10^{-11}$ inch $= 1{\cdot}2 \times 10^{-6}$ reflection fringe, on taking $\lambda = 2 \times 10^{-5}$ inch as the effective wave-length of the light used. Thus the error in equation (8) is negligible in these cases.

For most purposes it is sufficient to use the cruder approximation

$$P'G+PG\simeq 2\rho_0 \tag{9}$$

and to neglect the term in $\left(\frac{d}{\rho_0}\right)^2 u^4$. Equation (7) then yields the approximate formula

$$P'G-PG=\tfrac{1}{8}\rho_0\left(\frac{\rho_0}{d}\right)^2\left[\left(\frac{y}{\rho_0}\right)^2 u^2+\frac{1}{2}\frac{y}{\rho_0}\frac{d}{\rho_0}u^3\right]. \tag{10}$$

In the case of an $f/4$ paraboloid of 25 inches aperture, tested in zones of width $d=\frac{1}{300}\rho_0=0{\cdot}67$ inch, (10) gives at the edge of the mirror $\left(\text{where } y=\frac{1}{16}\rho_0\right)$

$$P'G-PG=\tfrac{1}{8}.8\times 25.\left(\frac{1}{300}\right)^2\left[\frac{1}{256}u^2+\frac{1}{2}\cdot\frac{1}{16}\cdot\frac{1}{300}u^3\right]\text{inch}$$

$$=\frac{1}{9{\cdot}22}u^2+\frac{1}{346}u^3 \text{ reflection fringe.} \tag{11}$$

The error in the coefficients of u^2 and u^3 is here less than $\frac{1}{5}$ per cent, while the discarded term

$$\tfrac{1}{8}.8\times 25.\left(\frac{1}{300}\right)^2.\frac{1}{16}.\left(\frac{1}{300}\right)^2 u^4 \text{ inch}=\frac{u^4}{51840}\text{reflection fringe}$$

is evidently negligible.

To predict, on the basis of ray theory, the shadows seen on a true paraboloid under the zonal knife-edge test, we consider a pair of apertures which expose two segments of the zone $y-\frac{1}{2}d\leq y'\leq y+\frac{1}{2}d$ on the mirror surface. The normal at P′, whose equation is $Xt'+Y=2at'+at'^3$, cuts the line $X=2a+at^2$ at the point where

$$\begin{aligned}Y&=2at'+at'^3-2at'-at^2t'\\&=at'(t'^2-t^2)\\&=a(t'-t)[t+(t'-t)][2t+(t'-t)]\\&=\tfrac{1}{2}d\left[2\left(\frac{y}{\rho_0}\right)^2 u+\frac{3}{2}\frac{y}{\rho_0}\frac{d}{\rho_0}u^2+\frac{1}{4}\left(\frac{d}{\rho_0}\right)^2 u^3\right].\end{aligned} \tag{12}$$

The solution of this equation in u gives the point of the right-hand zonal segment RS (see Fig. 2) which the edge of the geometrical shadow has reached when the knife-edge and pinhole are at a distance $\frac{1}{2}Y$ off axis in the plane through the point $G=(2a+at^2, 0)$. On the left-hand zonal segment, where we take u to run from -1 at R′ to $+1$ at S′, the edge of the geometrical shadow is at the point where

$$Y=\tfrac{1}{2}d\left[2\left(\frac{y}{\rho_0}\right)^2 u-\frac{3}{2}\frac{y}{\rho_0}\frac{d}{\rho_0}u^2+\frac{1}{4}\left(\frac{d}{\rho_0}\right)^2 u^3\right], \tag{13}$$

as may be seen by changing y into $-y$ in (12). (12) and (13) show that when the knife-edge is brought in, from the left, at the focal setting which makes the geometrical shadows reach the centres of the two zonal segments simultaneously *, the march of the shadows across the segments from left to right is not quite the

* The points $u=0$ on the zonal segments of the mirror surface may be supposed to project on to the centres of the zonal apertures when viewed from G, since the discrepancy is far too small to be detected by the eye. Thus G is also a focal setting at which the geometrical shadows appear to reach the centres of the screen apertures simultaneously as the knife-edge is brought across.

same in the two cases. The shadow will make its first appearance in the left-hand aperture when

$$Y=-\tfrac{1}{2}d\left[2\left(\frac{y}{\rho_0}\right)^2+\frac{3}{2}\frac{y}{\rho_0}\frac{d}{\rho_0}+\frac{1}{4}\left(\frac{d}{\rho_0}\right)^2\right], \tag{14}$$

while the shadow in the right-hand aperture will not appear until Y has been increased by a further amount $\frac{3}{2}d\frac{y}{\rho_0}\frac{d}{\rho_0}$. Similarly, the geometrical shadow first covers the whole of the left-hand zonal segment when

$$Y=\tfrac{1}{2}d\left[2\left(\frac{y}{\rho_0}\right)^2-\frac{3}{2}\frac{y}{\rho_0}\frac{d}{\rho_0}+\frac{1}{4}\left(\frac{d}{\rho_0}\right)^2\right], \tag{15}$$

while the right-hand segment is not completely covered until Y is increased by a further amount $\frac{3}{2}d\frac{y}{\rho_0}\frac{d}{\rho_0}$.

If these predictions of ray theory were in fairly good agreement with the appearances observed when the test is actually carried out, we might expect to be able to derive from them a theoretical estimate of the limit of sensitiveness of the zonal knife-edge test as applied to paraboloid mirrors, and of the order of magnitude of its systematic errors. However, an experimental trial shows at once that the appearances seen on the zones, and described in the previous section, are very different from those predicted by ray theory, and that only a discussion based on diffraction theory can be expected to provide valid estimates of the limit of sensitiveness of the test and of its systematic errors. In the next section we carry out such a discussion and use it to draw conclusions which can be compared with the results of experiment.

4. *Zonal testing of paraboloids: diffraction theory.*—We first consider the case of a single zonal aperture, illuminated by a point source and tested with the knife-edge centrally set at the "zonal focus" G (see Fig. 3).

If the edge of the screen aperture were in contact with the mirror surface, and if the viewing system were focused on this surface, the intensity $I(x', y')$ seen under the test at the point $P'=(x', y', z')$ on the mirror surface would be given, except in the immediate vicinity of the boundary of the aperture, by the equations *

$$2\pi D(x', y')=\pi E(x', y')+i\int_{-\infty}^{\infty}\frac{E(t, y')}{t-x'}dt, \tag{16}$$

$$I(x', y')=|2\pi D(x', y')|^2, \tag{17}$$

where

$$E(x', y')=e^{2\pi i\phi(x', y')} \tag{18}$$
$$=0,$$

according as P′ does or does not lie in the exposed area of the mirror surface, and $\phi(x', y')$ denotes the optical path difference PG − P′G (see Fig. 3), measured in reflection fringes. P is the point, midway on the zone † and lying on the horizontal diameter of the mirror surface, the normal at which passes through G.

* See (3), p. 81, where, however, it was assumed that $E(x', y')=0$ for $x'^2+y'^2>1$. The inequality can be replaced by $x'^2+y'^2>y_0^2$ without affecting the conclusions, provided that y_0/ρ_0 is small.

† As measured perpendicular to the axis of the mirror; we express this by calling P the "median point" of the zonal segment.

The integral on the right of (16) is to be interpreted as a Cauchy principal value when P′ is on the exposed part of the mirror surface; the range of integration is infinite only in appearance, since $E(t, y')$ vanishes outside a certain finite t-interval. At points close to the boundary of the aperture, (16) is no longer a valid approximation. At these points the intensities seen under the test depend critically on the aperture and optical aberrations of the viewing system, as well as on the shape of the mirror surface, and we therefore exclude them from the discussion. The proof of (16) was based on a double application of Huyghens' principle, in the surface of the mirror and in the plane of the knife-edge.

In the zonal test the flat screen is not quite in contact with the curved mirror surface and the viewing system is focused on the screen aperture. The application of Huyghens' principle in the surface of the mirror is therefore replaced by one in the plane of the screen aperture. The discussion is on the same lines as before and, in the result, (16) and (17) are now found to give the intensity seen under the test at the point of intersection Q′ of P′G with the plane of the screen. The space coordinates, x' and y', of P′, can now be regarded as two parameters which determine the position of Q′ and approximate closely in value to the Cartesian coordinates of Q′ in the plane of the screen. When Q′ runs over the screen aperture, P′ runs over a region of the mirror surface which we call the zonal area corresponding to the screen aperture.

To predict the appearances seen on the zone when pinhole and knife-edge are displaced together through a lateral distance $\frac{1}{2}c$ from the central position, we replace $E(x, y)$ by $E(x, y)e^{ic'x}$ and $D(x, y)$ by $D(x, y)e^{ic'x}$ in (16), where (to a sufficient approximation) $c' = \dfrac{2\pi cd}{\lambda\rho_0}$ and d is the width, measured perpendicular to the axis of the mirror, of the corresponding zonal area. In a mirror of focal ratio not shorter than $f/3$ it agrees to within 0·7 per cent with the width, $f/300$, of the screen aperture.

The resulting equation, namely

$$2\pi D(x', y') = \pi E(x', y') + i\int_{-\infty}^{\infty} \frac{E(t, y')}{t - x'} e^{ic'(t - x')}\, dt \qquad (19)$$

gives the new value of $D(x', y')$.*

The only change which is needed when two zonal apertures are open instead of one is the redefining of $E(x', y')$ as $e^{2\pi i\varphi(x', y')}$ when P′ lies on either of the two corresponding zonal areas on the mirror, and as zero elsewhere.

It is easy to show † that, with apertures of the form shown in Fig. 1, the predicted intensity distribution along any horizontal line crossing either aperture resembles that along its central line $y' = 0$ so closely that they appear identical under visual inspection. It is therefore sufficient to consider only the intensity distribution $I(x') = I(x', 0)$ along the central line $y' = 0$ of each aperture.

On writing for shortness $D(x') = D(x', 0)$, $E(x') = E(x', 0)$, equations (19), (17) become

$$2\pi D(x') = \pi E(x') + i\left(\int_{R'S'} + \int_{RS}\right) \frac{E(t)}{t - x'} e^{ic'(t - x')}\, dt, \qquad (20)$$

$$I(x') = |\, 2\pi D(x')|^2. \qquad (21)$$

* Compare (**3**), p. 83. The edge-vignetting which results from the fact that the light passes twice through the screen apertures only affects points very close to the edges of the zonal segments, and these points have already been excluded from the discussion.

† By an application of the reduction theorem. The property is of course familiar experimentally.

When x' is in RS, the expression

$$2\pi D_r(x') = \pi E(x') + i\int_{\mathrm{RS}} \frac{E(t)}{t-x'} e^{ic'(t-x')}\,dt \tag{22}$$

agrees with the value which $2\pi D(x')$ would have if the right-hand aperture alone were uncovered, while the remaining term on the right of (20), namely

$$2\pi D_l(x') = i\int_{\mathrm{R'S'}} \frac{E(t)}{t-x'} e^{ic'(t-x')}\,dt, \tag{23}$$

represents the contribution from the halo of the left-hand aperture.

This contribution is rather small except on the inmost zones; on the Nth zone, t runs from $(-N+\frac{1}{2})d$ to $(-N+\frac{3}{2})d$ in R'S', while x' lies between $(N-\frac{3}{2})d$ and $(N-\frac{1}{2})d$ on RS. Thus, for $N \geqq 2$, the absolute value of (23) does not exceed

$$\int_{(N-\frac{1}{2})d}^{(N-\frac{3}{2})d} \frac{dt}{t+(N-\frac{3}{2})d} = \int_{2N-3}^{2N-1} \frac{dv}{v+2N-3}$$

$$= \log_e \frac{4N-4}{4N-6} = 2\left\{\frac{1}{4N-5} + \frac{1}{3}\frac{1}{(4N-5)^3} + \ldots.\right\}, \tag{24}$$

which is less than

$$0{\cdot}69,\ 0{\cdot}29,\ 0{\cdot}19,\ 0{\cdot}14,\ \ldots. \tag{25}$$

on zones 2, 3, 4, 5, ... respectively.

It has been assumed so far that the dimensions of the light source can be neglected. In predicting the appearances seen under test on a single zonal aperture, the assumption is a legitimate approximation provided that the horizontal dimensions of the pinhole or slit are small compared with the horizontal resolving power of the zonal aperture. This condition is not difficult to satisfy in a practical case. For example, when an $f/300$ zonal aperture is illuminated from a slit 0·001 inch wide, the full width of the central bright area in the diffraction image of the aperture is more than ten times the width of the slit.

In predicting the appearances seen on a pair of apertures, however, we should only be justified in treating the pinhole as a point source *ab initio* if its horizontal dimensions were small compared with the horizontal resolving power of the two apertures taken together. This condition is not usually satisfied in practice, except on the first few zones near the centre of the mirror. On the other zones it is necessary, when discussing the influence of one aperture on another, to take account of the finite size of the pinhole or slit and of the coherence properties of the light issuing from it.

We suppose the pinhole aperture and the knife-edge both to lie in the plane through G perpendicular to the axis of the mirror. In the practical case where pinhole and knife-edge move together, we take the pinhole aperture to be a region S surrounding the origin of coordinates in this plane, using for convenience coordinates (u, v) moving with the pinhole carrier and connected with the ordinary Cartesian coordinates (ξ, η) in the plane by the change of scale

$$u = \frac{2\pi y_0}{\lambda \rho_0}\xi, \qquad v = \frac{2\pi y_0}{\lambda \rho_0}\eta.$$

A circular pinhole equal in size to the Airy disk of the mirror then has the radius 3·83 in (u, v) units. To specify the position of the knife-edge we use a second set of coordinates (u', v'), differing by a parallel displacement from the (u, v)

coordinates and having as origin O′ the intersection with the (u, v) plane of the reflection from the median point P on the zonal segment RS of the ray joining P to the (u, v) origin O. If the knife-edge covers the half-plane $u' \leq c'$, the value of c' specifies the stage of darkening of the aperture, independently of the amount of the fixed lateral displacement between knife-edge and pinhole.

In a practical case S is large compared with the wave-length and the illumination over S is neither coherent nor fully incoherent, nor is it of uniform intensity. It can be regarded as the sum of a large number of coherent illuminations, each originating in a single emitting particle W of the primary light source and contributing, after passage through a condensing system whose errors are usually not small, a complex displacement $e_W(u, v)$ in the plane of the pinhole aperture S. In saying this, we make the harmless simplification of supposing that each particle emits an infinite train of periodic waves of wave-length λ.

To reduce the formal complications a little, we may suppose that the zonal screen is everywhere in contact with the mirror surface, that the viewing system is focused on this surface, and that the (u, v) origin and the (u', v') origin both coincide with G. We use as reference surface the sphere M_0, with centre G and passing through the median point P of the zonal segment RS; in the two zonal areas M_0 lies everywhere within a few fringes of the mirror surface. The wave-fronts leaving the mirror surface and converging to a more or less imperfect focus in the neighbourhood of G can be described, as in (**3**), in terms of the corresponding complex displacements in the surface M_0.

Corresponding to each emitting particle W and each element $dudv$ of the pinhole aperture, there is a contribution $E(x', y')\, e^{iux'+ivy'}\, e_W(u, v)\, dudv$ to the complex displacement on M_0, where $E(x', y')$, as before, is the complex displacement which would be given by a unit source placed at G. The whole contribution from the particle W is thus

$$E(x', y') \iint_S e^{iux'+ivy'}\, e_W(u, v)\, dudv = E(x', y') h_W(x', y'),$$

where

$$h_W(x', y') = \iint_S e^{iux'+ivy'}\, e_W(u, v)\, dudv. \tag{26}$$

The corresponding intensity is

$$4\pi^2 |E(x', y')|^2 . |h_W(x', y')|^2$$

and the total intensity distribution, obtained by summing over all the particles W, is therefore

$$4\pi^2 |E(x', y')|^2 \sum_W |h_W(x', y')|^2.$$

For the mirror to appear uniformly lit, this has to be constant as x' and y' vary on the mirror surface.

In the case of an unmasked mirror of uniform reflecting power, this means that

$$J = \sum_W |h_W(x', y')|^2 \tag{27}$$

must be constant over the mirror surface. When, as here, the mirror is covered by a screen exposing only a pair of zonal areas, the condition is that J should be constant over these areas. For since the effect of the screen is to reduce the reflecting power to zero outside the zonal areas, the masked mirror can be treated

as a particular case of the unmasked mirror of variable reflecting power, provided that points close to the discontinuities in $E(x', y')$ are excluded from the discussion.

Now suppose that the knife-edge is inserted so as to cover the half-plane $u' \leqq c'$. A unit source at the point (u, v) of the pinhole aperture will then contribute, instead of $e^{iux'+ivy'} E(x', y')$, an amount

$$e^{iux'+ivy'}\left[\tfrac{1}{2}E(x', y') + \frac{i}{\pi}\int_{-\infty}^{\infty} \frac{E(t, y')}{t-x'} e^{i(c'+u)(t-x')}\, dt\right] \tag{28}$$

to the complex displacement $D(x', y')$ "seen" on M_0. Thus the particle W contributes altogether a complex displacement $D_W(x', y'; c')$, where

$$2\pi D_W(x', y'; c') =$$

$$\iint_S \left[\pi E(x', y') + i\int_{-\infty}^{\infty} \frac{E(t, y')}{t-x'} e^{i(c'+u)(t-x')}\, dt\right] . e^{iux'+ivy'} e_W(u, v)\, du dv$$

$$= \pi E(x', y') h_W(x', y') + i\int_{-\infty}^{\infty} \frac{E(t, y')}{t-x'} e^{ic'(t-x')} h_W(t, y')\, dt, \tag{29}$$

by (26). The corresponding intensity

$$I_W(x', y'; c') = |2\pi D_W(x', y'; c')|^2. \tag{30}$$

Finally, since the waves emitted from every two different particles are mutually incoherent, the observed intensity under the test

$$I(x', y'; c') = \sum_W I_W(x', y'; c'). \tag{31}$$

Equations (29)–(31) show that the reduction theorem ((**3**), p. 84), according to which the intensities seen under the test at a point (x', y') depend only on the properties of the mirror surface along the horizontal line through this point, remains valid when the point source is replaced by a large pinhole or by a slit. It was assumed in the above analysis that the slit is not so large that off-axis aberrations of the system under test vary appreciably from one point to another of the slit-area. However, this restriction is unnecessary; when it is removed, (29) takes the form

$$2\pi D_W(x', y'; c') =$$

$$\iint_S \left[\pi E(x', y'; u, v) + i\int_{-\infty}^{\infty} \frac{E(t, y'; u, v)}{t-x'} e^{i(c'+u)(t-x')}\, dt\right] . e^{iux'+ivy'} e_W(u, v)\, du dv \tag{32}$$

and the reduction theorem follows as before.

5. *Interaction between apertures. Effects of coherence.*—Fig. 4A–4C show the intensities seen at selected lateral settings of the knife-edge, using point source illumination, on the inmost pair of zonal segments of a spherical mirror. The corresponding intensity curves for a paraboloid do not differ appreciably from these in a practical case.

Fig. 4B shows the appearances seen at the central setting; Fig. 4A and 4C those with knife-edge and pinhole displaced to the left and to the right by amounts which introduce a path-difference of half a wave-length between the rays arriving via the centre points of the two zonal segments. For a mirror tested with $f/300$ zonal apertures, the amount of the displacement is 0·00075 inch to the left and to the right respectively.

The halo bands corresponding to two lateral settings at equal distances on either side of the central setting are really identical, but when the knife-edge is advanced beyond the central setting the apertures darken and the simultaneous

increase in brightness of the halo band is very conspicuous; at the setting of Fig. 4c, the halo is brighter than the aperture.

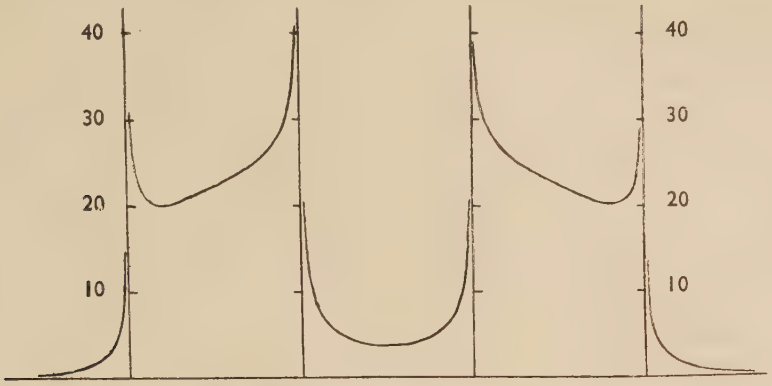

FIG. 4A.—*Intensities on inmost pair of f/300 zonal segments, and halo intensities, with knife-edge set 0·00075 inch short of central position. (Pinhole and knife-edge moving together.)*

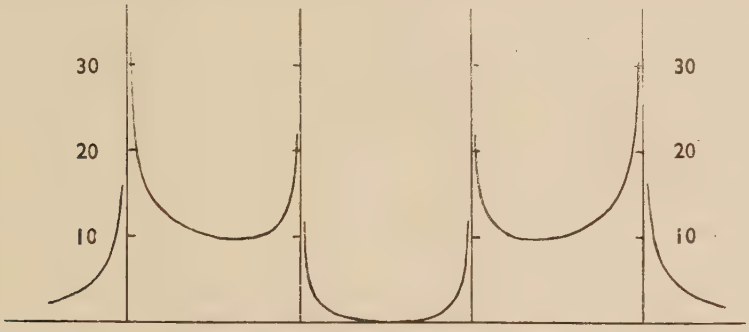

FIG. 4B.—*Intensities with knife-edge central.*

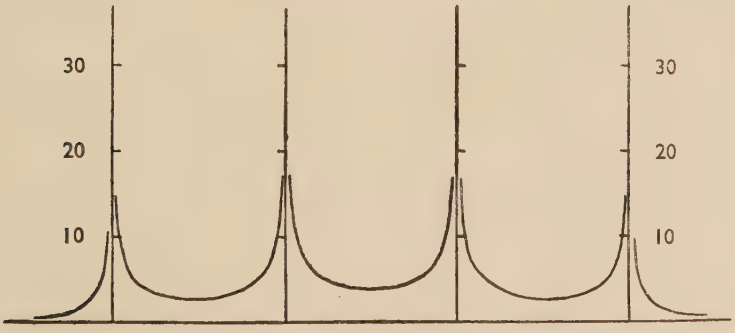

FIG. 4C.—*Intensities with knife-edge 0·00075 inch beyond central position.*

The asymmetry of the intensity distribution along each zonal segment can be regarded as due to disturbance by the halo from the other aperture, i. e. to interaction between the apertures.

If the illuminations of the two apertures are mutually incoherent, the effect of the halo of each aperture on the other is not complicated by interference phenomena and the intensity seen under the test with both apertures open is the sum of those due to the two separate apertures. Since the halo of either aperture is quite faint at the distance corresponding to the position of the other, interaction between the apertures is small.

If, in the other extreme, the illumination of the two apertures is fully coherent (as happens when the light source is a pinhole of negligible size), then it is the complex displacements corresponding to the two single apertures and their halos which have to be added, and the squared modulus of their sum which measures the resulting intensity, instead of, as formerly, the sum of their squared moduli. In this case an overlapping halo of intensity amounting to only four per cent of the main intensity at a point in the aperture which it overlaps may cause a 20 per cent change in the observed brightness.

In a practical case the illumination may be neither fully coherent nor fully incoherent; and it appears from the above that the effect of interaction between the zonal apertures cannot be dismissed as small merely because the intensity of each halo is small where it overlaps the other aperture. The order of magnitude of the interaction effect, as well as its more detailed characteristics, will depend on the coherence situation in the aperture of the pinhole or slit.

Of practical interest is the question whether this interaction can upset the determinations of the zonal foci near the centre of the mirror. With point source illumination, it follows from the general formulae that a pair of zonal apertures on a true sphere darkens symmetrically when the knife-edge is brought across at the geometrically correct focal setting. But even in the relatively simple case of a pair of zonal apertures uniformly lit from a slit whose width is not small compared with the resolving power of the two apertures taken together, it is not clear without analysis whether the two apertures will darken similarly. It could happen, for example, that the light issuing from the slit consisted of two mutually incoherent waves W and W′; W providing displacements 1 and $1/\sqrt{2}$ and W′ displacements 0 and $1/\sqrt{2}$ on the right and left-hand zonal segments respectively, as shown in Fig. 5. The pair of apertures will then appear uniformly lit with the knife-edge withdrawn, but when the knife-edge is centrally set the mechanism of the interaction between the apertures is not symmetrical, and hence the observed intensities on the zonal segments cannot be expected to be symmetrical.

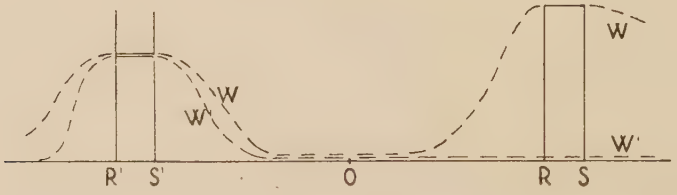

FIG. 5.—*Equal and uniform lighting of two zonal segments, with unsymmetrical coherence.*

Nevertheless, in the above example, and also in general, subject to certain conditions on the lighting which are easily realized in practice, a pair of zonal areas on a true sphere does darken symmetrically when the knife-edge is brought across at the geometrically correct focus; and the zonal focus determinations are consequently not affected by asymmetry of coherence in the lighting.

This result is a consequence of the following theorem:

(1) *If, in the carrying out of the zonal Foucault test, the lateral dimensions of the pinhole or slit are small compared with the horizontal resolution of a single zonal aperture; if*

(2) *the lighting is such that, in a given pair of zonal apertures, the two members appear uniformly and equally bright with the knife-edge withdrawn; and if*

(3) *the mirror figure is such that this pair of zonal apertures would darken symmetrically under point-source illumination*;

Then the pair of apertures will darken symmetrically under the actual illumination, and the focal reading for the zone will be the same with the actual lighting as with point-source illumination.

Condition (3) is satisfied on a true sphere and also, to a good approximation, on the central zones of an astronomical paraboloid. For example, on a 25-inch $f/4$ paraboloid the deviation of a pair of $f/300$ zonal apertures from the best-fitting sphere is less than $\frac{1}{50}$ fringe for the first eleven zones.

By the generalized reduction theorem, it is enough to prove the theorem along the main diameter $y=0$. Along this diameter each luminous particle W of the primary light source contributes a wave displacement

$$E_W(x)=A_W(x)E(x) \tag{33}$$

on the surface of the reference sphere M_0. Here

$$E(x)=\exp\left[\frac{2\pi i}{\lambda}d(x,0)\right] \qquad a<|x|<b$$
$$=0 \qquad \text{elsewhere.}$$

The factor $\exp\left[\frac{2\pi i}{\lambda}d(x,0)\right]$ expresses the distortion of the wave-fronts caused by the deviation of the mirror surface (amounting to $d(x,y)$ fringes at the point (x,y) from that of the reference sphere M_0). The masking of the mirror is expressed by setting $E(x)=0$ outside the two zonal segments $-b<x<-a$ and $a<x<b$.

The factor $A_W(x)$ describes the characteristics of the wave emitted by the W particle when, after passing through the condensing system and the slit, it arrives at the point $(x,0)$ on M_0. $|A_W(x)|^2$ measures the intensity of the wave at this point, so that if the two apertures are to appear uniformly and equally lit with the knife-edge withdrawn, the sum

$$\sum_W |A_W(x)|^2$$

must be constant for $a<|x|<b$. By a suitable choice of units, we can write this condition in the form

$$\sum_W |A_W(x)|^2=1 \qquad (a<|x|<b). \tag{34}$$

Further, since the slit-width is small compared with the resolving limit of each zonal segment, the value of $A_W(x)$ will be effectively constant over each of these two ranges.

The condition that the zones should darken symmetrically under point-source illumination is

$$E(-x)=\overline{E(x)}; \tag{35}$$

when it is satisfied,

$$\begin{aligned}2\pi D(-x)&=\pi E(-x)+i\int_{-1}^{1}\frac{E(t)}{t+x}e^{ic'(t+x)}\,dt\\&=\pi\overline{E(x)}-i\int_{-1}^{1}\frac{E(-t)}{t-x}e^{-ic'(t-x)}\,dt\\&=\pi\overline{E(x)}-i\int_{-1}^{1}\frac{\overline{E(t)}}{t-x}e^{-ic'(t-x)}\,dt\\&=2\pi\overline{D(x)},\end{aligned}$$

so that $I(-x)=I(x)$.

Now suppose the conditions of the theorem satisfied. Then

$$2\pi D_W(x) = \pi A_W(x)E(x) + i\int_{-\infty}^{\infty} e^{ic'(t-x)}\, A_W(t)E(t)\,\frac{dt}{t-x}$$
$$= \pi A_W(x)E(x) + i\left(\int_{-b}^{-a} + \int_a^b\right) e^{ic'(t-x)}\, A_W(t)E(t)\,\frac{dt}{t-x}.$$

Write

$$\alpha(x) = \int_a^b e^{ic'(t-x)}\, E(t)\,\frac{dt}{t-x}, \qquad \beta(x) = \int_{-b}^{-a} e^{ic'(t-x)}\, E(t)\,\frac{dt}{t-x};$$

then, by (35),

$$\beta(x) = -\int_a^b e^{-ic'(t+x)}\, E(-t)\,\frac{dt}{t+x} = -\overline{\alpha(-x)}.$$

For $a<x<b$, therefore,

$$2\pi D_W(x) = A_W(x)[\pi E(x) + i\alpha(x)] + iA_W(-x)\beta(x)$$
$$= A_W(x)[\pi E(x) + i\alpha(x)] + iA_W(-x)\overline{\alpha(-x)},$$
$$|2\pi D_W(x)|^2 = |\pi E(x) + i\alpha(x)|^2 |A_W(x)|^2 + |\alpha(-x)|^2 |A_W(-x)|^2$$
$$+ 2\mathscr{I}\{[\pi E(x) + i\alpha(x)]A_W(x)\,.\,\alpha(-x)\overline{A_W(-x)}\},$$
$$I(x) = \sum_W |2\pi D_W(x)|^2 = |\pi E(x) + i\alpha(x)|^2 + |\alpha(-x)|^2$$
$$+ 2\mathscr{I}\{[\pi E(x) + i\alpha(x)]\alpha(-x)\sum_W A_W(x)\overline{A_W(-x)}\}; \quad (36)$$

while for $-b<x<-a$

$$2\pi D_W(x) = A_W(x)[\pi E(x) + i\beta(x)] + iA_W(-x)\alpha(x)$$
$$= A_W(x)[\pi E(x) + i\beta(x)] - iA_W(-x)\overline{\beta(-x)},$$
$$I(x) = \sum_W |2\pi D_W(x)|^2 = |\pi E(x) + i\beta(x)|^2 + |\beta(-x)|^2$$
$$+ 2\mathscr{I}\{[\pi E(x) + i\beta(x)]\beta(-x)\sum_W A_W(x)\overline{A_W(-x)}\}. \quad (37)$$

On the right of (36), (37), the first two terms represent the intensity-contributions from the two apertures taken separately and the third term measures the interaction due to coherence.

From (36), (37) it follows that for $a<x<b$

$$I(-x) = |\pi E(-x) + i\beta(-x)|^2 + |\beta(x)|^2$$
$$+ 2\mathscr{I}\{[\pi E(-x) + i\beta(-x)]\beta(x)\sum_W A_W(-x)\overline{A_W(x)}\}$$
$$= |\pi\overline{E(x)} - i\overline{\alpha(x)}|^2 + |\overline{\alpha(-x)}|^2$$
$$- 2\mathscr{I}\{[\pi\overline{E(x)} - i\overline{\alpha(x)}]\overline{\alpha(-x)}\sum_W \overline{A_W(x)}A_W(-x)\}$$
$$= |\pi E(x) + i\alpha(x)|^2 + |\alpha(x)|^2$$
$$+ 2\mathscr{I}\{[\pi E(x) + i\alpha(x)]\alpha(-x)\sum_W A_W(x)\overline{A_W(-x)}\}$$
$$= I(x),$$

which proves the theorem.

6. *Comparability of the two zonal apertures under the test.*—On the median and outer zones of the paraboloid, interaction between the members of a pair

of $f/300$ zonal apertures is so small as to be negligible in visual testing. For example, on the Nth zone from the centre of any concave mirror the halo contribution from either aperture to the complex displacement near the centre of the other is, by (24), not greater than 0·05 if $N \geq 12$; that is to say less than two per cent of the total displacement with the knife-edge centrally set. Even with fully coherent lighting, this produces a change of less than four per cent in the intensities on the apertures; such a change is too small to be detected by the eye. In calculating the appearance under the test of the median and outer zones, we may therefore disregard the interaction between the two apertures.

The possibility of making accurate focal readings on the outer zones of a paraboloid depends on the fact that the run of the Foucault shadows is similar on the two apertures when the knife-edge is at the "correct" setting for the zone, namely the intersection G of the normals from the median points of the two zonal segments (see Fig. 3). But whereas on the central zones the shadows were shown to be inversely similar at this focal setting, i. e. symmetrical about the centre of the mirror surface, on the outer zones they are directly similar, both zonal apertures appearing darker on the side towards the knife-edge.

In order that the two members of every pair of zonal apertures shall darken similarly, and the sensitiveness of the test shall not be reduced by uncertainties of interpretation, it is necessary and sufficient that (i) interaction effects shall become inappreciable before the term in u^2 in equation (8) produces an appreciable effect on the observed intensities; (ii) even at the edge of the mirror, the effect of the term in u^3 in equation (8) shall be inappreciable to the eye. When these two conditions are satisfied, the sensitiveness of the test depends on the observer's power to judge which of two similarly lit apertures appears the brighter as the knife-edge is moved from side to side.

Experimental trials showed that condition (i) is satisfied with an ample margin in the case of a 25-inch $f/4{\cdot}9$ paraboloid. Even on the inmost pair of apertures (corresponding to zone 2) it was only with difficulty possible to make out any asymmetry in the brightness of the individual zonal apertures, although the halo band appeared quite vivid with the knife-edge nearly central.

To investigate whether condition (ii) is satisfied in a practical case, intensity distributions were computed for the edge-zones of a 25-inch $f/4{\cdot}9$ paraboloid and of a 75-inch $f/4$ paraboloid at selected knife-edge settings. In making the computations it is permissible, by what has been established above, to neglect the interaction between the two zonal apertures. It is also permissible to replace by a point source the fine slit or pinhole which would be used in practice. For the width, about 0·001 inch, of this slit or pinhole is only about $\frac{1}{12}$ of the width of the central maximum in the diffraction image of an $f/300$ zonal aperture.

The results of the computation are shown in Fig. 6 and Fig. 7. It will be seen that in both cases the intensity curves on the two zonal segments are so closely similar that their differences are hardly visible to the eye on the graphs. Much larger differences would be imperceptible to the eye in the actual carrying out of the test.

Some idea of the theoretical sensitiveness of the test can be found from Figs. 8 and 9. Fig. 8 shows the effect of a small lateral shift of pinhole and knife-edge on the intensities seen on the pair of $f/300$ zonal segments corresponding to the edge-zone of a 25-inch $f/4{\cdot}9$ paraboloid. In the upper curve, knife-edge and pinhole are centrally set at the intersection G of the normals from the median

points P of the two zonal segments (see Fig. 3); in the lower curve, knife-edge and pinhole are advanced 0·0005 inch beyond the central position. The effect of the lateral shift is an apparent tilt of the mirror surface, corresponding to a height difference of $\frac{1}{6}$ fringe between the two sides of each zonal aperture.

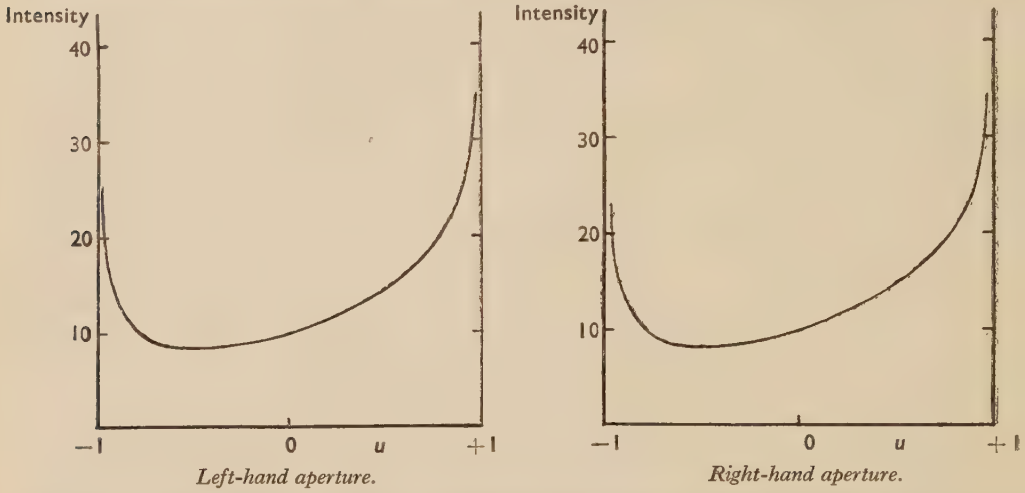

FIG. 6.—*f*/300 *edge-zone of* 25*-inch* *f*/4·9 *paraboloid with knife-edge at the focal setting G* (*Fig.* 3).

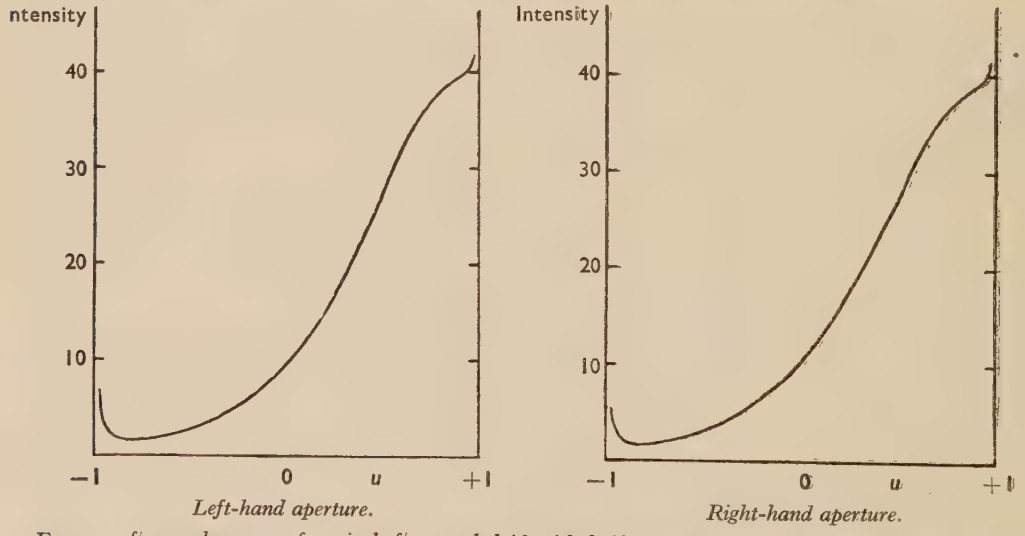

FIG. 7.—*f*/300 *edge-zone of* 75*-inch* *f*/4 *paraboloid with knife-edge at the focal setting G* (*Fig.* 3).

If the longitudinal setting of the knife-edge and pinhole is shortened by 0·005 inch, the effect on the intensities is (to a sufficient approximation) as though one of the zonal sectors received a tilt of the above amount relative to the other. Therefore the upper and lower curves in Fig. 8 will represent also the intensities seen, on the right and left zonal segments respectively, when the knife-edge and pinhole are 0·005 inch inside the zonal focus G and 0·00025 inch to the left of the axis.

Results of the same kind for the *f*/300 edge-zone of a 75-inch *f*/4 paraboloid are shown in Fig. 9. Here the difference between the upper and lower curves represents the effect of a tilt which raises the right-hand side of each zonal aperture

$\frac{1}{12}$ fringe relative to the left; it also shows the intensities seen along the two zonal segments when the pinhole and knife-edge are set 0·002 inch inside the zonal focus G and 0·00025 inch across the axis of the mirror.

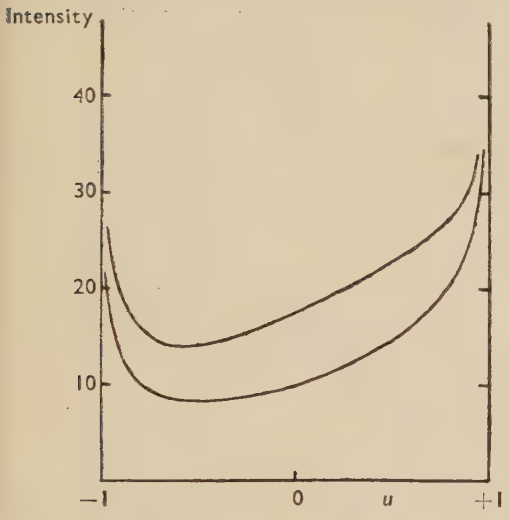

FIG. 8.—*f*/300 *edge-zone of 25-inch f*/4·9 *paraboloid with longitudinal setting of knife-edge* 0·005 *inch inside G* (*Fig.* 3). (*Pinhole and knife-edge moving together.*)

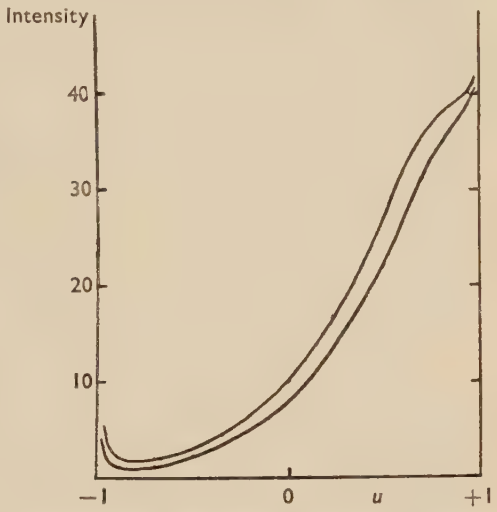

FIG. 9.—*f*/300 *edge-zone of 75-inch f*/4 *paraboloid with longitudinal setting of knife-edge* 0·002 *inch inside G* (*Fig.* 3). (*Pinhole and knife-edge moving together.*)

The zonal settings are most accurately determined, not by comparing the brightness of the apertures with the knife-edge stationary, but by observing which darkens in advance of the other as the knife-edge is brought across. It would therefore be unsafe to base any numerical estimate of the limit of sensitiveness of the zonal test on Figs. 8 and 9. We can, however, draw the conclusion from Figs. 6 and 7 that no difficulty arises, in the zonal testing of paraboloids of the dimensions and focal ratios ordinarily used in reflecting telescopes, through the Foucault shadows crossing the two zonal apertures at different speeds, or in a different manner, as the knife-edge is brought across the axis.* The appearances on the two members of a pair of zonal segments pass through the same sequence of changes as the knife-edge advances, the discrepancies being far too small to be detected by the eye. The accuracy of each zonal focus determination is therefore limited in a practical case only by the observer's limited power to perceive that one aperture is darkening a little ahead of the other.

The Observatory,
Cambridge:
1948 *September* 27.

References

(1) F. L. O. Wadsworth, *Popular Astronomy*, **10**, 337, 1902.
(2) R. Platzeck and E. Gaviola, *J.O.S.A.*, **29**, 484–500, 1939.
(3) E. H. Linfoot, *Proc. Roy. Soc.* (A), **186**, 72–99, 1946.

* The contrary has been asserted in the literature; see R. Platzeck and E. Gaviola (2).

INTERFEROMETRIC MEASUREMENTS OF SOLAR WAVE-LENGTHS AND AN INVESTIGATION OF THE EINSTEIN GRAVITATIONAL DISPLACEMENT

M. G. Adam

(Communicated by the Director of the University Observatory, Oxford)

(Received 1948 December 3)

Summary

Absolute wave-lengths are determined for selected lines in the solar spectrum near the atmospheric oxygen band at λ 6300, for 13 points across the polar diameter of a large solar image. The centre wave-lengths show a shift of +0·005 A. over the vacuum arc values; there is little change in wave-length with disk position until the last 10 per cent of the solar image radius, when a rapid increase to a shift of +0·013 A. is found. The observed wave-lengths are corrected for differences in physical conditions in the Sun and in the vacuum arc (Lindholm effect), and the interpretation of the residual shifts is considered. It is found that the usual Relativity-radial current hypothesis implies currents with impossibly large velocities. It is concluded that we have at present no adequate theoretical interpretation of solar wave-lengths, and suggestions are made for further observational investigations which should indicate the solution to this problem.

Introduction.—Precise values of solar wave-lengths are of especial interest and have been much discussed, because one of the three crucial tests given for the General Theory of Relativity is that the Fraunhofer lines should show a red shift in wave-length of 21 parts in 10^7 with respect to the lines from terrestrial sources. Although the reality of a red shift of the solar lines was established by Jewell in 1896, until 1928 the precise value of the shift was very uncertain, due in part to random errors in the wave-lengths of the solar lines observed, and in part to ignorance of the physical conditions which must be satisfied in a satisfactory laboratory source. In 1928 St. John (**16**) discussed the absolute wave-lengths of 1537 lines at the centre of the disk and 133 at the limb; the wave-lengths were based on standard iron arc lines (free from pole effect), and the values were compared with the laboratory vacuum arc wave-lengths. St. John's interpretation of his results was that the Einstein red shift was present, but that it was partly concealed at the centre of the disk by violet shifts due to radial currents, the effect of which disappeared at the limb. This work is the basis for the belief that the red shift predicted by the General Theory of Relativity is present. It is true that the solar wave-lengths could not wholly be accounted for by St. John's theory, but the discrepancies were small.

Further measurement and discussion of solar wave-lengths has not improved the position of St. John's theory (**7**). Burns (**4b**) has discussed the three series of solar wave-lengths which form the basis of the standard values adopted by the International Astronomical Union in 1928 (**2a**), from the point of view of the Relativity theory. He points out that in the red, where the agreement between the observers is best, the red shift has only half the Relativity value, and considers

that St. John's interpretation of this as due to radial currents is untenable, basing his objections chiefly on the systematic change in red shift shown by lines of different intensities.

Burns was considering primarily wave-lengths for the centre of the disk, or for the integrated disk, but the effect of radial currents depends upon the inclination of the line of sight to the normal to the solar surface, so that observations of changes in wave-length across the disk furnish valuable information for testing St. John's theory. Several investigations of this change, which in this paper is called "limb effect" * have been made (**6a**, **8**, **9**, **3d**). But neither centre absolute wave-lengths, nor differential measures across the disk can separately give a full test of the Relativity-radial current interpretation of solar wave-lengths. If radial velocities are deduced from "limb effect", then we must be able to show that the centre absolute values do in fact show the corresponding velocity shift. Any theoretical interpretation of solar wave-lengths must be tested by absolute values of the wave-lengths at each point of the disk.

In the present investigation an attempt is made to obtain a homogeneous set of wave-lengths, which are absolute, and refer to representative points from centre to limb of the solar disk. The observational procedure and reduction of the material to give absolute wave-lengths is described in Sections I and II of the paper, and the theoretical interpretation of the measured wave-lengths is considered in Section III.

I. *Apparatus and Observational Procedure*

Choice of a wave-length region and selection of lines.—For the measurement of absolute wave-lengths in the solar spectrum the first requirement is a number of standard lines of known wave-length. The standard lines should be photographed simultaneously with the solar lines, as it is otherwise extremely difficult to avoid errors due to slight changes in the dispersing apparatus during, and between exposures. The light from the standard source and from the Sun must also have identical paths in the apparatus to avoid "Hartmann" displacements due to variations in the illumination of the optical components. The absorption lines of atmospheric oxygen meet both these requirements, and Babcock's (**3a**, **3b**) careful investigations show that they form reliable wave-length standards at least for the higher solar altitudes. The wave-lengths of atmospheric oxygen lines have been carefully determined in terms of the neon secondary standards, and a number of the lines were adopted as standards by the International Astronomical Union in 1928. The selection of these atmospheric lines as standards means observing solar lines in their vicinity at λ 6280. This general region has the further advantage that the line density in the solar spectrum is fairly low, and also it is the wave-length region of the neon spectrum. It is here that the agreement between wave-lengths measured by different observers is best, and, as Burns (**4b**) points out, the region is therefore very important for testing the Relativity theory.

The 14 solar lines in Table I were finally selected as being freest from blends, and of a strength measurable with fair certainty. They are all designated "*m*" in Rowland's Table (**1**) indicating three or more independent measures. Columns 1, 2, 3 are taken direct from Rowland's Table, column 4 is from *Transactions*

* St. John's original meaning of "limb effect" was the excess of the extreme limb shift over the predicted Einstein shift.

of the I.A.U. 1928 (**2a**), except that the individual values for λ6022 Mn and λ6056 Fe of different observers are not averaged there to give a "recommended λ" as is done now, and λ6108 Ni does not appear at all, the value given is from Burns and Meggers' Table (**5a**). The 10 atmospheric oxygen lines selected as standards are all given "recommended" wave-lengths in the I.A.U. list (**2a**); the neon standards are from the I.A.U. list of 1935 (**2c**).

TABLE I

Lines selected for measurement

Solar lines				Atmospheric oxygen lines			Neon lines
Rev. Rowland Table			I.A.U. 1928 Wave-length	Rev. Rowland Table		I.A.U. 1928 Wave-length	I.A.U. 1935 Wave-length in A.
Wave-length in A.	El.	Int.		Wave-length in A.	Int.		
6013·503	Mn	6	·497	6281·185	1	·178	5944·8342
6016·653	Mn	6	·647	6281·961	2	·956	6074·3377
6021·808	Mn	6	[·801]	6283·799	1	·796	6096·1630
6024·073	Fe	7	·068	6290·224	2	·221	6163·5939
6027·064	Fe	4	·059	6292·170	2	·162	6266·4950
6042·108	Fe	3	·104	6292·967	3	·958	6334·4279
6056·018	Fe	5	[·010]	6295·966	3	·960	
6065·499	Fe	7	·494	6305·819	2	·810	
6108·130	Ni	6	[·120]	6306·575	2	·565	
6122·231	Ca	10	·226	6309·896	2	·886	
6200·327	Fe	6	·321				
6219·294	Fe	6	·287				
6265·148	Fe	5	·141				
6270·237	Fe	3	·231				

Experimental arrangements.—The wave-length region centred at λ6150 has the disadvantage that the Oxford Solar Spectroscope in its five-prism form gives here a dispersion of only 1·7 A./mm. This is too small for the determination of wave-lengths with an accuracy of ±0·002 A., and it was accordingly decided to cross the spectroscope with a Fabry-Perot interferometer. An interferometer plate separation of 5 mm., as finally used with a 15 cm. projecting lens, gives at these wave-lengths (for the inner rings of the interference pattern, which were chosen for measurement) an effective dispersion of 0·4 A./mm. to 1·0 A. mm. The measurement of rings to the nearest $\frac{1}{100}$ mm. will thus give an accuracy for a single setting of ±0·004 A. at the innermost ring, to ±0·010 A. at the outermost ring.

The channelled spectrum obtained for continuous light when a Fabry-Perot interferometer is crossed with a spectroscope has been fully described by Burns and Meggers (**5a**), who have pointed out the conditions and precautions necessary to obtain reliable wave-lengths.* The interferometer used in this investigation had both plates and separators made of fused silica. The reflecting surfaces were coated with aluminium to give about 50 per cent reflectivity. Separators of $2\frac{1}{2}$, 5 and 10 mm. were tried, but for the absorption lines of Table I the 5 mm.

* See also (**4a, 17, 3c, 13**) for general references.

separator gave the best spectra for wave-length measurements. This gives an order of interference of 16,700 at λ6000, and a separation of the continuous spectrum channels of 0·36 A. Experiment showed that a slit width of 0·227 mm. was the optimum for the disappearance of the channels over the 300 A. range, in close agreement with the theoretical value for the spectroscope dispersion.

The experimental set-up used is shown in Fig. 1. The solar image (180 mm. diameter) was focused on the guiding disk, and the spectroscope is then fed by the light from that region of the disk over the axial hole. The area of this hole should be as small as is possible, since it chiefly determines the resolution on the solar image. A circular area 3 mm. in diameter ($\frac{1}{30}$ of the image radius) gave exposure times for the spectra of reasonable length. The beam passing through the guiding disk filled the solar diaphragm D_S which was placed immediately in front of a convex cylindrical lens. This lens requires a word of explanation: the Cassegrain system of the solar telescope results in each point on the focused image receiving light from a hollow cone of rays, and it is necessary to increase the angular range and fill in the missing angles before the light crosses the interferometer. The use of a short-focus (2 cm. approx.) cylindrical convex lens for this purpose gave fairly good uniformity with the least reduction in intensity. The interferometer diaphragm D_I was placed as close as possible to the first plate, and its circular aperture (2·44 mm. diameter) was filled with light. The projection "ring" lens was a Beck "Neostigmar" of 15 cm. focal length, full aperture $f/4·5$ and used at $f/8$ approx. This optical train gave on the collimating lens of the spectroscope a central band of light running perpendicular to the slit and of width approximately $\frac{1}{3}$ of the lens diameter.

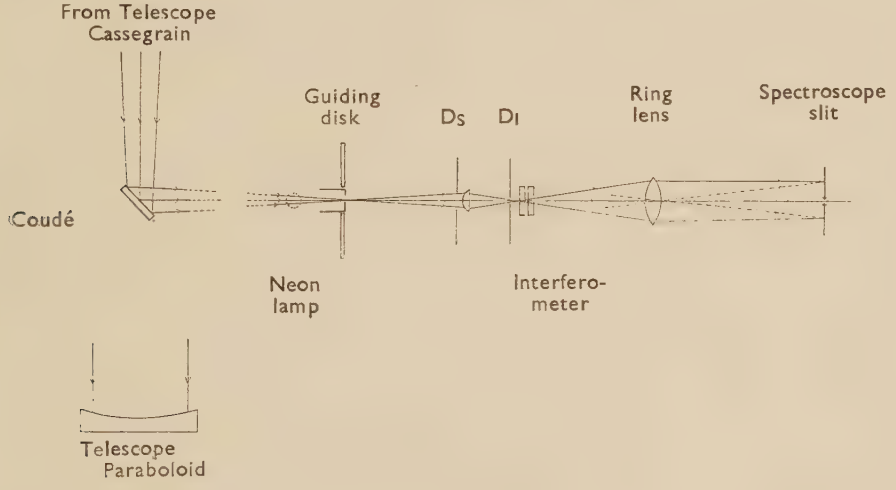

FIG. 1.—*Diagram of apparatus.*

Although the wave-lengths determined in this investigation are based on the atmospheric oxygen lines of Table I, neon comparison spectra were nevertheless obtained at intervals during a sequence of solar exposures, and provided a valuable confirmation of the stability of the set-up. Considerable difficulty was experienced in finding a convenient neon source of sufficient extent so that when it replaced the solar light in front of the guiding disk the illumination of the optical train was the same, and of sufficient intensity to give reasonable exposure times.

I am much indebted to Dr A. von Engel of the Electrical Laboratory, Oxford, and to the British Thomson-Houston Company for their cooperation in this matter.* For the final plates the B.T.-H. experimental lamp was used; it was essentially similar in construction and conditions of excitation to the B.T.-H. Sodra lamp, but contained neon alone. This lamp gave a long cylindrical discharge of luminous diameter 9–9½ mm., and a current of approximately 500 m.a. (465 volts A.C.), it was extremely simple to run, and the exposure times were practicable.

Details of exposures.—The spectroscope was carefully focused for the range λλ 6000–6300, and the ring lens placed on the optical axis with the focus at the slit. The procedure for obtaining a "set" of exposures on any one day was first to adjust the interferometer. This was carried on a rotatable table, so that it could be turned through 90°, and the plates made parallel and tested *in situ*. The cylindrical lens was then adjusted to give uniformity of illumination across the spectrum as far as possible, and the solar and interferometer diaphragms placed in position. The optical train from the guiding disk was then entirely untouched, while solar spectra from 13 points across a diameter of the image, and neon comparison spectra were obtained. A slit height of 12 mm. gave 13–14 rings on the spectrum lines, and enabled 5 spectra to be taken on each plate, of which one, generally exposure 3, was always a centre spectrum. The exposure times for the Sun ranged from 2¼ minutes at the centre of the disk to 8 minutes at the extreme limb position; for the neon lamp about 30 minutes was required.

The observations were made across a polar diameter to avoid wave-length shifts due to solar rotation. The east–west line on the image was determined from the drift of sunspots on changing the rate of the coelostat, and the orientation of the polar diameter was then deduced from the tabulated position angle of the pole. The linear motion of the guiding disk parallel to this direction enabled any predetermined point on the polar diameter to be brought over the axial hole. The image was guided during all exposures. Three complete "sets" of exposures each consisting of 4 plates and 18–20 spectra were obtained during 1946 September and October. The procedure for each set was identical except that the orientation of the interferometer plates was changed by 90° for each set. Ilford Process Panchromatic Plates (Rapid) were used throughout and developed in Parkhurst two-solution developer. The details for the plates are given in Table II; disk position in column 1 gives the ratio of the distance r of the "point" of observation (N. or S. of the equator) from the image centre, to the image radius R.

II. *Reduction of Observations*

Measurement of plates and determination of fractional orders.—The reduction of interference spectra for wave-length determinations has been fully described in the literature (**4a**, **17**, **3c**, **13**). There are two main steps in the procedure, the determination of the fractional orders of interference (ϵ) for each line, and the determination of the interferometer plate separation (t) from the standard lines. The approximate wave-length then gives the integral order of interference (n) and the accurate wave-length is $2t/(n+\epsilon)$, assuming that the interferometer is

* In 1945 Dr von Engel constructed two low voltage, low pressure, heated cathode neon lamps, the second of these gave a cylindrical discharge of good uniformity, luminous diameter 7 mm., nd length approximately 3 cm., with intensity somewhat greater than the B.T.-H. lamp.

TABLE II

Measured Plates

Disk Position r/R	Exposure	U.T.	Hour angle of Sun	Altitude of Sun
1946 *Sept.* 15. *Plate A* 325				
	m s	h m	° ′	° ′
N ·984	8 00	8 47	48 22	27 03
N ·959	7 00	8 58	45 30	28 30
·000	2 30	9 08	43 07	29 40
S ·984	8 00	9 23	39 22	31 26
S ·959	7 00	9 39	35 22	33 12
Plate A 326				
	m s	h m		
Neon	32 10	10 20	° ′	° ′
S ·884	5 00	10 52	17 00	39 23
S ·769	4 00	11 06	13 37	40 05
·000	2 30	11 21	9 52	40 43
Neon	30 00	11 45		
Plate A 327				
	m s	h m	° ′	° ′
S ·769	4 00	14 32	37 52	32 03
S ·577	3 00	14 46	41 30	30 23
·000	2 30	14 54	43 22	29 29
N ·577	3 00	15 03	45 45	28 17
N ·769	4 00	15 12	47 52	27 13
Plate A 328				
	m s	h m	° ′	° ′
N ·884	5 00	15 32	53 00	24 29
N ·918	6 00	15 41	55 07	23 20
·000	3 00	15 54	58 30	21 26
S ·918	5 30	16 09	62 07	19 21
Neon	30 00	16 42		
1946 *Sept.* 28. *Plate A* 335				
	m s	h m	° ′	° ′
N ·984	7 30	9 56	30 00	30 41
N ·959	6 00	10 06	27 30	31 33
·000	2 30	10 14	25 30	32 11
S ·984	7 30	10 25	22 45	33 01
S ·959	6 00	10 36	20 00	33 46
Plate A 336				
	m s	h m	° ′	° ′
S ·918	5 30	10 54	15 30	34 47
S ·884	5 00	11 00	13 52	35 06
·000	2 30	11 07	12 15	35 22
Neon	32 00	11 37		
N ·918	6 00	13 17	20 15	33 39
Sept. 28 (*cont.*). *Plate A* 337				
	m s	h m	° ′	° ′
N ·884	5 30	13 35	24 45	32 22
N ·769	4 00	13 45	27 15	31 34
·000	2 30	13 52	29 00	30 59
S ·769	4 00	14 04	32 00	29 53
S ·577	3 00	14 16	35 07	28 39
Plate A 338				
	m s	h m	° ′	° ′
N ·577	3 00	14 48	43 07	25 09
·000	2 30	14 55	44 45	24 23
Neon	30 00	15 23		
1946 *Oct.* 11. *Plate A* 352				
	m s	h m	° ′	° ′
S ·984	7 00	8 31	50 07	17 29
S ·959	5 30	8 42	47 22	18 49
·000	2 30	8 51	45 15	19 49
N ·984	7 00	9 06	41 22	21 34
N ·959	5 30	9 17	38 37	22 44
Plate A 353				
	m s	h m		
Neon	38 00	9 55	° ′	° ′
·000	2 20	10 27	21 15	28 37
N ·918	4 15	10 36	19 00	29 09
N ·884	3 45	10 45	16 45	29 37
S ·884	3 45	10 57	13 45	30 11
Plate A 354				
	m s	h m		
Neon	36 00	11 38	° ′	° ′
S ·918	3 45	13 08	19 00	29 06
S ·769	3 15	13 16	21 07	28 36
·000	2 15	13 24	23 00	28 06
N ·769	3 15	13 34	25 37	27 21
Plate A 355				
	m s	h m	° ′	° ′
N ·577	2 45	13 53	30 22	25 48
S ·577	2 45	14 07	33 52	24 33
·000	2 15	14 16	36 00	23 43
Neon	36 00	14 51		

used under the atmospheric conditions to which the standard wave-lengths refer. The fractional order for any line can be obtained from the ratio $D_p^2/\Delta D^2 = p - 1 + \epsilon$, where D_p is the diameter of the pth ring from the centre, and ΔD^2 is the constant difference of the squares of the diameters of successive rings for the line. The values of ϵ have been determined following the "plate constant" method described by St. John and Babcock (**17**), in which ΔD^2 is not obtained from the line itself, but is given a value deduced from all the lines from the expression

$$\Delta D^2/\lambda m^2 = 4f^2/t$$

in which λ is the wave-length, m the spectroscope magnification and f is the focal length of the ring lens. For any given set-up the quantity $4f^2/t$ is a constant for which a mean value of high accuracy can be obtained from all the lines from the measured ring diameters, the approximate wave-length and the spectroscope magnification at that wave-length.

Preliminary detailed measurements of the interference patterns, to test the performance of the ring lens and general accuracy of the optical system, showed that the 8 innermost rings were apparently free from systematic errors due to distortion, curvature, etc. As the effective dispersion decreases with increasing ring diameter it was decided to determine wave-lengths from the four innermost measurable rings on each line. Ring diameters were measured to the nearest $\frac{1}{100}$ mm. with a Hilger measuring micrometer using low magnification. The value adopted for each ring was the mean of two measures in reverse directions; for the 57 spectra of Table II, in all about 5000 mean diameters were determined. Each ring diameter leads to a value for the fractional order of interference ϵ, and the arithmetic mean for the 4 rings was used. The probable error of this mean was for the neon lines 0·002 approx. corresponding to 1 part in 10^7 of the order of interference or 0·001 A. The atmospheric and solar lines in a typical absorption spectrum showed a p.e. of the mean ϵ for any line of 0·004 approx. corresponding to 0·002 A.

Standard wave-lengths.—The interferometer plate separation t or path length $2t$ may be determined from the neon spectra, and from the atmospheric oxygen lines in each solar exposure. The path lengths deduced from both sets of standard lines (assuming standard atmospheric conditions) on each of the three days on which "sets" of spectra were obtained are shown in Fig. 2. The neon spectrum $2t$ is the arithmetic mean of the values from the 6 lines in Table I and the p.e. of the mean value is approximately 1 in 2×10^7. The absorption spectrum $2t$ is the arithmetic mean from the 10 oxygen lines of Table I, and the p.e. of the mean value is 1 in 7×10^6 approx.

Fig. 2 shows that the stability of the interferometer was on the whole very good, the same change during the day is shown both by the atmospheric lines and by the neon lines, at its worst on 1946 September 15, the rate of change of plate separation was only 1 part in 2×10^6 per hour. The atmospheric temperature and pressure will of course affect the optical path length, but for this day the estimated change in path length due to atmospheric conditions was only of the order 2 in 10^9 over the whole set of solar exposures. A slow change in $2t$ may, however, also arise from the mechanical effects of temperature and pressure on the interferometer springs. Our experimental arrangements do not provide for the simultaneous exposure of neon and solar spectra, and the systematically higher values for $2t$ given by the neon lines no doubt arises on this account.

The difference agrees with the effect observed by Burns and Meggers (**5a**) for non-simultaneous exposure of the Sun and neon lamp.

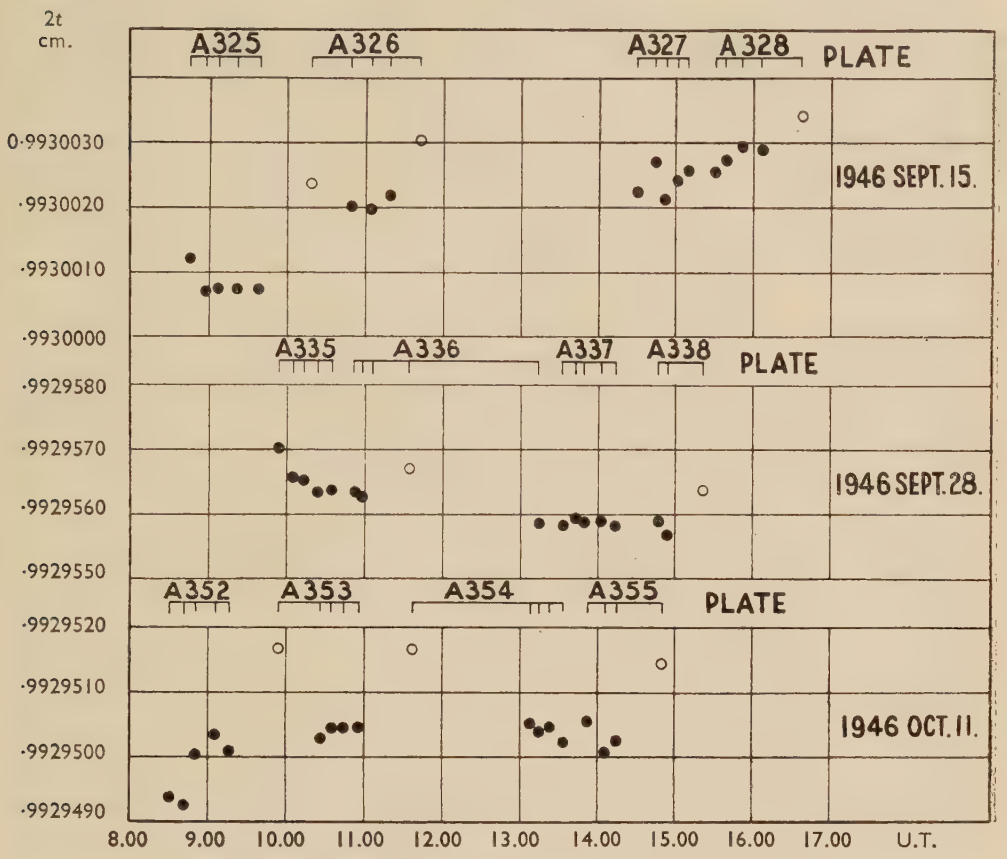

FIG. 2.—*Interferometer path length (2t) deduced from standard lines.*

Filled circles : Oxygen lines.
Open circles : Neon lines.

These continuous observations of the atmospheric oxygen lines during three days give further evidence of their suitability for wave-length standards. Fig. 2 demonstrates that for the rather low altitude Sun now used, there is no effect attributable to a systematic change in wave-length during the day such as might be feared for atmospheric lines (**21**). The individual $2t$ values for each of the 10 lines showed no outstanding discrepancies, nor was there evidence of a correlation between the $2t$ values and position on the solar disk. Wave-lengths in each solar spectrum were therefore based on the interferometer plate separation given by the atmospheric oxygen lines within the spectrum. The wave-lengths obtained refer to standard atmospheric conditions; close to the oxygen standards the solar wave-lengths are automatically corrected to the standard conditions of temperature and pressure, and the corrections to the observed wave-lengths for atmospheric dispersion over the small wave-length range from the solar lines to the oxygen standards were found to be negligible. No correction for the phase change at metallic reflection as a function of wave-length has been made, but this is probably also negligible over the short wave-length range with which we are concerned.

Corrections for the rotation of the Earth and for the orbital motion were applied to the measured wave-length for each solar line, corresponding to the time at which the spectrum was obtained. The velocity correction V for the rotation of the Earth was calculated from $V = 0{\cdot}464 \sin H \cos\delta \cos\phi$ km./sec. in which H is the hour angle of the Sun, δ its declination and ϕ the latitude of observation (51° 46′ N.). The maximum correction was 0·253 km./sec. recession at $16^h\ 09^m$ on 1946 September 15. The correction for the orbital motion of the Earth was derived directly from the decrease in the radius vector given in the *Nautical Almanac*: the maximum correction was 0·500 km./sec. approach on 1946 September 28.

TABLE III

Mean observed wave-lengths (centre) and comparisons

El.	Int.	Centre Obs. Wave-length	Prob. error	I.A.U. 1928 Wave-length	St. John	Bab-cock	A.O.–B.S.	Vac. arc* Wave-length
Mn	6	6013·493	±·0005	·497	...	·497	·497	·490
Mn	6	6016·643	±·0006	·647	...	·648	·646	·638
Mn	6	6021·798	±·0006	...	...	·803	·800	·791
Fe	7	6024·062	±·0006	·068	·068	·068	·069	·060
Fe	4	6027·058	±·0003	·059	·060	·058	·058	·048
Fe	3	6042·099	±·0007	·104	·104	·103	·104	·091
Fe	5	6056·007	±·0003	...	·012	·014	·005	·004
Fe	7	6065·490	±·0006	·494	·493	·494	·495	·483
Ni	6	6108·122	±·0003	...	...	...	·120	·121
Ca	10	6122·222	±·0005	·226	...	·226	·226	·216
Fe	6	6200·318	±·0007	·321	·321	·321	·320	·313
Fe	6	6219·285	±·0006	·287	·288	·288	·286	·282
Fe	5	6265·140	±·0006	·141	·143	·141	·138	·130
Fe	3	6270·229	±·0006	·231	·230	·232	·231	·229

* Vacuum arc wave-lengths are from the following sources: *Iron*, Burns and Walters (**5b**), direct measurements except λλ 6270·2, 6200·3 which are computed values (checked observationally). *Calcium*, Burns, Kiess (**2b**, page 79). *Nickel*, Kiess (**10**). *Manganese*, Burns, Kiess (**2b**, page 80).

Observed wave-lengths. Centre values.—The wave-lengths determined for the selected lines at the centre of the solar disk are given in Table III, column 3. The tabulated value is the mean from 11 spectra (4 on September 15 and October 11 and 3 on September 28), the probable error (column 4) of the mean value, as far as accidental errors are concerned, is for every line less than 0·001 A. Columns 5, 6, 7, 8 of Table III are from the I.A.U. Table (**2a**). The mean difference for the 11 lines in common from the I.A.U. values in column 5 is −0·0033 A. The present wave-lengths are essentially based, through the oxygen lines, on the neon scale of wave-lengths (**3b**), St. John's and Babcock's measurements in columns 6 and 7 of Table III are based on iron arc standards, the Allegheny Observatory—Bureau of Standards values in column 8 refer to direct comparisons with neon standards simultaneously exposed, and it is of some interest to compare with these measurements in particular. The mean difference of the present values from the A.O.—B.S. values is −0·0020 A.; this agreement in absolute values is on the whole satisfactory, and it is difficult to point with any certainty to the origin of the slight systematic difference. The A.O.–B.S. values for the 10 atmospheric lines used

as standards are all within 0·001 A. of the values in Table I, and the mean difference is only 0·0001 A., so that the two series of measurements are undoubtedly on the same scale. The outstanding difference between the two investigations is that our present values for solar lines refer to a small area at the centre of the disk, and the A.O.–B.S. values refer to the integrated disk. The slight violet shift found from the A.O.–B.S. values is in agreement with the statement in the I.A.U. Report 1932 (**2b**) on this question, a violet shift of 0·002 A. is there quoted for lines of Rowland Intensity 3, 4, 5 at λ 4600, for centre – integrated disk wave-lengths.

For comparison of the solar wave-lengths with laboratory values the vacuum arc wave-lengths of the lines are given in column 9 of Table III. The mean value Sun (centre)—vacuum arc for the 14 lines is $+0{\cdot}0050$ A. $\pm 0{\cdot}0006$ (p.e.); for the 9 iron lines it is $+0{\cdot}0053$ A.

Wave-lengths observed across the disk.—It is an essential feature of this investigation that the wave-lengths measured at each disk position are absolute, and independent of the measures at the centre, or any other disk position. The difference between a solar absolute wave-length and the laboratory wave-length we shall denote by Δ, and express the values in 1/1000 A. Δ_θ refers to λ Sun–λ laboratory for a point on the solar disk where the line of sight makes an angle θ with the normal to the solar surface. The "observed" Δ is then λ Sun–λ vacuum arc, and the values of observed Δ for the individual lines are given in Table IV. For all disk positions except the centre (Δ_0 is the mean of 11 values), each observed Δ is the mean of six observations, three for the disk position N. of the equator, and three for the same position S. of the equator. There is no evidence of systematic differences of behaviour across the disk with line strength, element, or Δ_0, and no justification for more than a statistical treatment of the present material. The wave-length shift henceforth used at each disk position is therefore the mean value for all 14 lines. The mean observed Δ for each disk position is given at the foot of Table IV, with the probable error of the mean deduced from the scatter of the tabulated values.

The $\sin\theta$ value corresponds to the centre of the guiding disk hole, the maximum range in $\sin\theta$ across the hole is $\pm 0{\cdot}016$, and the corresponding range in $\cos\theta$ is given with the $\cos\theta$ values. No attempt is made to estimate the uncertainty in $\sin\theta$ and $\cos\theta$ due to errors in guiding and "seeing" during exposures. The mean values of Table IV are shown graphically in Fig. 3, with the probable errors in Δ and the range in $\sin\theta$ indicated. We may compare the absolute wave-lengths at the limb now observed with the results obtained by Evershed (St. John's measures do not refer to this wave-length region). Evershed (**6b**) finds an observed Δ of 25 at $\sin\theta = 0{\cdot}98$ for 5 Fe lines of mean Rowland Intensity 8, which is about twice the value found in this investigation. Fig. 3 shows, however, that the red shift varies so rapidly near the extreme limb, that there is little to be gained from comparison of observations at a single disk position.

For the general form of the observed Δ, θ curve we may make comparison with the results of Evershed (**6a**) and Freundlich, Brunn and Brück (**8**), for limb effect. Limb effect comes from a differential measure, and in the present terminology corresponds to observed Δ_θ–observed Δ_0; for the purpose of comparison with Fig. 3 we have assumed for these two series of results the observed Δ_0 now measured. The form of the present curve agrees well with that of Freundlich, Brunn and Brück (see Fig. 4) and the differences from Evershed's curves suggests that the observed relation depends upon resolution on the solar disk. Evershed's results were obtained with the spectroscope slit diametrically across a 14 mm.

TABLE IV

Mean observed shifts (Δ) for individual lines

Disk Position			Centre	6	5	4	3	2	1
Sin θ			0·000	0·577	0·769	0·884	0·918	0·959	0·984
Cos θ			1·000 (1·000, 1·000)	0·817 (0·805, 0·828)	0·639 (0·619, 0·658)	0·468 (0·436, 0·498)	0·398 (0·357, 0·434)	0·282 (0·219, 0·333)	0·181 (0·000, 0·255)
Wave-length	El.	Int.	Δ_0	Δ_θ	Δ_θ	Δ_θ	Δ_0	Δ_θ	Δ_0
6013·5	Mn	6	+2·8	+ 3·8	+3·3	+ 4·2	+ 4·3	+ 5·0	+11·2
6016·6	Mn	6	+5·1	+ 5·8	+3·8	+ 5·0	+ 6·3	+ 9·8	+12·3
6021·8	Mn	6	+6·5	+ 7·0	+6·0	+ 7·5	+ 7·0	+10·0	+14·2
6024·1	Fe	7	+2·5	+ 1·5	+ 4·0	+ 2·8	+ 4·5	+ 7·7	+ 9·0
6027·1	Fe	4	+ 9·6	+ 8·7	+ 8·8	+ 7·0	+ 11·8	+14·7	+16·8
6042·1	Fe	3	+7·6	+ 9·3	+9·5	+11·3	+11·0	+13·2	+18·5
6056·0	Fe	5	+2·5	+ 3·5	+3·0	+ 3·5	+ 6·0	+ 7·3	+ 11·5
6065·5	Fe	7	+ 7·2	+ 7·8	+7·8	+ 9·7	+10·2	+12·0	+ 14·5
6108·1	Ni	6	+1·3	− 0·3	−0·7	+ 1·3	+ 2·7	+ 3·0	+ 8·3
6122·2	Ca	10	+6·3	+ 7·5	+7·3	+ 9·5	+10·7	+11·2	+14·0
6200·3	Fe	6	+5·5	+ 5·7	+ 7·3	+ 7·2	+ 6·8	+10·5	+ 13·8
6219·3	Fe	6	+3·2	+ 3·8	+4·7	+ 2·8	+ 7·0	+ 7·8	+10·8
6265·1	Fe	5	+9·8	+10·3	+9·0	+10·0	+12·2	+12·2	+19·2
6270·2	Fe	3	+ 0·4	+ 0·3	−0·7	+ 0·5	+ 0·3	+ 3·2	+ 7·0
Mean Δ			+ 5·0	+ 5·3	+ 5·2	+ 5·9	+ 7·2	+ 9·1	+ 12·9
prob. error			± 0·5	± 0·6	± 0·6	± 0·6	± 0·6	± 0·7	± 0·7

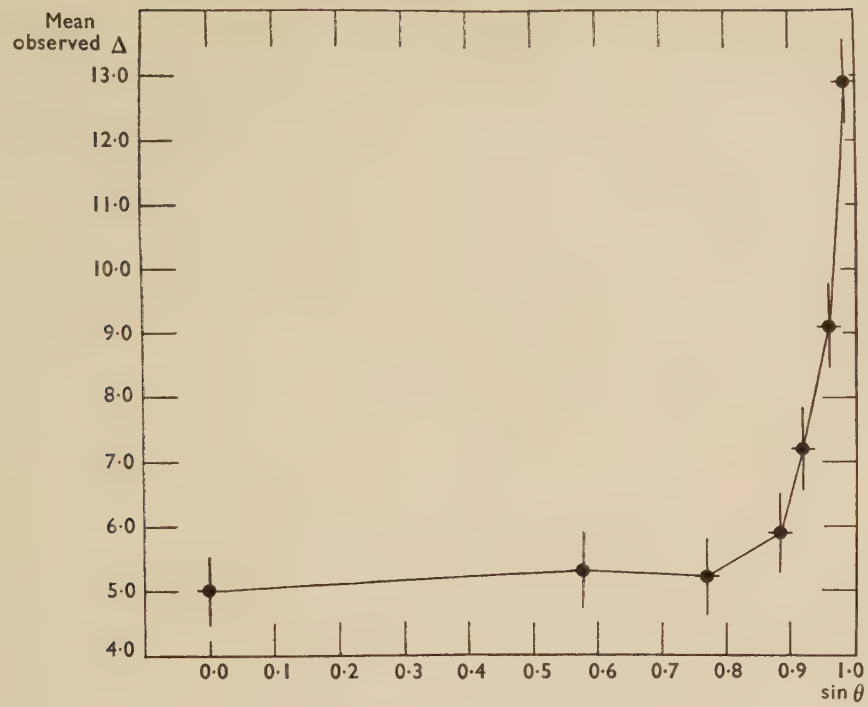

FIG. 3.—*Mean observed Δ as a function of disk position.*

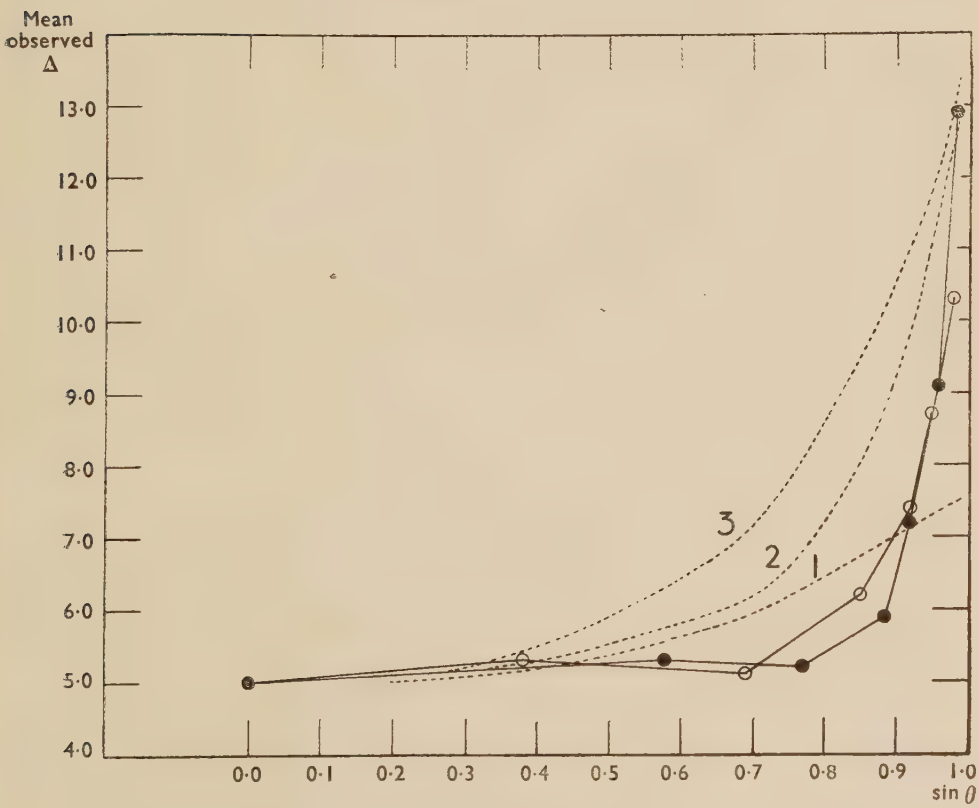

FIG. 4.—*Comparison of wave-length change across the disk with the results of other observers.*

● *Present values* λ 6100 14 *lines. Mean Int.* 6.
○ *Freundlich, et al.* λ 4420. 9 *Fe lines. Mean Int.* 3. (*All radii.*)
----- (1) *Evershed* λ 3930. 2 *lines Fe* 8.
----- (2) *Evershed* λ 6300. 3 *Fe lines. Mean Int.* 5.
----- (3) *Evershed* λ 4385. 2 *lines* Fe^+, Ti^+. *Mean Int.* 1·5.

solar image, the measures of Freundlich, Brunn and Brück were made with an image 130 mm. diameter, the present measures with an image 180 mm. diameter, and the larger images enable greater resolution to be obtained. The present resolution and that of Freundlich, Brunn and Brück are probably comparable, but even this is still lower than could be desired in view of the rapid increase in wave-length at the limb. The increase may well occur within an even more limited range on the disk, and achieve much higher values. The measures of Freundlich, Brunn and Brück show little variation in the wave-length–disk position relation with position angle of the solar radius along which observations are made, in particular their curves for a polar and equatorial diameter are practically the same. The comparison of their curves with the present results shows further that there is no significant change in the form of the relation with time, or with wave-length region in the solar spectrum.

III. *Theoretical Interpretation of Observed Wave-lengths*

Corrections to observed wave-lengths for physical conditions in the Sun.—The observed solar wave-lengths have so far been compared with vacuum arc values, but the Sun and the vacuum arc are not strictly equivalent sources. Before investigating hypotheses to account for differences between solar and terrestrial wave-lengths, we must allow for such shifts as are produced by well-established effects associated with the differences in the physical conditions in the two sources. Differences between solar and laboratory wave-lengths will arise in two ways; first, the spectrum at one level in the reversing layer may subsequently be modified in transmission through the solar atmosphere by effects such as anomalous refraction, Rayleigh scattering and electron scattering; and secondly, the frequency of an oscillator may be affected by the presence of other atoms through collisions, or the interaction of atomic fields. Now in view of the present estimates of conditions in the reversing layer (**18a**), hydrogen more than 10^3 times more abundant than the metals, total gas pressure 10^{-2} atmospheres, and electron pressure 10^{-6} atmospheres, the first group of processes cannot give rise to measurable effects. We must conclude that the outflowing radiation is subject only to selective absorption and re-emission, and at this stage we are only bound to consider the shifts in the frequency of an atom due to the influence of other particles.

Lindholm shift.—At the low pressures prevailing in the solar atmosphere and in the presence of Van der Waals' forces there will be no statistical broadening, and no displacement of the centre of gravity of solar lines through asymmetry. Further, collisional broadening, as first proposed by Lorentz and re-interpreted by Lenz and Weisskopf, does not give rise to line displacements. However, Weisskopf's theory contains an arbitrary assumption that only those collisions need be considered, in which the perturbing atom changes the frequency of the emitted radiation by such an amount that the phases of the wave emitted before and after collision differ by unity. This arbitrary limitation has been removed in a recent discussion by Lindholm (**11**), who shows that when all possible collisions are taken into account, namely those which produce phase changes less than unity, as well as those producing phase changes greater than unity, the emitted line will show the ordinary Weisskopf collisionally-broadened profile, and will be bodily displaced to the red by an amount in frequency units of $0{\cdot}36\gamma$, where γ is the collisional damping constant.

ten Bruggencate and Houtgast (**19**) have recently determined damping constants for a number of iron lines in the solar spectrum as a function of position on the disk. From their values, shown below, we may compute the Lindholm red shift, and the values so obtained may be applied to our measures, since their determinations were for lines of mean Rowland intensity 5 and the mean Rowland intensity of our 14 lines is 6.

Cos θ	1·0	0·20	0·14
γ (sec.$^{-1}$)	$0{\cdot}83\times10^{10}$	$0{\cdot}36\times10^{10}$	$0{\cdot}26\times10^{10}$
Lindholm shift	0·0041 A.	0·0018 A.	0·0013 A.

ten Bruggencate and Houtgast show that for the three disk positions observed the change in γ agrees with the values calculated for collisions with hydrogen atoms in a Strömgren (**18b**) atmosphere. In order to interpolate values for the Lindholm red shift for points between $\cos\theta = 1{\cdot}0$ and $\cos\theta = 0{\cdot}14$, we use their deduced relation

$$\log\frac{\gamma_\theta}{\gamma_0} = \log\frac{p_\theta}{p_0} + \frac{7}{40}\log\frac{1+1{\cdot}5\tau_0}{1+1{\cdot}5\tau_\theta},$$

where p_θ is the gas pressure and τ_θ the optical depth corresponding to disk position θ, and p_0, τ_0 refer to the centre. Using Strömgren's Table 14 for $\log A = 3{\cdot}8$ (A is the hydrogen/metal ratio) we can calculate γ_θ as a function of τ. We then relate τ and θ, by assuming as ten Bruggencate and Houtgast do, that τ is the mean optical depth in the continuous spectrum as given by Unsöld (**20**) for angle θ. The resulting calculated Lindholm shifts applicable to the solar lines at each disk position are given in column 3 of Table V.

The laboratory vacuum arc lines are very much narrower than the corresponding solar lines, as may be seen from Burns and Meggers' spectra with the iron vacuum arc lines photographed simultaneously within the solar lines (**5a**). We may further note that Burns and Walters' vacuum arc wave-lengths for iron lines agree well with the echelon measures of Williams and Middleton (**22**), and for the latter lines, obtained from a Schuler tube, we can estimate a width probably less than $\frac{1}{10}$ of the corresponding solar lines. We assume then, that for the laboratory vacuum arc lines the Lindholm shift is negligible.

When the Lindholm shift is allowed for in the solar lines, we are left with what we have called "residual Δ" in column 4 of Table V. These shifts we assume refer to equivalent sources on the Sun and on the Earth, and it is for these residual values of Δ that we must find a theoretical interpretation.

TABLE V

Mean line shifts for radial velocity calculations

Cos θ	Mean obs. Δ	Lindholm shift	Residual Δ	Velocity shift and p.e.	Velocity v_θ km./sec.
1·000	5·0	4·1	0·9	−12·0±0·5	·588±·026
·817	5·3	3·8	1·5	−11·4±0·6	·559±·029
·639	5·2	3·4	1·8	−11·1±0·6	·544±·029
·468	5·9	2·9	3·0	− 9·9±0·6	·485±·031
·398	7·2	2·6	4·6	− 8·3±0·6	·407±·032
·282	9·1	2·1	7·0	− 5·9±0·7	·289±·032
·181	12·9	1·5	11·4	− 1·5±0·7	·074±·032

Einstein effect and radial currents.—St. John's is the only theory nowadays remaining to account for the wave-length shifts of solar lines and we shall investigate the consequences of adopting his Einstein-radial current hypothesis. The Einstein red shift at $\lambda 6100$ is 0·0129 A., and we allow for this by subtracting 12·9 from the residual Δs. The resulting violet shifts given in column 5 of Table V, on St. John's theory are assumed to be due to radial currents and so are expressed in km./sec. in column 6. These line of sight velocities v_θ are shown as filled circles in Fig. 5; the vertical and horizontal lines through each point show respectively the probable error in v_θ (due to errors in wave-length measurement) and the uncertainty in $\cos\theta$ resulting from the diameter of the aperture which admitted light from the solar disk to the interferometer (*cf.* Section II). If the hypothetical radial currents had the same velocity at all optical depths and therefore at all values of θ, the observed line of sight velocity would show a linear dependence on $\cos\theta$. McCrea and Mitra (**12**) have, however, pointed out, that from the equation of continuity the radial velocity will vary inversely as the density, and since we see to smaller optical depths near the limb, the line of sight velocity may be expected to show a variation similar to that given in Fig. 5.

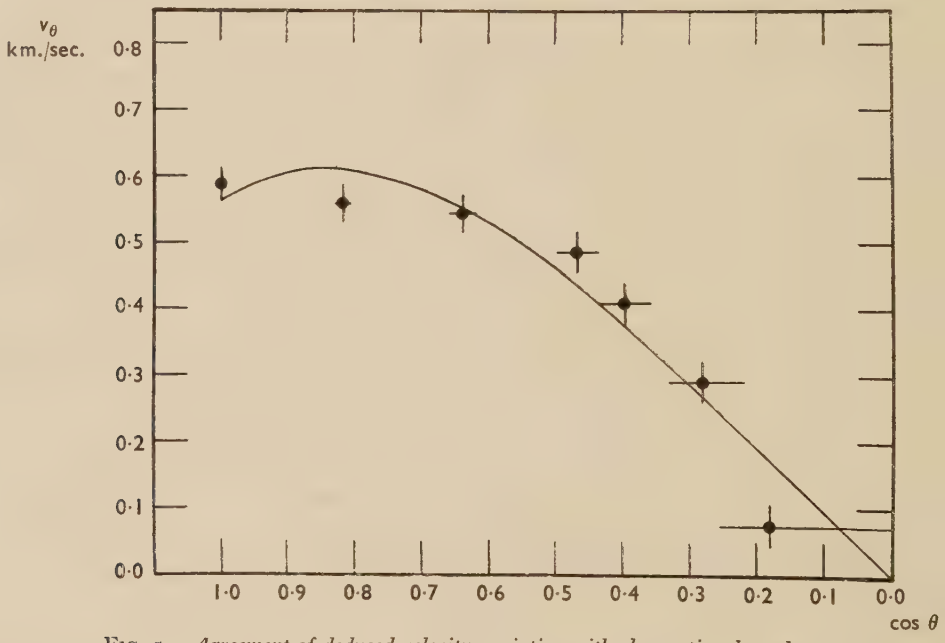

FIG. 5.—*Agreement of deduced velocity variation with observational results.*

For an Eddington model atmosphere Mitra (**14**) has derived the following expression for v_θ:

$$v_\theta = \frac{\int_0^\infty \omega(\tau) e^{-\tau \sec\theta} \cos\theta \, d\tau}{\int_0^\infty e^{-\tau \sec\theta} \, d\tau}, \qquad (1)$$

where $\omega(\tau)$ is the velocity of the assumed radial currents at optical depth τ. If for simplicity we represent the function $\omega(\tau)$ as a power series in τ,

$$\omega(\tau) = a + b\tau + c\tau^2 + \ldots,$$

equation (1) gives $v_\theta = a\cos\theta + b\cos^2\theta + 2c\cos^3\theta + \ldots$, and we can use our observed v_θ to solve for the constants a, b, c .... Taking the second order expression and giving all the observational equations equal weight, a least squares solution for a, b and c leads to the values:

$$v_\theta = 0{\cdot}858\cos\theta + 0{\cdot}559\cos^2\theta - 0{\cdot}853\cos^3\theta \qquad (2)$$

and

$$\omega(\tau) = 0{\cdot}858 + 0{\cdot}559\tau - 0{\cdot}426\tau^2, \qquad (3)$$

both v_θ and $\omega(\tau)$ being expressed in km./sec. The v_θ given by equation (2) is shown in Fig. 5; it will be seen that the curve is in good agreement with the observed values, considering their estimated uncertainty.

Fig. 6 shows the variation of the velocity $\omega(\tau)$ of the hypothetical currents with optical depth given by equation (3). The velocity decreases rapidly with optical depth, as we should expect from the equation of continuity. We see also that radial current velocities of the order of 1 km./sec. are reached in the small optical depths where the absorption lines may be assumed to arise. This hypothetical velocity is four times larger than that required by St. John. The higher values are a result in part of the fact that our measured solar wave-lengths show a violet displacement with respect to his, and in part of the correction for the recently discovered Lindholm effect.

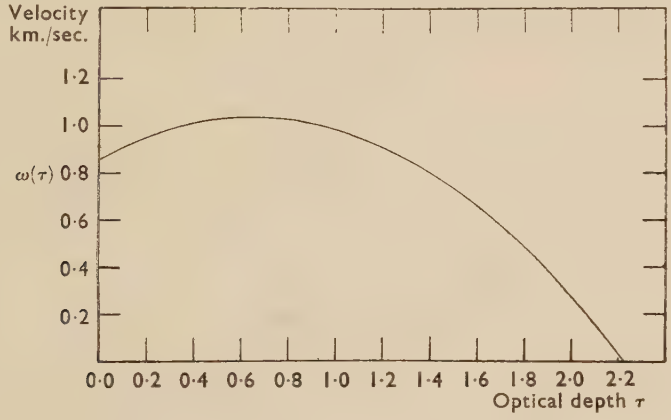

FIG. 6.—*Variation of velocity with optical depth deduced from* v_θ.

Interpretation of the radial velocities deduced.—We must now consider from what movement of the material of the solar atmosphere these hypothetical velocities, deduced from the observed absorption lines, could arise. It is clear that we cannot assume that the Sun is continuously losing matter at this rate, since it is more than 100 times smaller than the velocity of escape. Material that is observed to be rising must somewhere and somehow be returning. The possibility that there exists a large scale circulation in the solar atmosphere, of which we have observed a part, is ruled out by the fact that Freundlich, Brunn and Brück find practically the same limb effect over the whole of the disk. From this we are bound to conclude that the steady state, with as much material rising as falling, is maintained at each disk position and at each level in the atmosphere. Now we have observed only outward velocities, and it is possible that the downgoing material is represented by unobserved lines. If this were so we should

expect that the material going downwards from the cooler higher layers of the Sun, would be represented by low excitation potential lines of neutral atoms, while the upgoing material from the hotter lower layers would be indicated by the higher excitation potential lines, and by the lines of ionized atoms. But among lines of comparable intensity (presumably representing the same atmospheric level) there is no evidence of differential effects in the (centre) red shift with excitation potential, nor (but the observational evidence is less certain) between lines of ionized and neutral atoms. The only observational evidence which on the radial current hypothesis has been interpreted as indicating downward motion in the solar atmosphere, is for some of the stronger (high level) lines; but this would not give the required steady state at each atmospheric level, and would in fact lead to the impossible conclusion that there was an accumulation of material at a certain level.

We can then only conclude that the steady state is maintained by a microscopic circulation, and that the v_0 is a mean value of microscopic upgoing and downgoing streams. If, as seems reasonable, we associate this circulation with solar granulation, we can estimate the actual upgoing and downgoing velocities as follows. Assuming cellular flow, if at any level the granule of surface brightness J_1 occupies an area a_1 over which the upward velocity is v_1 and J_2, a_2, $-v_2$ are the corresponding quantities for the intergranular region at the same level, and if the spectra over a_1 and a_2 differ only in brightness, then the mean velocity $\bar{v}$ deduced at that level will be given by

$$\bar{v} = \frac{J_1 a_1 v_1 - J_2 a_2 v_2}{J_1 a_1 + J_2 a_2}.$$

If there is no accumulation of material at the level $\rho_2 v_2 a_2 = \rho_1 v_1 a_1$ and if the two streams are in pressure equilibrium laterally $\rho_2 T_2 = \rho_1 T_1$, where ρ_1, T_1 and ρ_2, T_2 are the densities and temperatures in the two streams. Taking (**15**) $J_1/J_2 = 1{\cdot}10$, $T_1/T_2 = 6100/6000$, and assuming $a_1 = a_2$ we find $v_1 = 18{\cdot}0\bar{v}$ and $v_2 = -17{\cdot}7\bar{v}$. Thus for our centre value of $\bar{v} = 0{\cdot}588$ km./sec. we find $v_1 = 10{\cdot}6$ km./sec., $v_2 = -10{\cdot}4$ km./sec., while for the higher τ levels (Fig. 6) we deduce $v_1 = 18{\cdot}0$ km./sec., $v_2 = -17{\cdot}7$ km./sec. Such large velocities are obviously unreal, the thermal velocity of hydrogen atoms at 6000 deg. Abs. is only 12 km./sec., and moreover the resulting absorption lines (at $\lambda 6000$) should show a red and violet broadening of 0·36 A. (corresponding to 18 km./sec.), whereas the turbulent velocities deduced from the contours of solar lines are only of the order 1·6 km./sec. There is at present no observational justification for modification of this interpretation of the hypothetical radial velocities deduced, so as to avoid these impossibly large stream velocities.

Conclusions.—St. John's radial current hypothesis when thus carefully examined on the basis of the present observational material leads to results which are inconsistent both with our knowledge of the solar spectrum and of the physical conditions prevailing in the solar atmosphere. If we assume that the solar lines do suffer an Einstein gravitational displacement, then we must find some mechanism other than radial currents which will effectively neutralize this displacement over 80–90 per cent of the solar disk, and yet leave the full Einstein shift near the limb. If on the other hand we assume that the solar lines show no gravitational displacement, we must find some mechanism which produces a reddening of solar lines of approximately the amount predicted by Einstein

but only near the limb of the Sun. There are obviously here problems which demand close theoretical investigation.

On the observational side the evidence is clearly incomplete. In particular it is of importance to determine absolute solar wave-lengths with high resolution on the disk much closer to the extreme limb of the Sun. The present observations suggest (Fig. 3), as Evershed finds, that the value of Δ for $\cos\theta < 0{\cdot}25$ is greater than the predicted Einstein red shift. If this proves generally to be the case, a choice between the alternative hypotheses mentioned above would be simpler. In addition it is equally important to determine absolute solar wave-lengths at the centre of the disk as a function of wave-length, line intensity, and state of excitation and ionization of the atoms. Earlier observations have revealed numerous anomalies, and until the observational data are more certain it will be impossible to find an adequate theoretical interpretation of solar wave-lengths. It is proposed to make investigations along these lines in the immediate future at Oxford; in view of the nature of the measures, it is clearly an observational problem in which similar independent investigations would prove most valuable.

Acknowledgments

In the computation of wave-lengths from measured ring diameters I have been most fortunate in having the assistance of Miss A. B. Hart and Miss S. M. Curtis (both of Somerville College). Their excellent work has considerably advanced the date of completion of the investigation. I should also like to thank Dr D. A. Jackson for the loan of the interferometer. Finally, to Professor Plaskett I am deeply indebted for advice and assistance at every stage of the work, and especially in the theoretical considerations and exposition of Section III.

University Observatory,
Oxford :
1948 *December* 1.

References

(1) *Revision of Rowland's Preliminary Table*, Mount Wilson, 1928.
(2a) *Trans. I.A.U.*, **III**, 93, 1928 (Table 4).
(2b) *Trans. I.A.U.*, **IV**, 62, 1932.
(2c) *Trans. I.A.U.*, **V**, 86, 1935.
(3a) H. D. Babcock, *Ap. J.*, **55**, 36, 1922.
(3b) H. D. Babcock, *Ap. J.*, **65**, 147, 1927.
(3c) H. D. Babcock, *Ap. J.*, **66**, 256, 1927.
(3d) H. D. Babcock, *P.A.S.P.*, **51**, 222, 1939.
(4a) K. Burns, *J.O.S.A.* and *R.S.I.*, **7**, 419, 1923.
(4b) K. Burns, *J.O.S.A.*, **20**, 216, 1930.
(5a) K. Burns and W. F. Meggers, *Pub. Alleg. Obs.*, **6**, Nos. 7, 8, 9, 1927.
(5b) K. Burns and F. M. Walters, Jr., *Pub. Alleg. Obs.*, **6**, No. 11, 1929.
(6a) J. Evershed, *M.N.*, **91**, 260, 1931.
(6b) J. Evershed, *M.N.*, **96**, 152, 1936.
(7) E. F. Freundlich, *Naturwissenschaften*, **18**, 513, 1930.
(8) E. F. Freundlich, A. v. Brunn and H. Brück, *Z. f. Ap.*, **1**, 43, 1930.
(9) A. Hunter, *M.N.*, **94**, 594, 1934.
(10) C. C. Kiess, *B.S.R.P.*, No. 4, 1928.
(11) E. Lindholm, *Arkiv. f. Mat., Astr. och Fys.*, **28**B, No. 3, 1941. Diss. Uppsala, 1942.
(12) W. H. McCrea and K. K. Mitra, *Obs.*, **57**, 379, 1934.

(13) K. H. Meissner, *J.O.S.A.*, **31,** 405, 1941; **32,** 185, 1942.
(14) K. K. Mitra, *Obs.*, **59,** 160, 1936.
(15) H. H. Plaskett, *M.N.*, **96,** 415, 1936; *Comm. U.O.O.*, No. 6.
(16) C. E. St. John, *Ap. J.*, **57,** 195, 1928.
(17) C. E. St. John and H. D. Babcock, *Ap. J.*, **53,** 260, 1921.
(18a) B. Strömgren, *Copenhagen Publications*, No. 127, 1940.
(18b) B. Strömgren, *Copenhagen Publications*, No. 138, 1944.
(19) P. ten Bruggencate and J. Houtgast, *Z. f. Ap.*, **20,** 149, 1940.
(20) A. Unsöld, *Physik der Sternatmosphären*, 95, 1938.
(21) H. C. van de Hulst, *Ann. Ap.*, **8,** 1, 1945.
(22) W. E. Williams and A. Middleton, *Proc. Roy. Soc.* A., **172,** 159, 1939.

ON THE ORIGIN OF COMETS

R. A. Lyttleton

(Received 1948 November 27)

Summary

During the passage of the Sun through a cloud of interstellar dust the particles converge to the accretion axis where their transverse velocities are destroyed by collisions. A stream of dust forms at the axis, and for low relative speed of the Sun and cloud that part of the stream within several hundred astronomical units is captured and flows towards the Sun. Internal gravitation causes the stream to divide into separate segments that contract lengthwise. The resulting aggregations are identified with the comets. The disruptive field of the Sun sets an upper limit to the initial length of a segment and thence to the initial mass of a comet. Several thousand such comets could result from a single passage of the Sun through a cloud of moderate dimensions. Owing to the presence of the major planets, some aggregations would have enough angular momentum to avoid falling directly into the Sun, but their initial orbits would be almost line-ellipses. Subsequent perturbations by passing stars when a comet is at great distance may endow it with greater angular momentum, but for it to have sufficiently small perihelion distance to become visible, the perturbed orbit must still be nearly parabolic. Earlier ideas relating to the origin of comets are briefly discussed.

---

1. *Introduction.*—Whereas a large number of speculations and hypotheses have been put forward during the past two centuries with a view to explaining the origin of the planets, and many of them investigated in detail, hypotheses on the origin of comets have been few and these mainly of so vague a nature that detailed examination of them has scarcely been practicable. It appears to have been widely accepted on general grounds that the planets and comets do not demand a common explanation, their properties being so markedly antithetical in almost all respects, but whether or not there is an essential cosmogonical difference is a question that can only finally be settled when dependable theories of the origin of both planets and comets are available. As far as the hypotheses on which recent progress with the planetary problem has been based are concerned, these have thrown no light whatever on the origin of comets, and it is difficult to imagine any development of them that could do so. The present paper has for its object an attempt to fill this gap in the theory of the solar system by giving an account of what seems to be a satisfactory mechanism for the formation of comets. The process proposed is, in brief, that of accretion of interstellar dust by the Sun during its passage through a dust cloud and the development from this material of more or less compact masses, composed of dust particles, describing almost parabolic orbits. It will be convenient to give first a general qualitative description of how it is considered the process would operate.

2. *General Description of the Process.*—Suppose the Sun to approach and enter a dust cloud whose particles for simplicity are assumed to be distributed uniformly in it with a common velocity relative to the Sun both in magnitude

and direction. The line through the centre of the Sun parallel to the direction of motion of the cloud defines the so-called accretion axis, and in the postulated conditions every particle will describe a hyperbolic orbit intersecting this axis. Thus even if, when undisturbed, the cloud is of extremely low density, the gravitational action of the star will cause its particles to converge towards the axis and thereby bring about a strong probability of collisions of some of them occurring at and near the axis. At a collision of two particles a portion of their kinetic energy of relative motion will be transformed into internal energy and heat the material. If they came originally from points on directly opposite sides of the accretion axis and in a plane with it, they would at impact have the same radial component velocity along the axis but equal and opposite transverse components, and only these would give them relative velocity. If the particles were of the same mass, and inelastic, as would be practically the case for dust particles, then in a head-on collision the whole of the kinetic energy of relative motion would be transformed into heat, and the velocity of the combined mass would be simply the former common radial component along the axis. As the radial and transverse components are comparable for a range of positions on the axis, an impact of this kind, by destroying the transverse component, could reduce the velocity to an elliptic value, so that the particles would be captured and thereafter move along the axis.

Instead of just two particles coming from opposite directions, the actual process even in a small length of the axis will involve a large number converging from different directions. The radial component away from the Sun will be the same for every particle, and apart from this velocity the effect will thus be as if particles were converging from all directions at right angles to the axis. This situation will clearly be highly favourable for the occurrence of collisions. Also, once collisions begin and introduce a random element of particles near the axis, further collisions will become even more probable, and indeed will occur with complete certainty once material has begun to collect round the axis. It is not necessary at this point to specify the sizes of the particles, though for a given density of the cloud the effective area for collisions becomes greater the smaller the dust particles are. There is however a critical range of size, radius $\sim 10^{-5}$ cm., for which particles would be repelled from the Sun by radiation pressure. Particles outside this range of size, larger or smaller, suffer negligible repulsion. In the initial stages dust particles smaller than this critical size would be most effective in starting an accumulation of material round the axis, but once this had begun almost all particles subsequently arriving at and near the axis would be intercepted and absorbed into the general stream along it.

There is however a restriction on the process if matter in solid form is to collect, for the energy converted into heat at impact must not be so great as to vaporize the particles completely. Evidently the transverse component of velocity must not be higher than a certain amount and this means that only material converging to the axis at more than a certain distance from the Sun would remain chiefly in the solid state.

On the other hand the distance from the Sun at which it joins the axial stream must not be so great that the material flows away from the Sun altogether to be lost from the solar system.

These two opposing requirements place upper and lower limits on the distance at which accumulations of solid particles can form and still be captured by the

Sun. Provided the extent of the cloud is large compared with the linear dimensions involved in the mechanism of accretion, the process will have time to approach a steady state, and in such circumstances the investigation given by Bondi and Hoyle will be closely applicable.* Their work considers a semi-infinite cloud with a plane boundary across which a star enters orthogonally along a rectilinear path, and their assumption that temperature effects due to collisions near the axis may be neglected is obviously valid in the present problem when only the motion of the solid material is of interest. On this basis they show that the steady state involves a stream of material along the accretion axis flowing towards the Sun at all distances less than about $1{\cdot}25\,GM/V^2$ (where G = constant of gravitation, M = mass of Sun, V = relative velocity of cloud), and away from the Sun at all distances greater than this. Particles whose paths intersect the axis within this distance join the inward stream and are swept towards the Sun, and at greater distances join the outward stream and are carried away to infinity in the opposite direction.

In the idealized circumstances to which the solution accurately applies, the process clearly cannot result in aggregations in orbital motion around the Sun, since the net angular momentum of accumulations on the axis must always be zero. There are however a number of additional factors that will be present in the actual problem whose influence is to give the material of the stream angular momentum round the Sun. First, as possibly the most important, may be mentioned the feature that at large distances the attraction is directed not towards the centre of the Sun but towards the centre of gravity of the whole solar system. This point may at times be a little over two solar radii from the Sun's centre, the main displacing agency being Jupiter and to a less extent Saturn. The distances at which aggregations first form, as will be shown, are of the order of several hundred astronomical units from the Sun, so the inward flow would be directed towards the centre of gravity until the orbital distance of Saturn is approached, and the attraction would not become towards the Sun's centre until some way within Jupiter's distance. For this reason the material may come to be endowed with angular momentum about the Sun corresponding to motion at about two solar radii simply as a result of the prevailing configuration of the planetary system. The time of passage through a cloud might be many thousand years and the time of fall of material towards the Sun is shown to be as much as a few thousand years, so that suitable configurations leading to angular momentum of this order would be bound to obtain for a considerable proportion of the time.

The foregoing effect is due of course to the gravitational action of the planets, but it can produce only small angular momentum per unit mass. There is the possibility of far stronger direct disturbance by a planet if the accretion axis happens to pass near its orbit, for then sooner or later an aggregation that had not been swept into the Sun would undergo a close approach in which the influence of the planet might become comparable with that of the Sun for a time, and the body would in general thereby receive angular momentum per unit mass about the Sun comparable with that carried by the planet.

Similarly there is the possibility of deflections by passing stars, a contingency by no means negligible for the ranges of distance from the Sun likely to occur. For low relative speed of the cloud the inward stream may extend to about 1000 astronomical units from the Sun, and during 10^9 years some 50 or 60 stars

* H. Bondi and F. Hoyle, *M.N.*, **104**, 273, 1944.

will have passed within, say, ten times this distance from the Sun. Only a small perturbation at such a distance is necessary to impart considerable angular momentum about the Sun to material.

All the foregoing influences will be operative at times to prevent parts of the stream from falling directly into the Sun, and as small effects are more likely than large ones it is evident that most of the resulting orbits will be nearly parabolic.

Although its action can have no appreciable effect on the orbit of an aggregation, there is also the self-gravitation of the material of the stream to be considered. At distances sufficiently far from other matter, any accumulation of material, however small its mass, will settle into as compact a body as possible consistent with its energy and angular momentum, which in the present instance is negligibly small, since the stream is formed at the axis by collisions. Owing to chance irregularities in the stream at different points of its length, it will tend to contract lengthwise and form a number of separate pieces of finite length, but this will be hindered by the tidal action of the Sun, and the combination of the two influences sets an upper limit to the length of a segment that can form at a given distance, and hence to the initial mass of a comet. An estimate of the mass of Halley's comet has been made by H. N. Russell and there is satisfactorily close agreement of the present value with this, considering the uncertainty attached to most of the factors involved in the calculations.

3. *Conditions for Capture of Particles in Solid Form.*—According to the investigation by Bondi and Hoyle, the neutral point on the accretion axis is at approximately $1{\cdot}25\,GM/V^2$ from the Sun. This gives at once an upper limit to the distance at which comets could form and remain associated with the Sun, since beyond this the material streams away to infinity. A lower limit can be estimated as follows.

At the axis the radial component of velocity of a particle is V, so that its transverse component is always precisely the parabolic speed at the distance concerned, and at the neutral point this is $\sqrt{(8/5)}V$. The particle will therefore enter the stream here with relative speed $\sqrt{(13/5)}V$, and this must not be such as to cause complete vaporization. If a proportion f of the kinetic energy per unit mass, $\frac{1}{2}u^2$ say, is converted by collisions into thermal energy in the material of the particle, and if E denotes the energy per unit mass required to vaporize the material, the condition that it is not entirely vaporized is $u^2 < 2E/f$. Near the neutral point this requires $V < 1{\cdot}25\sqrt{E/f}$, approximately.

The factor f for any particle may depend on the way it happens to be absorbed into the stream, especially if this consists of a loose aggregation and several collisions are involved in stopping an incoming particle. Also, as far as the general effectiveness of the mechanism for forming and maintaining a stream of material is concerned, it will be sufficient if part of the material remains unvolatilized. It is therefore difficult to assess a precise value for f, but as it does not enter to a high power in the calculation the use of a value of $\frac{1}{4}$ may not lead to serious error.

As for the value of E, according to an estimate made by Hoyle* for iron, the heat of evaporation at boiling-point is about 1000 calories per gram. The dust particles, which of course will probably not consist mainly of iron, will presumably have low initial temperature, so making some allowance for the thermal energy needed to raise the material to its boiling-point, E may be roughly estimated

* F. Hoyle, *M.N.*, **106**, 410, 1946.

for dust as, say, 2000 calories per gram, or about 10^{11} ergs per gram. The upper limit to V is then about 8 km. per sec., giving a distance for the neutral point of about 17 astronomical units.

This calculation shows that if V exceeds this amount (or some comparable value, bearing in mind the uncertainties involved), then as far as material capable of being captured by the Sun is concerned, impacts will volatilize most if not all of it and therefore greatly impair the efficiency of the process for capturing material in solid form. A stream of material in the steady-state motion has been assumed to be already present, but in the initial stages, while this forms, the particles arriving at the axis will have relative speeds at least of the same order as was used in the above calculation, so the result will still apply. A limiting value of 8 km. sec.$^{-1}$ seems reasonably satisfactory from the point of view of velocities likely to occur. Studies of stellar evolution strongly suggest that most stars must at times undergo encounters with interstellar gas at relative speeds appreciably less than this, and it may be supposed that dust clouds have motions similar to those of interstellar gas.

If, for example, $V = 1$ km. sec.$^{-1}$, the range of distance R from the Sun at which material can collect in non-gaseous form and still be captured is given, in astronomical units, by

$$1100 \geqslant R \geqslant 17.$$

The upper limit for different speeds varies as V^{-2}, while the lower limit is not changed. The corresponding periods in almost parabolic motion about the Sun in orbits having these limiting distances as major axes are given approximately by

$$13{,}000 \text{ years} \geqslant \text{Period} \geqslant 26 \text{ years},$$

and here the upper limit varies as V^{-3}.

The investigation by Bondi and Hoyle shows that the precise position of the neutral point is not determinable from the steady-state conditions alone, but depends on how the steady state happens to build up, and this would depend on the configuration of the cloud. It is shown, however, that its distance from the Sun must always lie between $2GM/V^2$ and GM/V^2, so that the upper limit to distance may extend to nearly 2000 astronomical units for $V = 1$ km. sec.$^{-1}$.

4. *The Occurrence of Collisions in the Initial Stages of the Process.*—Consider an element of volume of the space of the cloud before it has reached the Sun's neighbourhood and suppose it to be of annular shape between radii p and $p + dp$ from the axis, and of small length $2b$ parallel to the axis. It need not be supposed that the cross-section of this region is rectangular. Its area will be $2b\,dp$ and the volume generated by its rotation round the axis will be $4\pi bp\,dp$. Imagine each point of this element of volume to describe the hyperbolic path that a particle initially at the point and moving with the velocity V would describe. Under such a motion of all its points the annular region will converge towards the axis and in so doing will undergo a large contraction of radius, but its other dimensions will alter only by small factors. Thus for large values of p enormous compression of volume will occur. To calculate its amount: A point of the original volume that crosses the axis at distance R from the Sun has transverse speed $\sqrt{(2GM/R)}$ and hence its initial perpendicular distance from the axis is

$$p = \sqrt{(2GMR)}/V.$$

Thus a length dR on the axis corresponds to an initial difference in distance from the axis of amount

$$dp = \sqrt{(GM/2R)}\, dR/V.$$

In calculating the shape and volume that the original element takes up near the axis the common radial velocity component V can be ignored and the points regarded as approaching the axis at right angles. Near the neutral point (to take some definite distance) the transverse speed will be $\sqrt{(8/5)}V$ and the separation $2b$ will have changed to $2\sqrt{(8/5)}b$. Thus, as far as the question of collisions is concerned, the original volume will at its smallest be compressed effectively to a circular cylinder of radius $\sqrt{(8/5)}b$ and length dR surrounding the axis, and the least volume is effectively $8/5\pi b^2\, dR$. If the original volume $4\pi bp\, dp$ contained the centre of one particle only, then collisions will certainly occur at the axis if this reduced volume element is less than the effective volume of the particle. Taking it as a sphere of radius r, and its centre as being anywhere in the small element of volume at the axis, the conditions that it shall not overlap any other particle near the axis are

$$dR \geqslant 4r \qquad \text{and} \qquad \sqrt{(8/5)}b \geqslant 2r.$$

Using the values given by adopting the equals signs, it is found that

$$4\pi bp\, dp = 8\pi\sqrt{10}GMr^2/V^2.$$

Collisions will therefore occur if this volume originally contained more than one particle of the adopted size. If ρ is the density of the cloud and σ that of the material of the particles, then the average volume per particle will be $4\pi r^3\sigma/3\rho$, and for collisions to occur with certainty for every particle this must be less than the above value. Taking $\sigma = 3$ gm. cm.$^{-3}$ and writing $V = 10^5 v$ cm. sec.$^{-1}$, so that v is the speed in kilometres per sec., the condition becomes

$$\rho > 10^{-17} v^2 r \text{ gm. cm.}^{-3}.$$

For example, if $r = 10^{-7}$ cm. and $v = 1$ km. sec.$^{-1}$, then collisions will occur for every particle from the outset if $\rho > 10^{-24}$ gm. cm.$^{-3}$.

In an actual cloud the particles would not have uniform sizes and shapes, and they might also possess small velocities within the cloud in addition to the general velocity V. If however the cloud were accompanied by gaseous interstellar material, the relative velocities of the smallest dust particles would soon be reduced to zero by interaction with the gas, and it is just these smallest particles that are the most efficient, mass for mass, in producing collisions. All that is needed when the Sun first enters the cloud is for there to be a small but finite probability of a particle undergoing a collision at the axis, for there are so many particles that some collisions must then occur that leave material moving along the axis. Once it has begun to accumulate, collisions of further incoming particles with the material at the axis will proceed with certainty. Thus to start the process it is only necessary for there to be a small but sufficient proportion of the mass of the cloud in the form of particles of small radius. Also, it is clearly not essential to suppose that the whole of the material crossing within the capture radius is necessarily absorbed into the stream and captured by the Sun. A particle whose initial velocity differed slightly from V (in direction) would have a path not passing accurately through the accretion axis, and might therefore not be absorbed into the stream even when this had an appreciable radial extent round the axis. The focusing action of the mechanism will result, to begin with, in

the capture of particles of negligible internal velocities in the cloud, but as the stream builds up, its radial extent will increase till the steady state is reached, and thus some latitude in the internal velocity will become permissible. Thus in any case a finite proportion of the material passing within the capture radius will be absorbed into the stream at the axis. The particles of small relative velocity will be sorted out, as it were, and captured, while those of larger relative velocity (in directions not parallel to V), supposing such to be present in a cloud, may escape capture. The quantity ρ will evidently refer to what may be termed the "effective density" of the cloud.

5. *Estimate of the Possible Mass of a Comet.*—According to Bondi and Hoyle the line density m on the axis in the steady state is of order $2\pi\rho G^2M^2/V^4$, and for $\rho = 10^{-24}$ gm. cm.$^{-3}$ this gives

$$m = 10^9 v^{-4} \text{ gm. cm.}^{-1},$$

where v is the velocity in kilometres per second. If this material were in a solid stream round the axis, its radius would be of order $10^4 v^{-2}$ cm. (for density $\sigma = 3$ gm. cm.$^{-3}$). Thus even if, as seems likely, the stream is far from being packed solid, its radial extent would be small compared with the general order of distance otherwise involved in the process, which is many astronomical units. It is therefore valid to treat the stream as a line distribution, as Bondi and Hoyle have done in their investigation.

The discussion by these authors, however, was aimed principally at the calculation of the rate of accretion by the Sun, and for this it was permissible to ignore the self-gravitation of the stream of material at the axis. But there is the possibility that its comparatively slight internal gravitation will cause it to collect into a series of separate pieces. The tidal action of the Sun, however, tends to disrupt the stream into portions of infinitesimal length, and the expression of the condition for the former influence to prevail enables an upper limit to be found for the length of a stable segment and hence to the mass of a comet. The existence in the stream of centres of attraction about which aggregations would tend to collect would probably be brought about by chance irregularities arising from such factors as departure from uniform density in the cloud. Supposing such centres to occur, then were it not for the Sun, the stream would break up into a number of finite segments each of which would contract under its own gravitation. The presence of other segments would not assist the contraction in any one of them.

If d is the initial length of such a segment, its attraction at points near its ends will be of order $4Gm/d$. Also, if $R(\gg d)$ is its distance from the Sun, the differential disruptive field to which the segment is subject as between its centre and either end will be GMd/R^3. The internal gravitation will therefore be the stronger influence if

$$d < 2(mR^3/M)^{\frac{1}{2}}.$$

If R is measured in astronomical units and the velocity in kilometres per second, with the above value of m this condition becomes

$$d < 8 \times 10^7 R^{\frac{3}{2}} v^{-2} \text{ cm.}$$

The mass of the segment would therefore satisfy

$$md < 8 \times 10^{16} R^{\frac{3}{2}} v^{-6} \text{ gm.}$$

For example, if $v = 1$ km. sec.$^{-1}$ and a segment starts to develop about halfway between the neutral point and the Sun, so that $R = 550$ astronomical units, it is

found that

$$d < 10^{12} \text{ cm.}$$

$$md < 10^{21} \text{ gm.}$$

For other values of v, remembering that R also depends on v, the mass md varies as v^{-9}, so that a slight increase in v will lower the upper limit considerably, and *vice versa*. Where ρ is concerned, md depends directly on the assumed value.

This result, which is essentially an upper limit, appears to be satisfactorily consistent with the value 10^{18} gm. for the mass of Halley's comet obtained by Russell * from entirely different considerations, and his estimate (without calculation) of 6×10^{21} gm. for the great comet of 1729.

6. The time taken for a segment of length d to contract substantially under its own field will be of the same order but less than the time of parabolic fall from distance $\frac{1}{2}d$ to a point mass md, and this is $\pi d/8\sqrt{(Gm)}$. From the above inequality for d, this value is itself less than $\pi R^{\frac{3}{2}}/4\sqrt{(GM)}$. On the other hand, the time of free fall to the Sun from distance R is $\pi R^{\frac{3}{2}}/2\sqrt{(2GM)}$. This is not only greater than the former value but it will also be less than the actual time to fall into the Sun, because in the steady state the stream does not flow in at the parabolic rate owing to the outward momentum of the particles being continually added to it. Hence for values of d below the limit the internal forces act sufficiently rapidly for the material to collect together before reaching the immediate neighbourhood of the Sun where the tidal field is so much greater. Moreover the time $\pi d/8\sqrt{(Gm)}$, for values of R comparable with GM/V^2, is also of the same order but less than GM/V^3 the time required to build up the steady state. Thus the contraction of segments will not proceed so quickly as to cause the process to depart far from the steady-state conditions by the creation of gaps along the axis.

The total amount of matter added to the Sun during its passage through a dust cloud can also be readily estimated, for from the nature of the process it is evident that a high proportion of the material will fall directly into the Sun. If the cloud were, say, 0·1 parsec in depth, the time of passage would be $10^5 v^{-1}$ years, and since material is captured at the rate $2\pi G^2 M^2 \rho / V^3$, the total amount added would be not more than $2 \cdot 10^{-7} v^{-4} M(\odot)$, for an effective density of 10^{-24} gm. cm.$^{-3}$. Apart from the factor v^{-4} this is less than a tenth the mass of the Earth, and it would provide enough material for $4 \cdot 10^5 v^5$ comets of mass equal to the maximum value calculated above. Thus if not more than one per cent of the captured material failed to be absorbed directly into the Sun it would yet be enough to provide material for several thousand comets.

The major axes of the orbits of comets formed in this way during the passage of the Sun through a single cloud would all be practically in the direction of the accretion axis, that is in the direction of the relative motion, and even after there had been time for considerable chance disturbances of the orbits some evidence of the original direction might probably remain. But during its lifetime the Sun must have passed through many clouds and the directions of the relative velocities of the encounters would probably be widely scattered over the celestial sphere. Thus the distribution of the axes of cometary orbits could be explained by attributing the comets as a whole to the result of several encounters with separate clouds, and of course the additional after-effects of perturbations of their orbits

* Russell, Dugan and Stewart, *Astronomy*, I. *The Solar System*, 1945, p. 446.

through causes of the kind discussed earlier. There is no objection to postulating a number of suitable encounters with dust clouds, indeed a hundred of them similar to that adopted above would result in negligible addition of material of a non-hydrogen character to the Sun, and also negligible addition of angular momentum.

Deflection of a comet by a star passing at great distance from the Sun will be effective only when the comet itself is at great distance, so that of necessity the greatest focal distance $a(1+e)$ of the resulting orbit will be several hundred astronomical units. On the other hand, for such a body to become observable requires its least focal distance $a(1-e)$ to be less than, say, ten astronomical units. That is

$$a(1+e) \gg 100 \quad \text{and} \quad a(1-e) \leqslant 10,$$

and hence the eccentricity of the new orbit must necessarily be near to unity. This suggests however that there must be many comets of long period whose orbits do not pass near enough to the Sun for them to be observed.

The value 10^{-24} gm. cm.$^{-3}$ adopted for the density for the purposes of numerical illustration, while probably a satisfactory average for some clouds, can scarcely be expected to be generally applicable. The estimates of masses derived above depend directly on ρ and are therefore subject to a corresponding uncertainty.

The structure of comets appears to raise interesting questions of a dynamical nature. Possibly, when sufficiently far from the Sun, the composing particles are in an almost steady dynamical state, perhaps analogous in some respects to the conditions in globular clusters. If this is so, every particle will be in orbital motion under the action of the rest of the system as a whole and the density would probably increase towards the centre, the distribution of particles being such as to reduce the frequency of collisions to a minimum. Comets have of course long since been regarded as diffuse aggregates of dust particles with possibly a small nucleus or nuclei at the centre, for they become invisible in transit over the Sun's disk, and also at all times reflect far less light than would continuous distributions of solid matter with the same general extent.

Although such an aggregation may be capable of forming and holding together while at large distance, it might nevertheless be disrupted later if it approached sufficiently near the Sun. As is well known, instances have been recorded of comets changing shape and sometimes actually dividing into parts, which thereafter follow separate but similar orbits.

Furthermore, if an appreciable proportion of the mass of a comet is in the form of particles of very small size, the comet as a whole may experience a resistance to its motion when near the Sun. This may arise possibly from the presence of gaseous material near the Sun and from the Poynting-Robertson * effect, resulting from the absorption and re-emission of solar radiation, which may be highly effective for small particles. Some slow secular development of cometary orbits, particularly those of short period, might take place through such causes.

The directions of the axes of those orbits studied (excluding the short-period comets) are widely distributed over the celestial sphere, but according to Bobrovnikoff † they nevertheless show a decided preference for the galactic plane. He has also examined the question of the rate of loss of mass of comets and believes that the majority of them must have been added to the solar system within the last few million years.

* H. P. Robertson, *M.N.*, **97**, 423, 1937.
† N. Bobrovnikoff, *Lick Obs. Bull.*, XIV, No. 408, 37, 1929.

7. *Previous Hypotheses on the Origin of Comets.*—Following Aristotle the ancients considered comets to be some kind of exhalations from the Earth itself inflamed in the upper air, and even the great Galileo failed to improve much on this in holding them to be atmospheric emanations that reflected sunlight. In more recent times Proctor, about 1870, proposed that certain of the comets, whose orbits pass so near that of a planet to suggest an intimate connection, may have been expelled from the body of the planet when in some form similar to that of the Sun. At a later date Crommelin suggested a solar origin for the family of comets grazing the Sun's surface and appearing in the years 1843, 1880, 1882 and 1887, proposing that their formation was in some way associated with solar prominences. These ideas however are of obviously little value, quite apart from the feature that they would apply only to an extremely small proportion of the whole vast number of comets in the solar system, estimated by Russell to exceed 100,000. Nevertheless, that there are groups of comets with orbits demanding a certain amount of special explanation seems definite enough, and it has long been generally accepted that several of the short-period comets must have been diverted into their present orbits by the action of Jupiter. This has led to the idea that these comets may have been captured from an originally hyperbolic orbit (about the Sun) as a result of a three-body encounter of the comet with the Sun and planet, energy being conserved in the process. It has further been suggested, with less plausibility, that all comets may have been added in this way, even though for most comets the orbits do not at present pass near that of any planet and no truly hyperbolic orbit has ever been found.

The dynamical capture idea, however, in no way explains the origin of the comets themselves as more or less compact masses of dust particles, which simply have to be postulated as already existing in space, a postulate for which there is no observational evidence and which is not justified by theoretical considerations. H. N. Russell, in discussing the problem in his book "The Solar System and Its Origin", has put forward a modification of the capture notion, though only in general descriptive terms, which bears some degree of resemblance to certain features of the process given in this paper. Thus Russell discusses the possibility of the Sun passing through a nebula, and actually writes of a "decided temporary concentration in the axial line behind the Sun" (p. 128), and he goes on to suggest that a gaseous cloud would result, associated with the Sun but almost stationary behind it, and that this would offer a resistance to the motion of comets initially describing hyperbolic orbits round the Sun, thereby possibly converting some of them to elliptic ones. The comets again were supposed already present in the nebula as condensations and in sufficiently great profusion for the process to explain the huge number left behind in the solar system. The discussion given is brief and does not suggest any great confidence in the idea. It is not perceived that the convergence of material towards the axis may itself bring about the necessary concentrations of particles, or that their capture may simultaneously be effected.

Several years earlier E. W. Brown * had discussed the passage of a star through a nebula consisting of dust particles, but with the object of attempting to explain the form of the variable nebula N.G.C. 2261. In this study Brown discerned the importance of collisions at the axis, but he assumed that all the material would be vaporized and by its subsequent expansion give rise to a gaseous conical appendage following the star as long as it remained within the nebula.

* E. W. Brown, *Ap. J.*, **53**, 169, 1921.

8. As far as the present paper is concerned, its initial hypotheses are philosophically on a sounder basis than those of earlier attempts to explain the origin of comets, for the existence of dust clouds is an accepted observational conclusion, and the effect of the passage of a star through such clouds is therefore a theoretical problem automatically arising. As has been seen, the hypotheses are capable of some quantitative investigation, though as for most cosmogonic hypotheses restricted mainly to order of magnitude considerations. Even so, the results suggest that the origin of comets can probably be satisfactorily explained along such lines. If this is correct, the theory confirms what has long been conjectured, that the comets and planets do in fact represent two solar families having essentially different origins. Moreover, in view of the large number of comets in the solar system, and the fact that most stars must from time to time pass through dust clouds, it may well be that of all celestial objects comets are possibly the most numerous in the universe.

3 *Grosvenor Court,*
Woodlark Road,
Cambridge:
1948 *November* 25.

A PHOTOELECTRIC PHOTOMETER EMPLOYING AN ELECTRON COUNTING TECHNIQUE

G. G. Yates

(Communicated by the Director of the Cambridge Observatories)

(Received 1948 December 10)

Summary

The chief instrumental problem in photoelectric stellar photometry is that of measuring the minute photoelectric currents. A method of performing this measurement by counting the electrons into which the current is resolvable is discussed; an apparatus for achieving the electron counting is described and some preliminary observational results obtained with an unselected 931–A tube are quoted, which indicate that with a 15-inch telescope it should be possible to make photometric measures down to 12^m.

The central problem of photoelectric stellar photometry is that of measuring the minute photo-currents which flow when the photosensitive cathode of a photoelectric cell is exposed to star-light. The currents encountered may be of the order of 10^{-15} to 10^{-18} amperes. This may be expressed otherwise by saying that the number of electrons emitted from the cathode per second is of the order of 10^4 to 10. This latter viewpoint suggests that if the electrons could be counted as they left the cathode, then a powerful method of measuring these minute currents would be available.

A combination of an electron multiplier type of photocell with a pulse amplifier, an electronic counter and an electronic timer enables this electron counting to be achieved. It is fundamental to the method described here that the secondary emission multiplier type of photocell be employed. When an electron is emitted from the cathode of this type of cell it is accelerated by an electric field and is caused to strike a target electrode, where it knocks out a number of secondary electrons which are in turn accelerated and directed towards a second target. The multiplier contains nine such targets (dynodes), at each of which "multiplication" takes place. The final burst of electrons, which may number from 100 to 1,000,000, depending on the accelerating fields applied to the tube, is collected at the anode of the multiplier. The whole multiplying process has been found to take place in about 10^{-8} second (1). Thus a single electron of charge e emitted from the cathode will cause a charge Me (M being the multiplying factor of the tube) to flow in the anode circuit.

The load circuit of the multiplier consists of a resistance R (this also forms the grid-resistance of the first valve of the succeeding pulse amplifier, Fig. 3B) and a capacity C in parallel with R. This capacity will normally be the inevitable anode to earth capacity of the multiplier, the capacity of the feeder coupling the multiplier to the succeeding amplifier and the input capacity of the amplifier, making a total capacity of at least $20\,\mu\mu$F. Since the M electrons which arrive at the anode consequent on the emission of one electron from the cathode do so in less than 10^{-8} second, the effect is to impress a negative potential on the capacity C of magnitude Me/C. The charge Me then leaks away through R at a rate

depending on the time constant CR in the usual manner. Thus each electron emitted from the cathode gives rise to a voltage pulse on the anode of the type shown in Fig. 1B. It is not necessary that all the charge on C should have leaked away before the arrival of another charge. Each primary electron will always give rise to a voltage drop Me/C at the anode, but varying rates of emission of primary electrons will cause the mean potential at the anode to vary. Fig. 1C shows the effect of a train of pulses at the anode. The mean potential is, however, subject only to slow changes and the pulse amplifier does not amplify these, but only the sharp pulses.

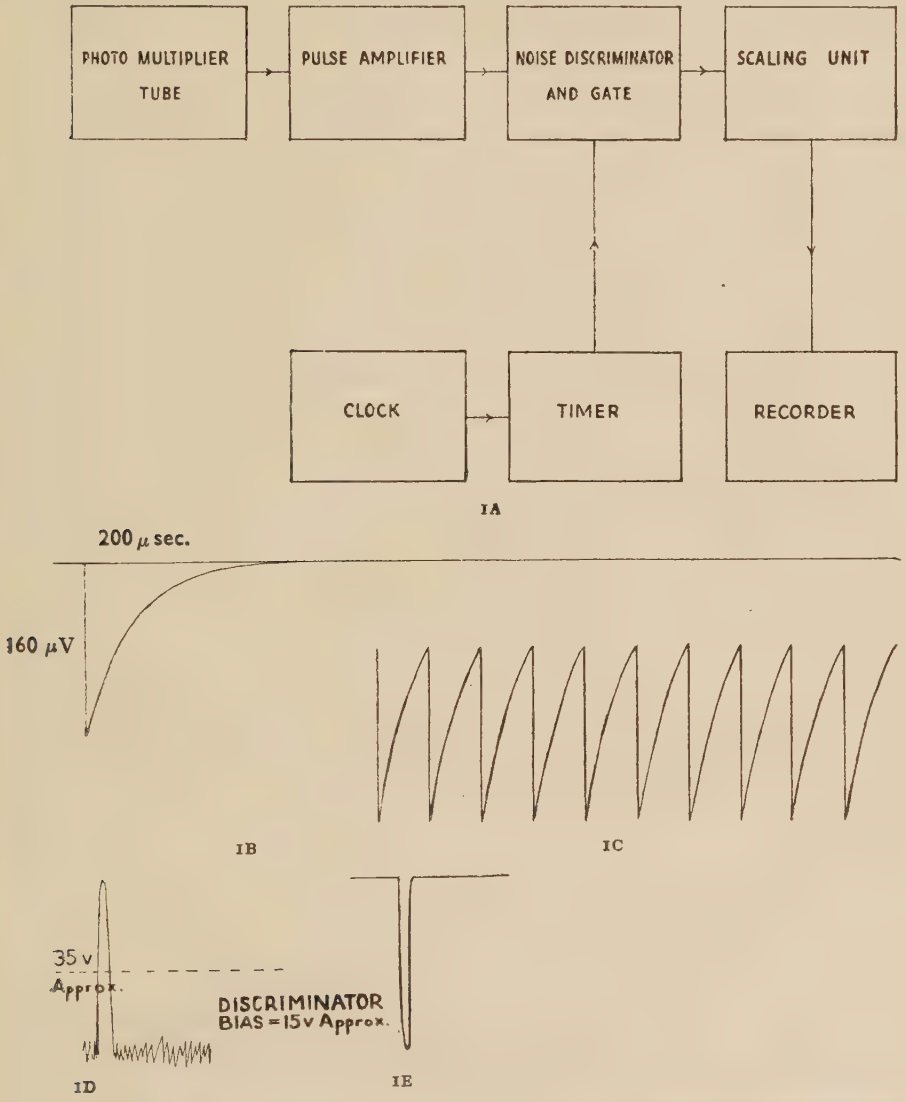

FIG. 1.—*Layout of Equipment and Voltage Wave-forms from Multiplier and Amplifier.*

1A : *Layout.*
1B : *Single voltage pulse from multiplier.*
1C : *Train of pulses from multiplier.*
1D : *Output from amplifier.*
1E : *Output from discriminator.*

The arrangement of the various units comprising the photometer is shown schematically in Fig. 1A. The pulses from the photocell pass to the pulse amplifier where they are amplified to about 35 volts, the output being then fed through a noise discriminator and gate circuit, thence to the scalers, and finally to the counter, where the number of pulses is recorded. An automatic timer, driven from a clock, is coupled to the gate circuit. Its purpose is to permit pulses to pass only for a predetermined interval. Since the whole apparatus is devoted to counting electrons, rather than measuring their rate of appearance, as in more conventional photocell plus amplifier units, we are integrating the response, and speak of an "exposure" analogous to a photographic exposure. The timer ensures that these exposures are always accurately of the required length.

It will be noticed (see Fig. 3A) that the photocell V_1 is being operated at a voltage considerably below its maximum, with consequent diminution in gain. R. W. Engstrom (2) discovered as a result of a thorough investigation of the properties of these photocells that the "dark current" can be considerably reduced if the tube is operated at a low voltage; a further reduction in dark current is also obtained by refrigerating the cell. By reducing the voltage on the cell the multiplication M is reduced and the pulses then require greater amplification in the succeeding pulse amplifier, so that this process of reducing the voltage on the cell cannot be carried on indefinitely, since the usable gain of a thermionic amplifier is limited by the noise inherent in its input circuit. It will be shown that a practical compromise leads to a multiplication of about 20,000, corresponding to a working voltage of about 550 to 600.

Now, the total input capacity of the amplifier is about 20 $\mu\mu$F, and the R.M.S. noise voltage at the input of the amplifier is given by $E_n = \sqrt{(kT/C)}$, where k is Boltzmann's constant ($\approx 1{\cdot}4 \times 10^{-23}$ watts sec./deg.) and T is the absolute temperature ($\approx$300 deg. K.), whence

$$E_n = \sqrt{\left(\frac{1{\cdot}4 \times 10^{-23} \times 300}{20 \times 10^{-12}}\right)} \cdot 10^6 \,\mu\text{V}.$$

$$= 14{\cdot}5 \,\mu\text{V}.$$

In order that the pulses shall be well above this amplifier noise level, we choose the pulse amplitude to be about $10 E_n$, say 160 μV. Now the pulse amplitude is given by Me/C, where $e = 1{\cdot}6 \times 10^{-19}$ coulombs.

Therefore

$$M = \frac{160 \times 10^{-6} \times 20 \times 10^{-12}}{1{\cdot}6 \times 10^{-19}}$$

$$= 20{,}000.$$

From the published characteristics of the 931–A it is seen that such a gain is obtained by using about 55 to 60 volts per stage, or 550 to 600 volts overall. Fig. 1D shows approximately the relative amplitude of amplifier noise and pulse as seen on a cathode-ray oscilloscope at the output of the amplifier.

Pulses are also obtained from the photocell even when it is not being illuminated. These constitute the "dark current" and they have their origin in electrons which are emitted from the cathode or the several dynodes, either by thermionic action, or under the influence of the interdynode electrostatic fields. These "dark current" pulses are amplified along with the signal pulses and are counted

with them. It should be noted however that the electrons which are emitted from the various dynodes are subject to less multiplication in the multiplier than the electrons emitted from the cathode, and consequently the "dark current" output contains pulses which are smaller than the average signal pulses. These small pulses may be removed by an amplitude discriminator circuit.

The pulse amplifier circuit is shown in Fig. 3B. The amplifier utilizes miniature valves and components and so can be mounted close to the photocell on the telescope itself. This reduces to a minimum the length of feeder coupling the photocell to the amplifier. The pentode valves have a mutual conductance of 4·5 mA./V. and each has an anode load of 15 KΩ which would give a stage gain of about 67·5. However, some rounding of the leading edge of the pulse is caused by the finite charging time of the valve capacities, which reduces the effective stage gain to about 60 and the overall gain to about 220,000. The resulting positive pulses of about 35 volts amplitude are fed by the cathode follower V_5 along a coaxial cable to the rest of the equipment, which is mounted in a rack separate from the telescope. It will be noted that the time constants of the interstage couplings are extremely short (27 μ sec.). Such a time constant is long enough to pass the pulses but ignores any change in mean potential at the input due to variation in the rate of arrival of the pulses.

The amplified pulses are passed from the amplifier to the discriminator (Fig. 3C). This circuit performs a dual function; firstly, it removes the amplifier noise and the smaller "dark" current pulses, and secondly, it acts as a "gate", permitting pulses to pass on to the scalers only during the exposure set by the timer. These results are achieved as follows. The valve V_7, a pentode, has about 18 volts negative bias applied to its control grid and about 60 volts negative bias applied to its suppressor grid. Since the valve will not conduct until the grid bias is less than -5 volts, it transmits only those pulses having an amplitude greater than 13 volts. Thus the amplifier noise and smaller pulses due to "dark current" electrons emitted from the various dynodes of the photocell are eliminated (see Figs. 1D and 1E). Further, not even the larger signal pulses will appear at the anode of V_7 until the suppressor bias has also been removed, either by closing the switch and putting the suppressor at earth potential (manual operation), or by applying a positive potential (about 200 V.) to R_{35} (automatic operation). Clean negative pulses (Fig. 1E) then appear at the anode of V_7.

The negative pulses from the discriminator pass into the scaling unit for counting and recording. This consists of a series of scale-of-sixteen units in cascade. Three such units are employed at the moment, but if a faster counting rate is required, four could be used. Fig. 4 shows the circuit of such a unit along with the circuit (V_{20}, V_{21}) for driving the mechanical counter. These scalers have been described elsewhere (**3**), so only a brief description is required here.

A simple type of electronic scaler naturally scales in a binary system and it was decided not to introduce extra complications necessary to scale in the decimal system. Each scale-of-sixteen unit consists of four halvers in cascade. The circuit of a halver is given in Fig. 4, valves V_8, V_9, V_{10}. The two triodes are connected as a multivibrator, which is stable with either of the valves conducting and the other cut off. In operation the Reset Line is connected to -125 volts, but in order to set the multivibrator with V_8 cut off, it is momentarily disconnected, by pressing a push button (Fig. 5), which causes the grid potential of V_{10} to rise

and the valve to conduct. The potential of the anode of V_{10} falls, driving the grid of V_8 negative, and so cutting off V_8. The halver is switched to its other position by applying a negative pulse through the diodes V_9. This cuts off V_{10}; and V_8 then conducts. The next pulse reverses the procedure, and the potential of the anode of V_{10} drops. This potential drop is passed through the condenser C_{31} to switch the next halver for the first time. Finally one negative impulse is passed forward from the whole unit after sixteen have been received. The number of received pulses is recorded directly on the meter and the electromechanical counter moves forward one for every sixteen of these. When three scale-of-sixteen units are employed before the counter, the counter moves forward one for every 4096 pulses received.

The circuit of the automatic timer is shown in Fig. 5. The voltage wave-forms at various points are shown in Fig. 2. Electrical impulses of about $\frac{1}{10}$ second duration and 15 volts (negative) amplitude are generated once every second when the input terminals are connected by a contact on a clock. These are differentiated by the network $C_{42}R_{85}$, to give negative clock pulses of about $\frac{1}{100}$ second duration at the grid of V_{22}. They are then amplified by valves V_{22} and V_{23} to negative pulses of about 200 volts in amplitude. These pulses do not appear at the anode of V_{23} until the start button (which removes the bias from the suppressor of V_{23}) has been pressed, after which the next clock pulse to pass triggers the single-stroke multivibrator $V_{24}V_{25}$, at the same time switching the halver $V_{28}V_{31}$, so that the anode potential of V_{28} falls and V_{33} is cut off. The relay A then closes the contact A/1 and holds the suppressor of V_{23} at earth potential. Simultaneously, with the arrival of the first clock pulse, the anode potential of V_{23} rises (Fig. 2B) and this turns on the pulse gate valve, V_7. The multivibrator resets after about $5\frac{1}{2}$ seconds (Fig. 2D), the anode potential of V_{24} falling and cutting off V_{32}. The relay B closes contact B/1 and causes the uniselector to advance one position. The next impulse from the clock triggers the multivibrator again, so that the uniselector is caused to advance one step every six seconds. After a predetermined interval, depending on the setting of the time-selector switch, the uniselector advances to a position where it earths the suppressor of V_{27}. The next impulse from the clock can then pass through V_{27} and switch the halver back to its initial state. This in turn causes V_{33} to conduct, opens contact A/1, and terminates the exposure. The various wave-forms shown relate to an exposure of 18 seconds. The lengths of exposure available on the present unit are 6, 12, 18 and 30 seconds; 1, 2 and 4 minutes. This circuit ensures that the accuracy of timing is that of the good astronomical clock from which the initiating signals are taken.

The photomultiplier is mounted in the refrigerating chamber, which is shown diagrammatically in Fig. 6. When it is required to cool the cell, dry ice is placed in the Dewar flask housed in the lower compartment of the chamber. Cooling is achieved mainly by conduction along the electrode leads and to increase the efficiency of the process each of the ten leads connected to the valve holder is brought through a separate brass tube (being electrically insulated from it), and each tube is in contact with the dry ice. It was at first found that leakage across the valve holder and valve base formed a serious source of noise. This was entirely eliminated by removing the anode pin and clearing a fairly large hole in the side of the ebonite valve cap through which to bring the anode wire; a further wire was soldered directly to this lead to convey the pulses to the output plug mounted on the side of the refrigerating chamber.

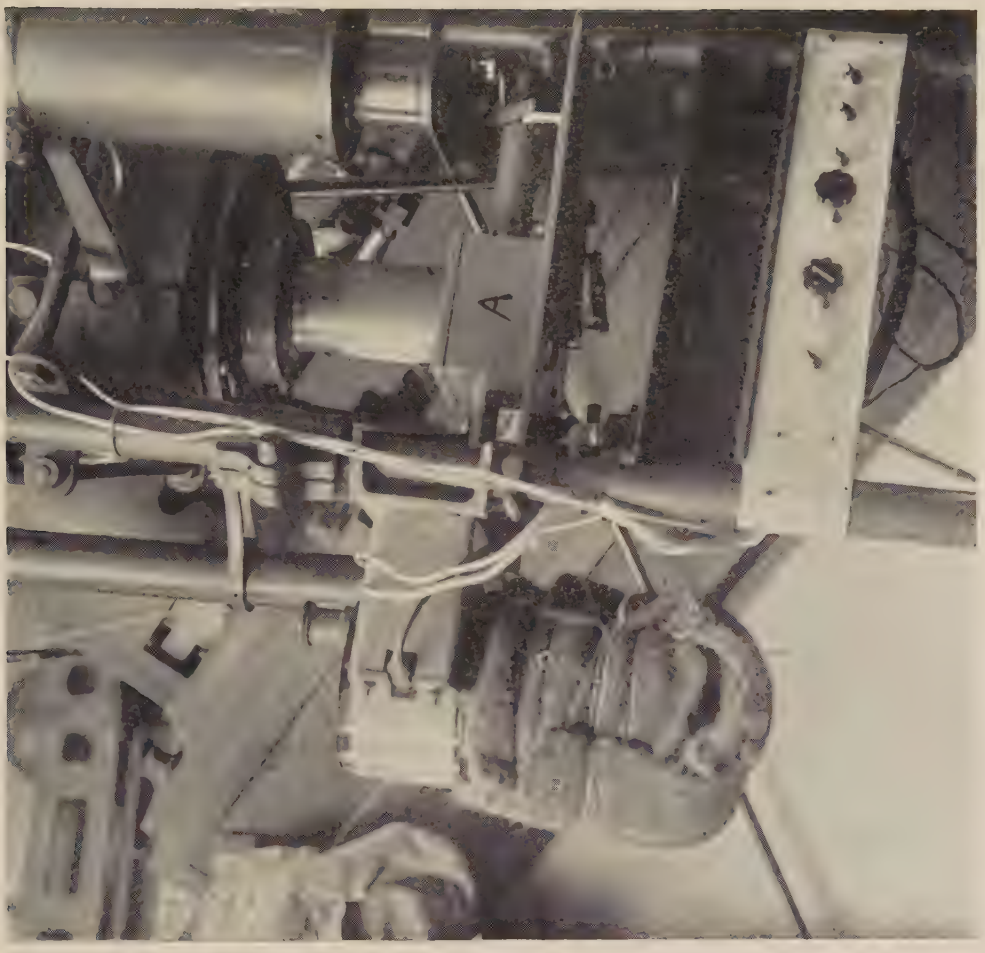

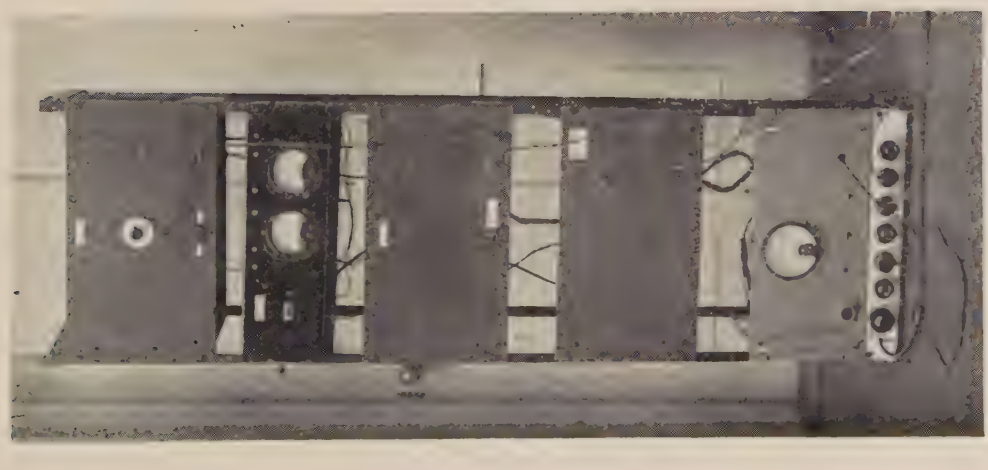

G. G. Yates, *A Photoelectric Photometer employing an Electron Counting Technique.*

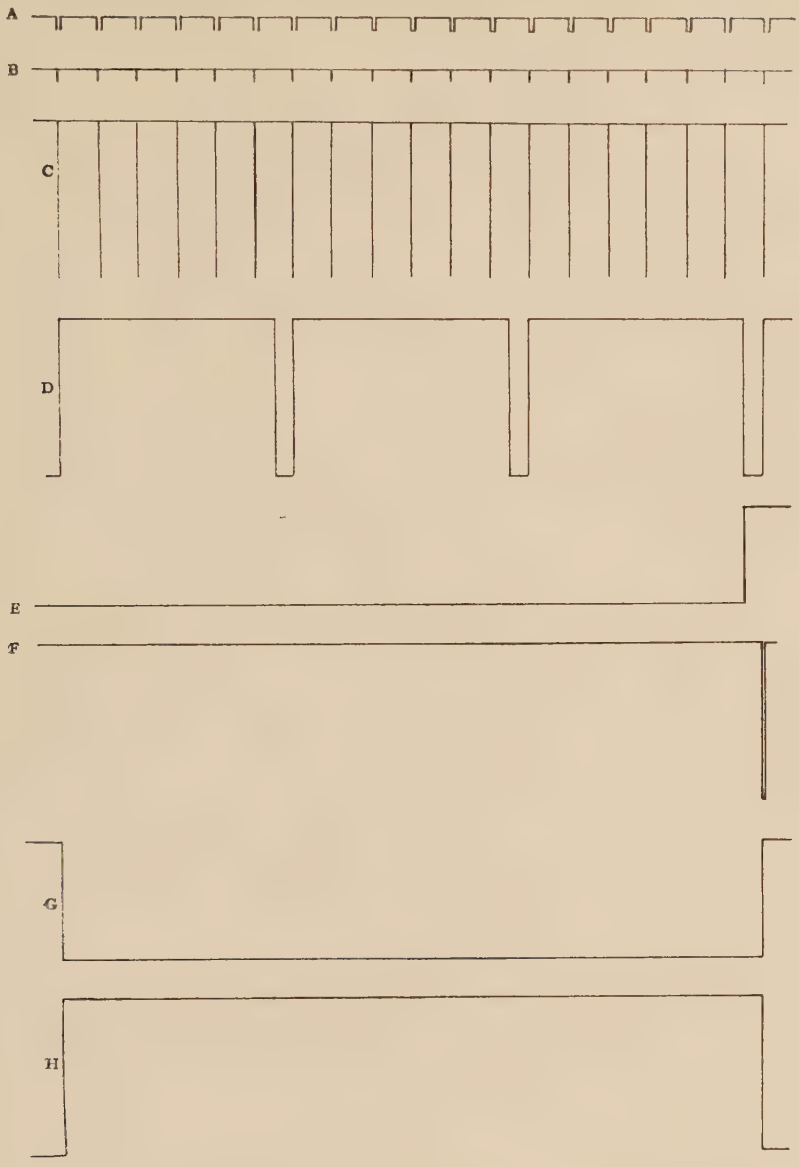

FIG. 2.

A : 1 *sec. pulses from clock.*
B : *Pulses at grid of* V_{22}.
C : *Pulses at anode of* V_{22}.
D : *Wave-form at anode of* V_{24}.
E : *Wave-form at suppressor of* V_{27}.
F : *Wave-form at anode of* V_{27}.
G : *Wave-form at anode of* V_{28}.
H : *Wave-form at anode of* V_{33}.

The photometer is being used in conjunction with the Huggins 15-inch Refractor at the Cambridge Observatories. Plate 9 shows on the left the scaler recorder, timer and power supplies and on the right the refrigerating chamber and the associated optical system mounted on the telescope. The box A contains a right-angled prism which can be turned to direct the light beam either into an eyepiece on the right, or into the photocell chamber on the left. A Fabry lens and a diaphragm about 1 mm. in diameter are mounted at the telescope focus, which is about $2\frac{7}{8}$ inches in front of the photocell. The Fabry lens forms

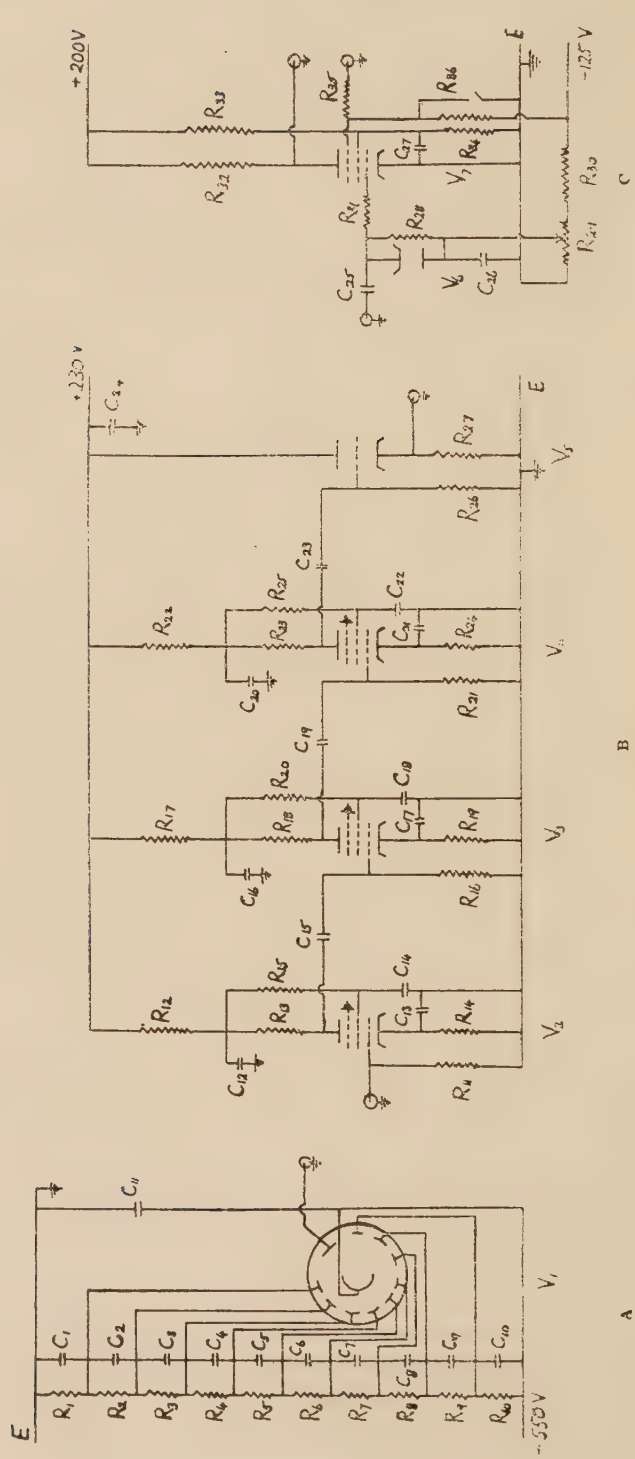

FIG. 3.

A : *Photocell circuit.*
B : *Pulse amplifier circuit.*
C : *Discriminator circuit.*

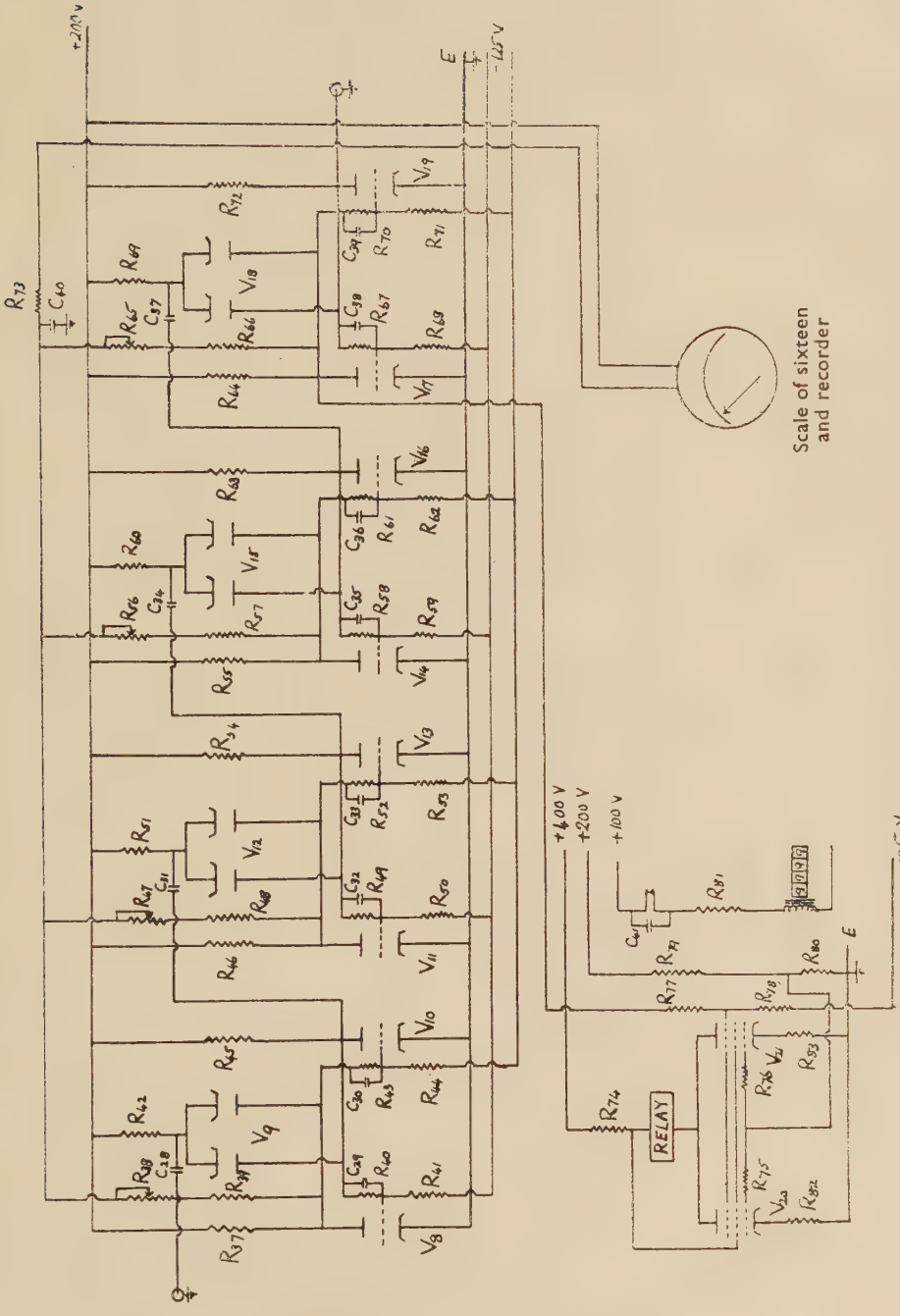
+200 V
E
-125 V
Scale of sixteen and recorder
+400 V
+200 V
+100 V
-125 V
RELAY
E

FIG. 4.

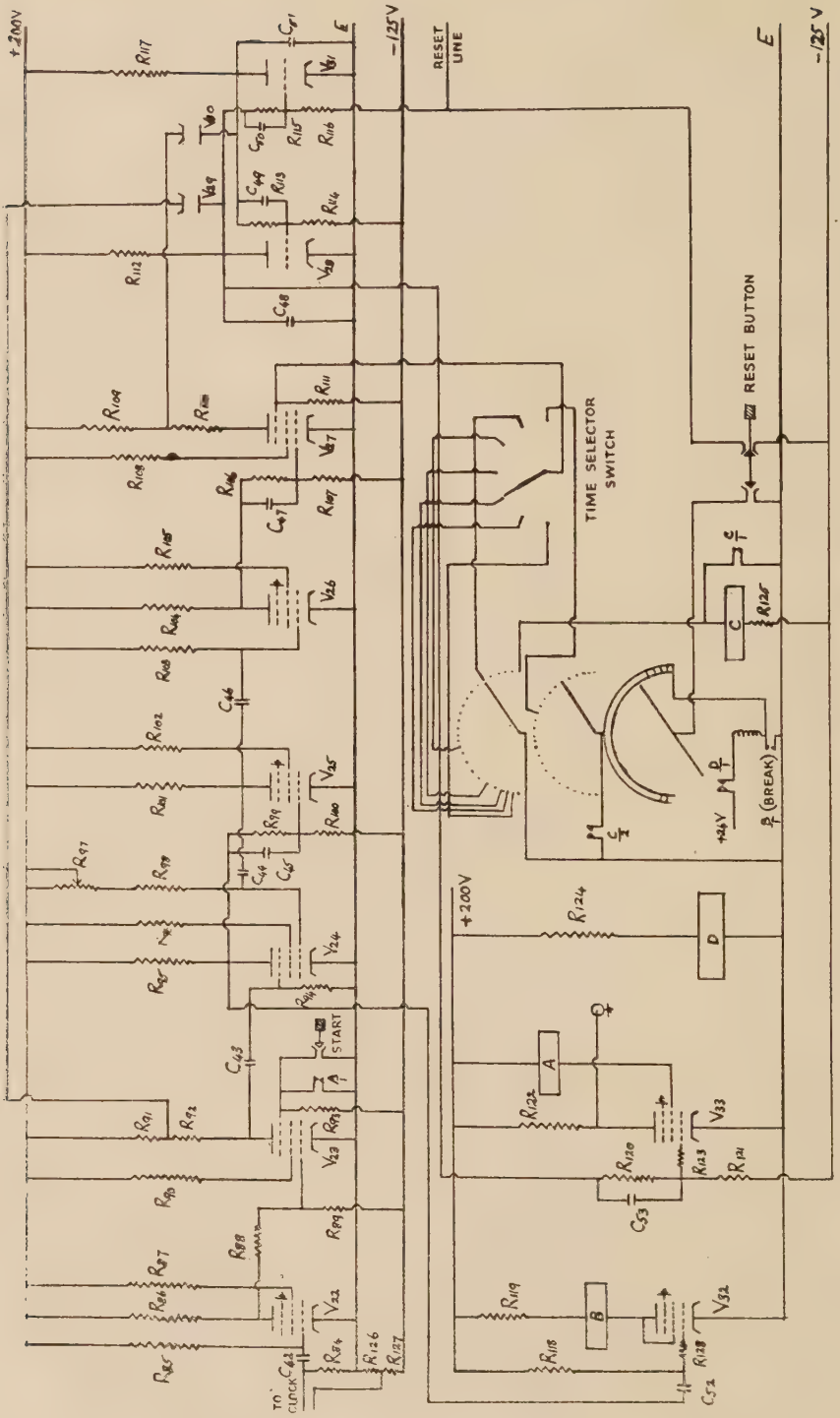

FIG. 5.—*Circuit of automatic timer.*

SCHEDULE OF COMPONENTS

Resistors

R_1	22 KΩ	R_{33}	56 KΩ	R_{65}	50 KΩ	R_{97}	5 MΩ (variable)
R_2	22 KΩ	R_{34}	56 KΩ	R_{66}	40 KΩ	R_{98}	13 MΩ
R_3	22 KΩ	R_{35}	2·2 MΩ	R_{67}	470 KΩ	R_{99}	1 MΩ
R_4	22 KΩ	R_{36}	1·5 MΩ	R_{68}	470 KΩ	R_{100}	1 MΩ
R_5	22 KΩ	R_{37}	28 KΩ	R_{69}	12 KΩ	R_{101}	100 KΩ
R_6	22 KΩ	R_{38}	500 KΩ	R_{70}	470 KΩ	R_{102}	56 KΩ
R_7	22 KΩ	R_{39}	330 KΩ	R_{71}	470 KΩ	R_{103}	2 MΩ
R_8	22 KΩ	R_{40}	470 KΩ	R_{72}	27 KΩ	R_{104}	100 KΩ
R_9	22 KΩ	R_{41}	470 KΩ	R_{73}	300 Ω	R_{105}	56 KΩ
R_{10}	22 KΩ	R_{42}	12 KΩ	R_{74}	10 KΩ	R_{106}	1 MΩ
R_{11}	2·7 MΩ	R_{43}	470 KΩ	R_{75}	470 Ω	R_{107}	1 MΩ
R_{12}	10 KΩ	R_{44}	470 KΩ	R_{76}	470 Ω	R_{108}	56 KΩ
R_{13}	15 KΩ	R_{45}	27 KΩ	R_{77}	1 MΩ	R_{109}	56 KΩ
R_{14}	100 Ω	R_{46}	30 KΩ	R_{78}	1·5 MΩ	R_{110}	56 KΩ
R_{15}	56 KΩ	R_{47}	250 KΩ	R_{79}	180 KΩ	R_{111}	470 KΩ
R_{16}	100 KΩ	R_{48}	150 KΩ	R_{80}	56 KΩ	R_{112}	56 KΩ
R_{17}	10 KΩ	R_{49}	470 KΩ	R_{81}	6·6 KΩ	R_{113}	2 MΩ
R_{18}	15 KΩ	R_{50}	470 KΩ	R_{82}	4·7 KΩ	R_{114}	2 MΩ
R_{19}	100 Ω	R_{51}	12 KΩ	R_{83}	4·7 KΩ	R_{115}	2 MΩ
R_{20}	56 KΩ	R_{52}	470 KΩ	R_{84}	330 KΩ	R_{116}	2 MΩ
R_{21}	100 KΩ	R_{53}	470 KΩ	R_{85}	1·5 MΩ	R_{117}	56 KΩ
R_{22}	10 KΩ	R_{54}	27 KΩ	R_{86}	100 KΩ	R_{118}	2 MΩ
R_{23}	15 KΩ	R_{55}	32 KΩ	R_{87}	56 KΩ	R_{119}	15 KΩ
R_{24}	100 Ω	R_{56}	100 KΩ	R_{88}	1 MΩ	R_{120}	1 MΩ
R_{25}	56 KΩ	R_{57}	82 KΩ	R_{89}	2·7 MΩ	R_{121}	1 MΩ
R_{26}	680 KΩ	R_{58}	470 KΩ	R_{90}	56 KΩ	R_{122}	100 KΩ
R_{27}	4·7 KΩ	R_{59}	470 KΩ	R_{91}	56 KΩ	R_{123}	470 Ω
R_{28}	1 MΩ	R_{60}	12 KΩ	R_{92}	56 KΩ	R_{124}	22 KΩ
R_{29}	25 KΩ	R_{61}	470 KΩ	R_{93}	470 KΩ	R_{125}	15 KΩ
R_{30}	100 KΩ	R_{62}	470 KΩ	R_{94}	470 KΩ	R_{126}	27 KΩ
R_{31}	100 KΩ	R_{63}	27 KΩ	R_{95}	100 KΩ	R_{127}	220 KΩ
R_{32}	22 KΩ	R_{64}	49 KΩ	R_{96}	56 KΩ	R_{128}	470 Ω

Condensers

C_1	0·1 μF	C_{14}	0·1 μF	C_{27}	0·01 μF	C_{40}	8 μF
C_2	·1 μF	C_{15}	270 μμF	C_{28}	80 μμF	C_{41}	2 μF
C_3	·1 μF	C_{16}	0·1 μF	C_{29}	80 μμF	C_{42}	0·1 μF
C_4	·1 μF	C_{17}	·1 μF	C_{30}	80 μμF	C_{43}	·1 μF
C_5	·1 μF	C_{18}	0·1 μF	C_{31}	80 μμF	C_{44}	·5 μF
C_6	·1 μF	C_{19}	270 μμF	C_{32}	80 μμF	C_{45}	·005 μF
C_7	·1 μF	C_{20}	0·1 μF	C_{33}	80 μμF	C_{46}	·02 μF
C_8	·1 μF	C_{21}	·1 μF	C_{34}	80 μμF	C_{47}	·001 μF
C_9	·1 μF	C_{22}	0·1 μF	C_{35}	80 μμF	C_{48}	·1 μF
C_{10}	·1 μF	C_{23}	270 μμF	C_{36}	80 μμF	C_{49}	·1 μF
C_{11}	·1 μF	C_{24}	0·5 μF	C_{37}	80 μμF	C_{50}	·1 μF
C_{12}	·1 μF	C_{25}	·01 μF	C_{38}	80 μμF	C_{51}	·1 μF
C_{13}	0·1 μF	C_{26}	0·1 μF	C_{39}	80 μμF	C_{52}	·2 μF
						C_{53}	0·0001 μF

Valves

V_1	931–A	V_9	VR54	V_{17}	CV1135	V_{25}	VR56
V_2	6AG5	V_{10}	CV1135	V_{18}	VR54	V_{26}	VR56
V_3	6AG5	V_{11}	CV1135	V_{19}	CV1135	V_{27}	VR56
V_4	6AG5	V_{12}	VR54	V_{20}	VR65	V_{28}	CV1135
V_5	RL16	V_{13}	CV1135	V_{21}	VR65	V_{29}	VR92
V_6	VR54	V_{14}	CV1135	V_{22}	VR56	V_{30}	VR92
V_7	VR56	V_{15}	VR54	V_{23}	VR56	V_{31}	CV1135
V_8	CV1135	V_{16}	CV1135	V_{24}	VR56	V_{32}	VR65
						V_{33}	VR65

an image of the object glass on the cathode of the photocell. The eyepiece on the right is fitted with cross wires which are so adjusted that after the star image has been brought into the square defined by the cross wires, rotation of the prism will throw the image into the diaphragm. In order to check that the star image is within the diaphragm, the tube G (Fig. 6), which carries a right-angled prism and an eyepiece, is pushed down to intercept the beam, and the diaphragm and

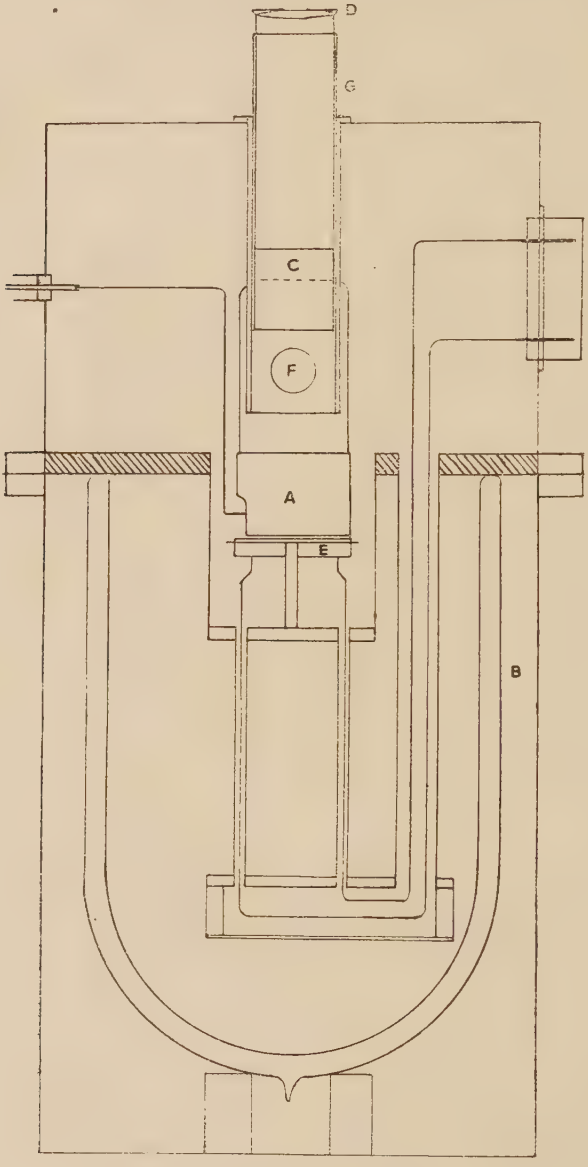

FIG. 6.—*Refrigerating Chamber.*

A : *Photocell.*
B : *Dewar flask.*
C : *Right-angled Prism.*
D : *Eyepiece.*
E : *Valve holder.*
F : *Opening exposing cathode to light.*
G : *Tube carrying prism and eyepiece.*

The cathode is parallel to the plane of the paper, the light beam enters the chamber along a line perpendicular to this plane at F.

star may be viewed through the eyepiece. Withdrawal of the tube allows the light to fall on the cathode of the photocell.

Since much of the "dark current" has its origin in electrons emitted thermionically from the cathode and the various dynodes of the photocell, it is reduced by cooling. The graphs (Fig. 7) show how the "dark count" varies with the voltage applied to the photocell and also demonstrate the improvement to be obtained by cooling to the temperature of dry ice. At all voltages the "dark count" is reduced by a factor of approximately 20 when the temperature is reduced from 10 deg. C. to −80 deg. C.

Using a battery-fed lamp as an artificial source of light, with neutral filters to reduce the amount of light to a suitable level, a number of observations were made to check the reliability of the instrument as a photometric device. In this experiment the photocell was refrigerated with dry ice to keep the "noise" (or dark count) down to a minimum. The results of the measurements are shown in the accompanying table. The figures in the columns headed Signal + Noise and Noise are the recorded number of pulses per minute with and without the lamp respectively. The fourth column is the difference between the preceding two, whilst the standard deviation of one reading is shown in the final column.

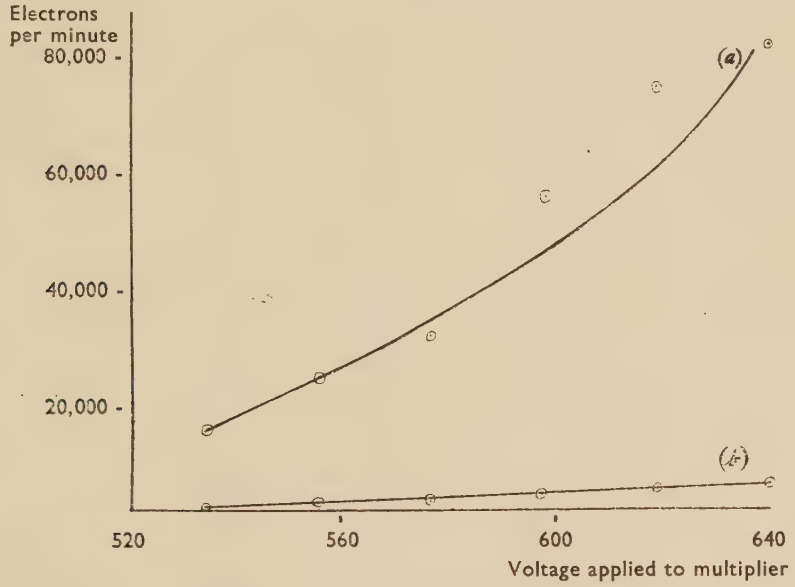

FIG. 7.—"*Noise*" *Count as a function of Voltage and Temperature.*
(*a*) : 10 deg. C. *approx.*
(*b*) : −80 deg. C. *approx.*

Since the electron counting method measures the primary (photoelectric) current by counting the individual electrons as they are emitted, the count should be independent of the size of the output pulses provided only that these are above the minimum size required to operate the scalers. Any increase in size of the pulses will not affect the count, and hence the equipment should be insensitive to changes of applied voltage. This would be strictly true if the pulses appearing at the anode of the multiplier were all of the same size. In fact the sizes vary about a mean value and a few of the smaller ones will normally be lost; when the

Measures on an Artificial Source

Photocell refrigerated to −80 deg. C.

Voltage applied to cell	Signal+Noise	Noise	Signal	Standard Deviation of a single reading
	266016	5872	260144	
	265936	5728	260208	
640 volts	264672	5392	259280	545
	265824	5136	260688	
	266448	5488	260960	$=0^{m}\cdot002$
	266000	5200	260800	
		Mean Signal	260347	
	260608	4096	256512	
	260640	3824	256716	
619 volts	261152	4224	256928	309
	260944	4080	256864	
	260608	3880	256728	$=0^{m}\cdot001$
	260064	4064	256000	
		Mean Signal	256625	
	252416	3104	249312	
	250816	2768	248048	
597 volts	249920	2576	247344	727
	249696	2592	247094	
	251104	2672	248432	$=0^{m}\cdot003$
	250912	2720	248192	
		Mean Signal	248070	
	241696	1744	239952	
	240176	1744	238432	
576 volts	240480	1760	238720	1245
	241872	1936	239836	
	244224	1952	242272	$=0^{m}\cdot005$
	242272	2032	240240	
		Mean Signal	239909	
	231264	1248	230016	
	227216	1216	226000	
555 volts	231520	1264	230256	1563
	229216	1344	227872	
	232080	1360	230720	$=0^{m}\cdot007$
	231072	1280	229792	
		Mean Signal	229109	
	211344	688	210656	
	210464	704	209760	
534 volts	211488	672	210816	1031
	211520	720	210800	
	211232	688	210544	
	208608	688	207920	$=0^{m}\cdot003$
		Mean Signal	210083	

voltage is increased some of these smaller ones will be raised above the minimum level and so counted. The graph (Fig. 8*a*) shows how the counting rate increases slowly as the voltage is raised. Fig. 8*b* shows how the multiplication of the photocell increases over the same range of voltage. As these photocells are normally used, the quantity measured is directly proportional to the multiplication of the photocell as well as to the illumination. Thus it will be seen that relative to the voltage supply on the dynodes a considerable increase in stability is achieved by the electron counting technique.

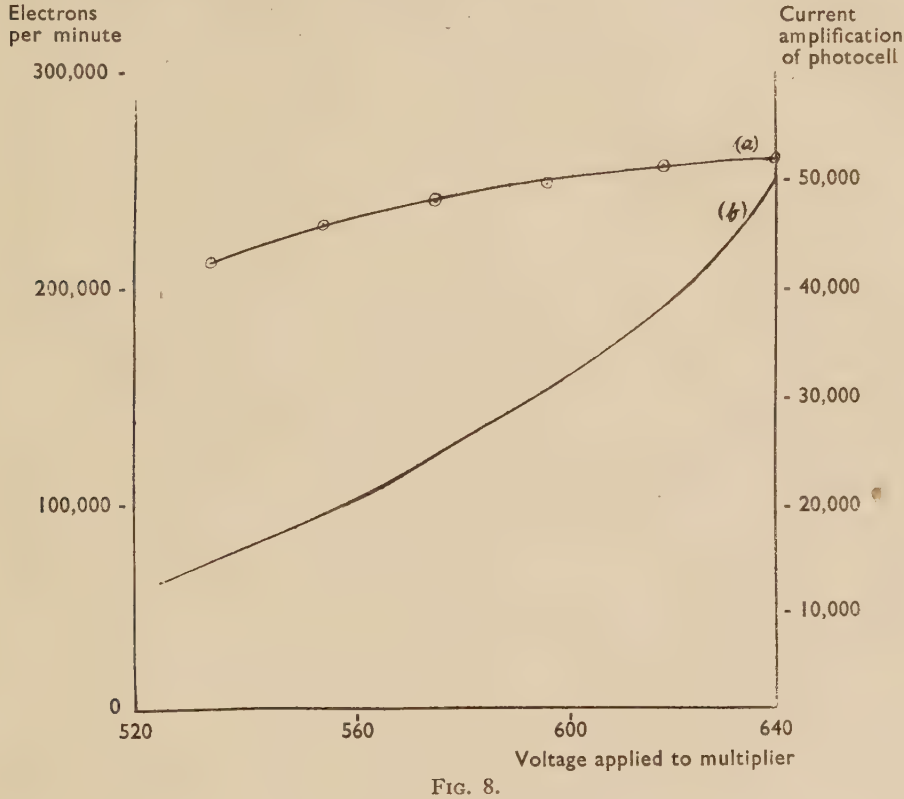

FIG. 8.

(*a*): *Variation of count with voltage.*
(*b*): *Variation of multiplication with voltage.*

A limited amount of observing has been done using the equipment. The following average figures were obtained with the telescope aperture stopped down to 7 inches, with a voltage of 540, and without refrigeration. At the time of the observations the temperature was between 0 deg. and 5 deg. C. The measurements were made during the night 1948 November 26, on the planet Uranus and the nearby Ko star G.C. 7739, the following results obtained with one-minute exposures:—

Object	*Intensity (Electrons per minute)*
Uranus + Background	901300
G.C. 7739 + Background	310900
Background	7700
Uranus	893600
G.C. 7739	303200

$$\Delta m(\text{G.C. } 7739 - \text{Uranus}) = 1^{m}\cdot 17$$

These figures enable one to make a rough estimate of the limits of the instrument. Of the above background count, the noise count (arising in the instrument itself) was roughly 6000 electrons per minute, leaving a sky count of 1700 electrons per minute. Refrigeration with dry ice would reduce the noise count at least to 600 electrons per minute. If now the full aperture of 15 inches is used, the sky count would go up to about 6800, giving a total background count of 7400. The count for the star G.C. 7739, using the full aperture, would be about 1,200,000 per minute, so that a star giving a count equal to the background of 7400 would be some $5^{m}\cdot5$ fainter than G.C. 7739. According to the catalogues the magnitude of this latter star is $6^{m}\cdot9$, so that photometric measures of stars down to 12^{m} should be possible with the present telescope and photometer. Theoretically, if observing conditions could be held perfectly constant, it should be possible to measure quite accurately stars giving a smaller count than the background, the limiting luminosity diminishing with increasing exposure time. The figure given is suggested as a conservative practical limit. It should be noted that all this work has been done with an unselected 931–A tube, and with no filter.

It is of interest to note that G. E. Kron (**4**) was already speculating in 1946 on the possibility of counting the output pulses from a multiplier type photocell as a means of measuring the primary photo-current and also suggested the use of a discriminator circuit to eliminate the smaller noise pulses. The method of pulse counting was used by R. W. Engstrom (**2**) when investigating the properties of the multiplier photocell and the present writer is much indebted to the information contained in Engstrom's paper. A brief account of an electron counting photometer which has been constructed at the Flower Observatory was given in the *Bulletin of the Panel on the Orbits of Eclipsing Binaries*, No. 4. To that account the writer is indebted for suggesting the general scheme of the photometer; as, however, no circuit details were published the present instrument represents an independent design.

Thanks are due to Mr R. S. Overhill, Observatory instrument maker, for making the refrigerating chamber and various optical parts and assembling these on the telescope, and also to Mr A. G. Wallman, assistant, for help in constructing the electronic equipment.

In conclusion it is a pleasure to thank Professor R. O. Redman for helpful criticisms and suggestions in connection with this project.

The Observatories,
Cambridge:
1948 *December* 8.

References

(1) R. D. Sard, *Journal of Applied Physics*, **17**, 768, 1946.
(2) R. W. Engstrom, *Journal of Optical Society of America*, **37**, 420, 1947.
(3) J. Rotblat, E. A. Sayle, D. G. A. Thomas, *Journal of Sci. Inst.*, **25**, 33, 1948.
(4) G. E. Kron, *Ap. J.*, **103**, 326, 1946.

THE SUN'S STELLAR MAGNITUDE

R. v. d. R. Woolley and S. C. B. Gascoigne

(Received 1948 October 6)

Summary

Monochromatic magnitude differences between the Sun and Sirius were measured by photographic spectrophotometry at the focus of the Mt. Stromlo solar tower, using diaphragms to weaken the intensity of the solar spectrum. The results at the four wave-lengths chosen are :—

λ 6209	λ 5550	λ 4945	λ 4510
25·85±04	25·59±04	25·34±04	25·15±04

Adopting a photovisual magnitude for Sirius of −1·52, the photovisual magnitude for the Sun is −27·07, and its absolute magnitude 4·52. The gradient of the Sun on the Greenwich system is 1·11.

1.—The importance of the accurate determination of the Sun's stellar magnitude is twofold. First, the Sun, being the most easily measured star, forms a strong point in mass-luminosity comparisons, provided that its characteristics can be expressed on the same scale as those of the stars, and secondly, since the flux of energy from its surface is accurately known, determination of the Sun's stellar magnitude gives one means of calibrating the stellar magnitude system in C.G.S. units (the other means being the direct comparison of starlight with a terrestrial source of known output).

The determination of the Sun's stellar magnitude has frequently been performed (**1**). It was decided to undertake a new determination on Mount Stromlo not only because the general advance in photometric methods of recent years justified the expectation that a new determination would be more accurate than earlier ones, but also because it was considered that this greater precision could be adequately exploited only if *monochromatic* rather than *integrated* magnitudes were measured.

In the observations briefly described in this note, spectra of the Sun, suitably weakened, and of Sirius were photographed on the same plate with the same exposure times, and the intensities at four selected wave-lengths compared by the standard methods of photographic photometry. The note describes, in fact, determinations of the monochromatic magnitude differences between the Sun and Sirius.

2.—The programme was carried out on the solar telescope of the Commonwealth Observatory (described by C. W. Allen in Memoir No. 5). In this instrument a coelostat and mirror feed a vertical telescope of 30 cm. aperture and 13 m. focal length, a diagram of the arrangement being shown in Fig. 1. The converging beam descends into a basement, where it is reflected into a horizontal direction by a 45° diagonal flat, to form an image at the focus of a specially constructed spectrograph. The low light level and general stability of conditions in the basement were found most convenient, as was the fact that equipment could be left set up for long periods without denying the use of the solar tower to other programmes.

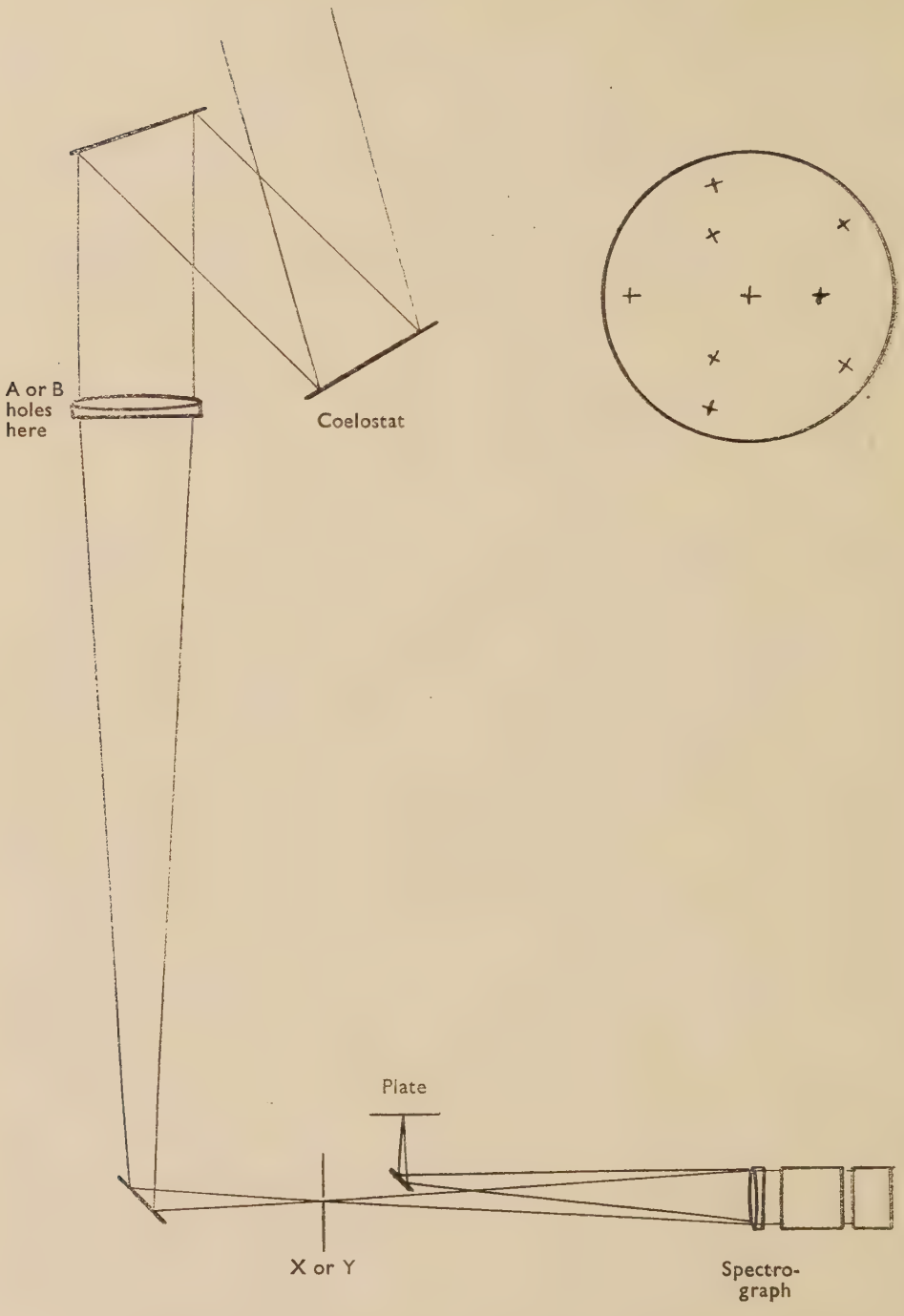

FIG. 1.—*Diagram of the optical train. The inset shows the arrangement of holes A and B.*

The image of the Sun was weakened in two stages. In the first the objective was diaphragmed with nine small circular apertures, distributed, as shown in Fig. 1 (inset), to make a fair sample of the optical train. In particular, the absorption introduced by the prism train into the diaphragmed beam was, for practical purposes, identical with that introduced into the full beam. (The extreme

differential absorption of the prism train, due to a difference in glass path of about 10 cm. of light flint, would hardly exceed 0·15 mag.) No attempt was made to locate the apertures in a fixed azimuth, and the day-to-day distribution of azimuths thus being random, any systematic effects due to irregularities in the optical train, specifically in the silvering of the coelostat mirrors, should average out.

Two sets of apertures were used. Set A, of mean diameter 0·51 mm., transmitted $0{\cdot}263 \cdot 10^{-4}$ of the incident light, a reduction of 11·45 mag., and set B, of mean diameter 1·01 mm., transmitted $1{\cdot}031 \cdot 10^{-4}$, a reduction of 9·97 mag. It was found necessary to include a (computed) correction for light lost by diffraction from the centre of the Sun's image. In the extreme case of holes A at λ 6209 this amounted to 0·075 mag. The intensity distribution over the Sun's image was substantially that produced by *one* of the diaphragming holes, the effect of the multiplicity of holes being (*a*) to increase the overall intensity without changing its distribution, (*b*) to introduce sets of "interferometer" fringes quite negligible in practice. Darkening to the limb had to be taken into account, the loss for a uniform disk being only about two-thirds that for a limb-darkened disk.

The second stage in the weakening was to select a fraction of the solar disk (the diameter of which is 122 mm. when the Sun is at mean distance and the objective at full aperture) by a small hole at the focus of the spectrograph.* Two such holes were constructed and carefully measured, with the following results :

Hole X	Diameter 0·516 mm.	Reduction 11·87 mag.
Y	0·239 mm.	13·54 mag.

A third hole Z, of diameter 0·101 mm. (reduction 15·41 mag.), was also constructed. It had been intended to use the combination BZ as an alternative to AY, but the Z hole proved difficult to measure and to handle, and after some trials was discarded. The X and B holes were therefore used only to check the transmission of the A and Y holes, as described at the end of the next section.

Final figures for the reduction in magnitudes of the Sun's intensity by the actual combination of holes used (AY) are:

	λ 6209	λ 5550	λ 4945	λ 4510
AY	25·07	25·06	25·05	25·05

The variation is due to change of diffraction correction with wave-length.

3.—The plates were taken on a Littrow spectrograph built for the purpose in the Observatory shops. The spectrograph lens had aperture 35 mm. and focal length 500 mm., and three equivalent prisms gave a dispersion ranging from 110 A./mm. at $H\alpha$ to 30 A./mm. at λ 4500. The optical parts were bloomed to reduce internal reflections. The returning beam was intercepted by a small aluminized mirror and reflected through 90° to a plate-holder at the focus. Between this diagonal mirror and the plate-holder was a glass plate about 10 mm. thick (not shown in the figure), mounted on an axis about which it could be rocked by a specially cut cam. The rocking widened the spectra to about 1 mm. Spectra of the Sun were secured by placing the Y hole at the focus. For the star the hole was removed, the image of the star itself defining the spectrum. The

* Notice that the amount of light passed by a fixed hole is independent of the solar distance, and that by choosing the solar diameter at mean distance we make the comparison refer to the apparent magnitude of the Sun at mean distance.

resolving power for solar spectra was effectively determined by the diameter of the hole used as slit. With the Y hole the magnesium lines λ 5167·3 and λ 5172·7 were barely resolved, but λ 4274·8 and λ 4271·7 were definitely resolved.

In front of the hole (or of the image of the star) could be placed a number of substantially neutral filters, of nominal absorptions ¼, ½ and 1 magnitude. These filters were used to calibrate each plate exposed; corrections for inter-reflection were small but were applied where necessary. In addition, a blue filter (*b*) was used with both the Sun and Sirius, to equalize densities at the red and blue ends of the spectrum, and a further blue filter (β) to make the colour of the Sun approximate to that of Sirius. A careful calibration of all these filters was carried out, using the spectrograph as a monochromator and a KMV–6 Osram photocell as light-sensitive element. The calibration was checked at the National Standards Laboratory, with results in good agreement with our own. It is worth mentioning, however, that as a substantial overlap in density between spectra of the Sun and Sirius was secured in each comparison plate, the final result is not very dependent on the filter calibration. This does not hold with filter β, of course, errors in which will enter with full weight. The reductions, in magnitudes, of this filter at the four wave-lengths used are:—

	λ 6209	λ 5550	λ 4945	λ 4510
(Mt. Stromlo)	1·008	0·620	0·488	0·222
(N.S.L.)	1·006	0·610	0·490	0·222

Great care was exercised to ensure that throughout the observations the telescope objective was filled with light, that all this light passed through the spectrograph and was received on the plate, and that all small holes were properly clean. Holes and filters were measured before and after carrying out the programme, with substantially the same results.

To confirm the measurements of holes A, B, X and Y, and as an overall check on the photometry, the ratios of the amounts of light transmitted by various combinations of holes were measured both photographically and photoelectrically. The photocell was not sufficiently sensitive to check directly the differences AY–BY and AX–BY. To measure A–B photoelectrically, the light flux was increased by using in the spectrograph an ordinary slit open to about 1 mm., the photocell being placed behind the position normally occupied by the plate. A diaphragm in the focal plane of the plate isolated any required spectral region. (Apart from differential diffraction, which should not have exceeded 0·01 mag., no dependence on colour should have been present, and none in fact was found.) To measure X–Y photoelectrically, the objective was diaphragmed with nine holes of diameter about ¾ mm., located in the positions usually occupied by the A or B holes. We found in this way:—

	Photoelectric	Computed
A–B	$1^m{\cdot}54 \pm 0{\cdot}02$	$1^m{\cdot}52$
X–Y	$1^m{\cdot}72 \pm 0{\cdot}02$	$1^m{\cdot}67$

Photographic comparisons of the solar spectrum weakened by various hole combinations were also made, with the following results:—

	Observed		Computed	
	λ 6209	λ 4510	λ 6209	λ 4510
AX–BY	$0^m{\cdot}18 \pm 0{\cdot}03$	$0^m{\cdot}20 \pm 0{\cdot}02$	$0^m{\cdot}15$	$0^m{\cdot}16$
AY–BY	$1^m{\cdot}54 \pm 0{\cdot}04$	$1^m{\cdot}525 \pm 0{\cdot}04$	$1^m{\cdot}52$	$1^m{\cdot}51$

"Computed" results are those computed from measurements of diameter, corrected for diffraction. (Without the diffraction correction A–B is $1^{m}\cdot48$.) Errors are standard (r.m.s.) errors.

The results indicate that the computed transmissions are reliable and, so far as they go, that they confirm the diffraction correction.

4.—In one day's (or night's) observing, one plate was used solely for determining atmospheric extinction, by securing spectra of the Sun or star as the secant of the zenith distance changed from about 1·5 to about 3·0. Between extinction exposures spectra were taken on comparison plates, each comparison plate having at least one series of calibrating spectra, together with from two to four spectra taken on each of a number of days and nights. (The reduction of a sample plate is shown in Table II.) One day or night might appear on up to four comparison plates, and one comparison plate might take from two to ten days to fill, depending on the weather. Mornings and afternoons of a single day, for which extinctions were determined separately, were counted as separate "days".

Kodak Panatomic–X plates were used, as the only red-sensitive plates available at the time. They proved very satisfactory. Exposure was for 60 seconds, and twenty spectra were normally secured on one (quarter) plate. Development was for five minutes in Kodak D–19, mostly in a tank with a plunger for agitating the developer. In all, 37 plates were retained, 14 for solar extinction, 9 for stellar extinction and 14 comparison plates. The results of this paper thus depend on the measurement of about 750 spectra.

Densities were measured on a projection photometer built to the design of Mr H. J. M. Abraham. An image of the plate, magnified sevenfold, was thrown on a screen, in which was a rectangular hole $1\frac{1}{2}$ by 1 mm. in size, i. e. of projected dimensions 0·21 by 0·14 mm. The short side was parallel to the direction of the dispersion. Behind the screen was a photocell on which fell the light transmitted by the hole. The resulting photo-current was amplified in a conventional one-tube circuit and read on a microammeter.

Measurements were made at the four wave-lengths mentioned above. These were chosen to be fairly equally spaced and as free as possible from the influence of absorption lines. (Three of them were used by H. H. Plaskett (**2**).) With the slit widths used it was of course impossible to avoid absorption lines entirely. The spectral purity was about the same as that of the slitless spectra used in such spectrophotometric work as the Greenwich gradient programme. The required spectral region was located by moving the plate—which could readily be done with two rack-and-pinion movements—until a prominent absorption line coincided with an appropriately placed mark on the screen. The whole was remarkably quick and convenient to use, an important consideration when several thousand densities had to be measured.

A complication was introduced by the non-uniformity of the spectra perpendicular to the dispersion, illustrated in the microphotometer tracings of Fig. 2. These show in order spectra 9 (star), 8 (Sun), 7 (Sun) and 6 (star) of plate 114 at λ6209, and spectrum 6 at λ4945. Plate 114 was chosen for illustration because the out-of-focus effect seemed most marked in spectrum No. 9. The solar spectra, being defined by the hole, have sharper edges than the stellar spectra, which were diffused both by seeing, by trailing of the star during exposure and by any imperfections in the definition of the solar telescope. The most important of these factors was the secondary spectrum, which prevented the star from being

in good focus throughout the spectral range used. The objective, being "photographically" corrected, should have a longitudinal secondary spectrum in the range $\lambda 4510$–$\lambda 6209$ of rather less than 0·3 per cent of the focal length, say 40 mm. The attempt was always made to focus near the middle of this range, so that the maximum out-of-focus widening (the telescope working at $f/40$) should not be much in excess of 0·5 mm. The star was not guided, and during the 60-sec. exposure should have drifted about 0·1 mm. diagonally across the spectrum.

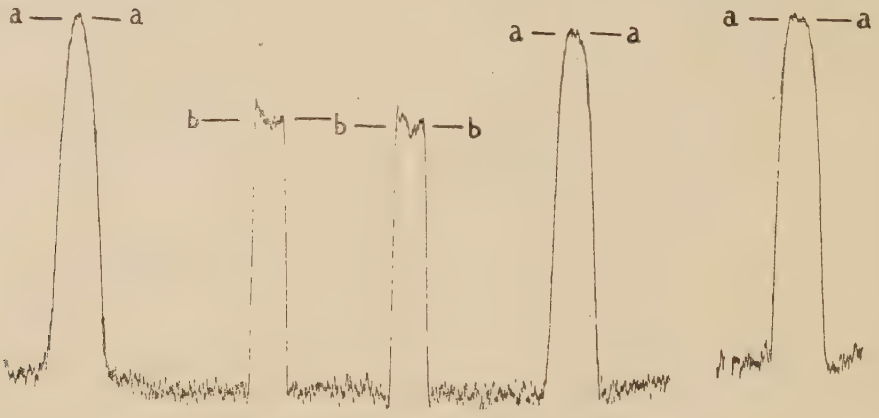

FIG. 2.—*Microphotometer tracings of plate* 114.

The one millimetre by which the spectra were broadened by the cam should be sufficient to offset these effects, in the sense that the central part of the spectrum should not show any out-of-focus or other weakening. It was, of course, necessary to check this point. Now the measurements actually made on the projection photometer were, with the stellar spectra, the transmission at the region of maximum photographic darkening, and with the solar spectra the mean transmission across the spectrum; these measures correspond to the lines *a–a* and *b–b* in Fig. 2. To check whether they gave (as they should do theoretically) a correct indication of the total light in the spectrum, equivalent widths were determined from microphotometer tracings of about 30 spectra made at wave-lengths $\lambda 6209$ and $\lambda 4945$. The means found were $1{\cdot}06 \pm 0{\cdot}01$ mm. for stellar spectra and $1{\cdot}04 \pm 0{\cdot}01$ mm. for solar spectra, with no dependence on wave-length. The resulting correction of 0·02 mag. was applied, although it is not much larger than the uncertainty of its determination. Part at least of this uncertainty lies in the difficulty of measuring the equivalent widths.

Most of the irregularity in the solar spectrum was due to a small fault in the profile of the cam.

5.—Extinction was measured in the usual way by plotting magnitude differences from an arbitrary zero against $\sec z$. If the resulting points did not lie close to a satisfactory straight line the day or night was rejected. The collected results for extinction are shown in Table I, the coefficients being hundredths of a magnitude per unit of $\sec z$.

Reductions were carried out both with individual extinction coefficients and with the adopted mean at the bottom of the table. The use of the latter led to an appreciably lower probable error in the final results (see Table III). From this, and the general lack of correlation between apparent high and low extinction

factors and apparent faint and bright objects on the comparison plates, it was concluded that the variations in Table I do not wholly correspond to real differences in extinction from night to night, but that they are partly observational and partly due to changing atmospheric conditions in the course of one night. It is perhaps not irrelevant that the observations were secured during the wettest summer in the history of the locality.

TABLE I

Determinations of absorption, in hundredths of a magnitude per unit of sec z

Plate	Object	Date	λ 6209	λ 5550	λ 4945	λ 4510
75	Sirius	Jan. 18/9	13	15	22	28
78	Sun	19 a.m.	9	13	20	24
82	Sirius	21/2	11	20	20	30
83	Sun	22 a.m.	10	13	21	26
85	Sun	22 p.m.	17	20	26	31
89	Sun	Jan. 30 p.m.	12	15	24	24
90	Sirius	Feb. 1/2	14	22	27	30
91	Sun	2 a.m.	14	18½	20½	25
94	Sirius	5/6	...	16	19	21
105	Sun	20 p.m.	20	23	29	35
107	Sun	Feb. 26 a.m.	...	15	18½	24
109	Sun	26 p.m.	9	14	17	23
111	Sirius	26/7	4 :	10 :	10 :	21 :
113	Sun	27 p.m.	10	11	25½	24
115	Sun	Mar. 2 a.m.	...	17	23½	29
119	Sirius	Mar. 2/3	18	20	24	31
124	Sun	3 p.m.	22 :	22	26	27
125	Sirius	3/4	14	18	20	25
127	Sun	6 a.m.	13	15	15	24
129	Sun	6 p.m.	9	14	24	28
131	Sirius	Mar. 6/7	19	17	19	...
133	Sun	7 a.m.	11	12	13	19
135	Sirius	7/8	16	21	22	24
Mean	Sun (a.m.)		11½	15	19	24½
,,	Sun (p.m.)		13½	17	24	27
,,	Sirius (p.m.)		14	18	21	26½
Adopted mean			13	17	21	26
Rayleigh value *			6	9	14	21

* I. e. value due to molecular scattering (taken from Allen (3)).

The tabulated extinctions will include any effects due to the varying with time of the angle of incidence on the coelostat mirror. The weight of evidence seems to be against variation of reflecting power with angle of incidence (4). The effect of varying polarization was examined theoretically and found to be negligible. In any case, these effects can only enter differentially, and as the greatest difference between the declinations of the Sun and of Sirius was only 10°, one would not expect them to be very large.

6.—The reduction of a typical comparison plate is shown in Table II. Column 5 gives the percentage transmission, column 6 the corresponding magnitude differences from an arbitrary zero, determined from the characteristic curve of the plate, column 7 atmospheric extinctions computed from the mean coefficient

0·26 mag./sec z, column 8 the absorptions of the filters designated in column 3, and column 9 the difference between 6 and the sum of 7 and 8. Column 9 thus exhibits the magnitude differences between the object photographed (corrected to zero atmosphere) and an arbitrary standard, a negative difference meaning that the object is brighter than the standard. All exposures except No. 13 include filter *b*, which is therefore not mentioned in column 3. The derived means and corrections for filter β are shown at the foot of the table.

TABLE II

Reduction of Comparison Plate 114 *at* λ 4510

(Unit : hundredth of a magnitude)

1 Exposure	2 Object	3 Filter	4 Sec z	5 transmission per cent	6	7 26 sec z	8 Filter Constant	9
1	115 ⊙	¼	1·24	33½	52	32	35	−15
2	117 ⊙	rejected						
3	119 *	½	1·66	55	101	43	55	3
4	115 ⊙	¾	1·24	57½	107	32	90	−15
5	113 ⊙	¾	1·61	65½	126	42	90	− 6
6	125 *	...	1·25	31	46	32	...	14
7	115 ⊙	½	1·24	44	76	32	55	−11
8	113 ⊙	¼	1·62	41½	70	42	35	− 7
9	119 *	...	1·65	32	48	43	...	5
10	115 ⊙	...	1·23	23	28	32	...	− 4
11	113 ⊙	...	1·64	29	41	43	...	− 2
12	125 *	¼	1·26	41½	70	33	35	2
13	119 *	−*b*	1·64	27½	38	43	−15	10
14	113 ⊙	½	1·65	50	90	43	55	− 8
15	121 ⊙	...	1·25	20½		32	not used	
16	119 *	¾	1·62	72	140	42	90	8
17	117 ⊙	rejected						
18	121 ⊙	...	1·24	21		32	not used	
19	119 *	¼	1·61	47½	84	42	35	7

Means

Plate	Sun AY β	β	Sun AY	Sirius
113	− 6	22	−28	...
115	−11	22	−33	...
119	...	...	...	+7
125	...	...	...	+8

The results to be carried forward to the ledger, of which Table III is a summary, are

* 119 − Sun AY 113 + 35; * 119 − Sun AY 115 + 40

* 125 − Sun AY 113 + 36; * 125 − Sun AY 115 + 41

However, these results are only contributions towards the mean entries shown in Table III, as a particular comparison may occur on more than one plate : for example, the entry 35 for *119 − ⊙113 is the mean of 35 from plate 108, 43 from plate 110, and 35 from plate 114, etcetera.

The collected results are assembled in Table III. This shows, in hundredths of a magnitude, the amount by which the reduced Sun is brighter than Sirius, for each day and night between which a comparison was secured. As comparisons were usually made on more than one plate, most of the entries in Table III are the means of two or three plates. Mean extinctions have been used. Column 8 contains the relative gradients (in the same units), determined from the slope of the least squares line through the four magnitude differences. These have been corrected for diffraction by the objective diaphragms.

TABLE III

Collected Results

Columns 4 to 7 express the amount, in hundredths of a magnitude, by which the reduced Sun is brighter than Sirius

1 Stellar plate	2 Solar plate	3 Interval in days	4 λ 6209	5 λ 5550	6 λ 4945	7 λ 4510	8
75	78	−0·4	112	97	69	50	99 Half weight
	83	−3·4	114	77	47	32	128 ,,
82	78	2·6	111	104	86	75	63 ,,
	83	−0·4	112	92	67	63	79 ,,
90	83	10·6	106	85	72	64	... Omit
	85	10·4	112	93	67	65	... Omit
	89	0·6	107	80	64	47	97
	91	−0·4	116	78	74	44	98
94	83	14·6	...	93	78	74	... Omit
	85	14·4	...	95	67	75	... Omit
	89	4·6	87	82	64	44	68 Half weight
	91	3·6	76	76	72	52	38 ,,
111	105	6·6	100	87	57	43	93
	107	0·6	90	75	56	40	77
	109	0·4	89	65	38	29	95
	113	−0·6	108	87	72	48	90
	115	−3·4	112	91	60	57	93
119	107	4·6	94	73	51	35	93
	109	4·4	85	60	30	17	109
	113	3·4	104	82	63	38	102
	115	0·6	112	86	51	44	110
	124	−0·6	116	83	54	36	125 Half weight
	127	−3·4	130	101	67	55	121 ,,
125	113	4·4	93	69	53	39	82
	115	1·6	104	75	45	45	98
	124	0·4	94	71	48	45	79
	127	−2·4	114	92	60	58	94
	129	−2·6	110	86	62	44	103
131	129	0·4	93	71	54	28	100
	133	−0·4	91	71	46	32	96
135	129	1·4	105	83	64	43	96
	133	0·6	105	86	60	48	93
Means (*a*)			102·3	80·2	57·1	42·8	94·1
Standard error			±2·6	±2·1	±2·1	±2·1	±2·6
Means (*b*)			101·3	77·2	61·0	42·2	
			±3·6	±2·8	±3·4	±3·2	
Means (*c*)			103·3	80·9	59·9	44·3	
			±2·4	±2·6	±2·4	±2·9	
Adopted mean			102	80	58	43	

Column 3 shows in days the interval between exposures, in the sense, date of stellar exposure minus date of solar exposure. This is of importance in assessing the ageing of the mirror train and of the photographic emulsion. Barbier and Chalonge (**5**) have found emulsion effects to be small, and this seems to be general experience. The mirror reflectivity was not constant, however, the coelostat mirror deteriorating rapidly and visibly on the afternoon of February 6. This deterioration can be traced back, through comparisons of 90 and 94 with 83 and 85, for at least two weeks, over which period it seemed to proceed, at λ 4510, at the rate of 0·02 mag. per day. The mirrors were resilvered on February 8 and thereafter there is no evidence for ageing. In any case, most of the time intervals are short and, after the rejection of the four comparisons quoted above, near zero in the mean. It will be seen that most of the comparisons prior to February 6 receive half weight; this is partly because of mirror ageing, and partly because some comparisons were made at too great a zenith distance. The observations in the period March 2 to March 8 were made during an extensive anticyclone, during which conditions seemed very stable.

Of the various means at the foot of Table III, (*a*) is the mean of the columns of the table as they stand, i. e. adopting mean extinctions and giving equal weight (unless otherwise stated) to each day–night combination. With (*b*), individual extinctions from Table I have been used, the weighting remaining the same, and (*c*) uses mean extinctions but gives each night equal weight. It can be seen that the adopted mean is effectively independent of the method of extinction correction and of the system of weighting, and that the standard errors, representing the combined effect of extinction and "night errors", and of the photographic photometry, are satisfactorily small. The mean sec z at which comparisons were made was, for plates 75–94, 1·67 for the Sun and 1·55 for Sirius; for plates 105–135 it was 1·69 for the Sun and 1·65 for Sirius.

The final result is deduced as follows, the unit being now a magnitude:—

	λ 6209	λ 5550	λ 4945	λ 4510
Mean from Table III	1·02	0·80	0·58	0·43 ± 0·02
" Profile " correction (Section 4)	−0·02	−0·02	−0·02	−0·02 ± ·02
AY	25·07	25·06	25·05	25·05 ± ·02
Sirius—centre Sun	26·07	25·84	25·61	25·46 ± ·04
Limb darkening	−0·22	−0·25	−0·28	−0·31
Sirius—Sun	25·85	25·59	25·33	25·15 ± ·04

The standard errors may be considered common to all columns. The limb-darkening figures were taken from Minnaert (**6**). They depend on Abbot's work, and seem correct to within 0·01 mag.

To compare our results with those of other observers we have first to interpolate to the effective wave-length of the *IPv* scale, for which we take λ 5430, the mean of Seares' figures (**7**) for spectral types A1 and G2. We have then to assign a magnitude to Sirius; we adopt −1·52, from Kuiper's (**8**) reduction of Zinner's catalogue, bearing in mind that other determinations may differ from this by a good tenth of a magnitude. The resulting magnitude of the Sun is −27·07. The two most recent determinations are those of Calder (−26·22) and Pettit (−26·94), while Kuiper (**1**) has adopted from the work of many observers (excluding Calder) a mean of −26·84.

As the figures stand, we make the Sun about a fifth of a magnitude brighter than has hitherto been assumed, the exact figure to depend on the finally adopted magnitude for Sirius. (A photoelectric determination of this is to be carried out at Mt. Stromlo next summer.) We have given a figure of $\pm 0{\cdot}04$ for the standard error of our determination: we believe that our limits of error are $\pm 0{\cdot}10$ magnitude. The position of this important constant is then not altogether satisfactory, and it is proposed to undertake further work on it at Mt. Stromlo, namely a comparison of the brighter stars with a standard terrestrial source, which will check the present work through Abbot's determination of the solar constant.

For the Sun's absolute magnitude we find $+4{\cdot}52$, which again is brighter, though not unduly so, having regard to the dispersion in the main sequence, than Kuiper's *Mpv* for G2 stars (**9**).

Turning now to colour, we find for the gradient of the centre of the Sun relative to Sirius 0·93, and for the mean Sun relative to Sirius 1·06. The residuals in each case are -2, $+2$, $+2$, -2, hundredths of a magnitude at the four wave-lengths, in the sense that at the intermediate wave-lengths the Sun is fainter than the Planck curve of best fit. The residuals are small but seem real, in that they occur with the same sign regardless of the weighting of the data of Table IV. Sirius was not included in the Greenwich programme, but the gradient estimated from its spectral type (A1V on the Yerkes system) should be reasonably reliable (**10**). This figure of 0·05 is confirmed by Barbier and Chalonge's (**11**) gradient of 1·00 which, reduced to the Greenwich system, becomes 0·06 (assuming the Greenwich zero to be 1·0 on the French observers' scale.)

The gradient of the mean Sun on the Greenwich system is then 1·11, which is rather less than the 1·2 or 1·3 its spectral type G2V would suggest. Adopting as zero of the Greenwich system 1·10 (**12**), the absolute gradient of the centre of the Sun is 2·07, corresponding to a temperature of 7030 deg. K. For the mean Sun the absolute gradient is 2·21, corresponding to $T = 6570$ deg. K. These results may be compared with those of Plaskett (*loc. cit.*), who found for the centre of the Sun a colour temperature of 6700 deg. to 7000 deg. If we accept Plaskett's result we find for the zero of the Greenwich gradients 1·15, corresponding to $T = 14{,}500$ deg., a by no means unreasonable result.

Acknowledgments.—The authors wish to refer to the late J. R. F. Jeffreys, who carried out a number of preparatory experiments on calibrating filters by photoelectric spectrophotometry at Cambridge in 1939, at a time when it was proposed that he and one of us (R. W.) should make a comparison of this kind at Calvinia after the eclipse of 1940. Jeffreys' untimely death in 1945 prevented him from taking part in the actual comparisons, but his work at Cambridge was followed in determining the filter constants at Mount Stromlo. Miss Beryl Mason has given extremely valuable assistance in the arduous work of reducing the plates, and she, together with Miss M. L. Woods, has assisted in securing many of the solar exposures. We are indebted also to the National Standards Laboratory for their careful calibration of several of the filters used.

Note added in proof. (1949 March 1.)—Preliminary results of the Mount Stromlo photoelectric monochromatic magnitude differences, measured by

A. R. Hogg and Miss Mason, indicate that the magnitude of Sirius quoted above is too high ; it is expected that the magnitude on the *IPv* scale will be about $-1{\cdot}3$. This will bring the Sun's absolute magnitude to about $-26{\cdot}9$, in very satisfactory agreement with earlier determinations.

Commonwealth Observatory,
Mt. Stromlo,
Canberra, A.C.T. :
1948 *August* 11.

References

(1) G. P. Kuiper, *Ap. J.*, **88,** 429, 1938.
(2) H. H. Plaskett, *Pub. D.A.O.*, **2,** 211, 1923.
(3) C. W. Allen, *Ger. Beit.*, **46,** 32, 1935.
(4) J. S. Hall, *Ap. J.*, **79,** 163, 1932. F. Benford and W. A. Ruggles, *J. Opt. Soc. Amer.*, **32,** 174, 1942.
(5) D. Barbier and D. Chalonge, *Journ. des Obs.*, **19,** 149, 1936.
(6) M. G. J. Minnaert, *B.A.N.*, **2,** 79, 1924.
(7) F. H. Seares and M. C. Joyner, *Ap. J.*, **98,** 302, 1943.
(8) G. P. Kuiper, *loc. cit.*, p. 477.
(9) G. P. Kuiper, *Ap. J.*, **95,** 201, 1942.
(10) W. W. Morgan and W. P. Bidelman, *Ap. J.*, **104,** 245, 1946. Spectral types of the Sun and Sirius are taken from Kuiper's 1942 paper.
(11) D. Barbier and D. Chalonge, *Ann. d'Ap.*, **4,** 30, 1941.
(12) Council Report, *M.N.*, **101,** 148, 1941, and the discussion on the following pages.

A VERY RED STAR: Co.D. $-62°466$

J. v. B. Lourens

(Communicated by H.M. Astronomer)

(Received 1948 November 30)

Summary

It has generally been assumed that Co.D. $-62°466$ is identical with C.P.D. $-62°1643$. Actually there are two stars about 17″ apart, the Co.D. star being about three magnitudes brighter visually than the C.P.D. star but about two magnitudes fainter photographically. The colour index of the Co.D. star must be about five.

In the course of measurement of plates taken with the Wide Angle Lens (W.A.L.) of the Cape Observatory it was found that the star measured as C.P.D. $-62°1643$ was 17″ away from the position of G.C. 14544, which had been identified as this star. To investigate this unexpected displacement in position, all the available meridian observations were examined. These positions, reduced with Newcomb's precessions to the Equinox of 1950·0 and the FK3 system by means of corrections given in the G.C., are given in Table I, numbers 1–5. Number 6 gives the W.A.L. position of the star measured on the same system.

TABLE I

Serial Number	Catalogue and Number	Catalogue Magnitude	Epoch: Number of Observations	R.A.	Dec.
				h m s	° ′ ″
1	Cordoba Zone (1875·0) 2159	8 to 8½ (Red)	1874·7 : 3	10 32 31·71	−62 27 7·2
2	Argentine General (1875·0) 14446	7½ (Red)	1875·4 : 4	31·87	9·3
3	Third Melbourne (1890·0) 1357	8·2	1885·4 : 3	31·78	9·2
4	Cape General (1900·0) 3737	8·3	1901·9 : 3	31·76	8·1
5	San Luis (1910·0) 6632	8·6	1910·0 : 4	31·72	8·0
6	Cape W.A.L. Zone −60° −64°	11½ Pg	1946·3 : 2	30·48	22·8

The data 1–5 support the results given for G.C. 14544, but an explanation was required for the W.A.L. position. As it appeared possible that we were dealing with two separate stars a plate was taken with the 24-inch Victoria Refractor on the morning of 1948 October 22. This plate confirmed that two stars were involved and their positions were deduced relative to eight nearby reference stars which had been specially measured on the W.A.L. plates. In Table II the positions of the two stars are given, as deduced from the Victoria plate, together

with the positions of the eight reference stars measured at first on the W.A.L. plates and smoothed by the Victoria plate. The positions are directly comparable with those given in Table I and their probable errors will not greatly exceed 0″·1.

TABLE II

		Pg. (Mag.)	Pv.	R.A.	Dec.
				h m s	° ′ ″
	C.P.D. −62° 1643	11·8	>10·5	10 32 30·48	−62 27 22·8
	Co.D. −62° 466	>13·0	8·8	31·75	7·9
Reference Stars Serial Number	C.P.D. Number				
1	−62 1636	10·2	10·3	10 31 50·20	−62 30 5·0
2	...	11·9	>10·5	32 25·71	16 53·5
3	−61 1719	11·4	10·4	32 43·51	20 25·3
4	...	11·8	10·4	32 44·45	30 33·7
5	−61 1720	10·1	10·0	32 49·61	16 45·2
6	−62 1648	10·8	9·7	33 6·81	24 9·7
7	−61 1724	10·6	9·8	33 19·56	14 36·9
8	−61 1730	11·5	9·7	33 29·14	14 46·8

The magnitudes given in Table II were found from photometric measures of a pair of plates taken in 1946 at the Radcliffe Observatory, Pretoria, with the Cape Photometric Cameras. These magnitudes are on the International Scale and the outstanding fact is the very large colour index of Co.D. −62° 466. Its position identifies it as G.C. 14544, which is thus not C.P.D. −62° 1643. On account of the very weak photographic response of Co.D. −62° 466, the spectral type, Fo, provided by the G.C. probably refers to C.P.D. −62° 1643.

The photometric plates, both of 15 minutes exposure, were also measured positionally to check the identification of the two stars and their magnitudes. The visual plate showed only one star of Pv. mag. 8·8, whereas the photographic plate showed a star of Pg. mag. 11·8 and also a very faint image of the companion 17″ n.f. of Pg. mag. fainter than 13·0. Accurate measures confirmed that the visual star was the very faint (photographic) companion.

The Catalogue of Red Stars of 1890 by Birmingham and Espin contains a star (No. 312, page 50) whose approximate position there is roughly that of Co.D. −62° 466. Observed by Russell in 1883 he makes the following comment on his observation: "This is a remarkably red star, 9½. The colour is as brilliant as that of the companion of β Crucis".

The A.G.C. and Z.C. observations also note the star as "Red" and our variable star observer, Mr de Kock made a first estimate of magnitude 8·5 during 1948 October, remarking that the star is "Very Red".

An examination of all the available data provided no evidence of any variation in visual magnitude exceeding $0^m·5$, this estimate being somewhat reserved, as individual observers sometimes differ largely in response when very red stars are estimated visually.

Royal Observatory,
Cape :
1948 *November* 16.

MEAN AREAS AND HELIOGRAPHIC LATITUDES OF SUNSPOTS IN THE YEAR 1942

Royal Observatory, Greenwich

(Communicated by the Astronomer Royal)

(Received 1948 November 24)

The following results are in continuation of those given in *M.N.*, **108,** 420, 1948, and are derived from the measurement at Greenwich of photographs taken at the Royal Observatories of Greenwich and the Cape and at the Kodaikanal Observatory, India. A photograph for one day unrepresented in the series was kindly supplied by the Superintendent, U.S. Naval Observatory, Washington.

Table I gives the mean daily areas of umbrae, whole spots and faculae for each synodic rotation of the Sun included in the year 1942; the means for the year as a whole are included in Table II, which summarizes the yearly values from 1933–42.

TABLE I

No. of Rotation	Rotation Commenced U.T.	Days Photographed	Mean Daily Areas: Projected* Umbrae	Projected* Whole Spots	Projected* Faculae	Corrected for Foreshortening† Umbrae	Corrected for Foreshortening† Whole Spots	Corrected for Foreshortening† Faculae
	1941							
1181	Dec. 23·74	27	115	656	1087	78	443	1269
	1942							
1182	Jan. 20·08	27	94	533	861	69	399	1020
1183	Feb. 16·42	28	280	1423	779	192	1016	955
1184	Mar. 15·74	27	236	1205	1034	162	837	1273
1185	Apr. 12·04	27	270	1429	862	197	1049	1116
1186	May 9·28	28	59	311	618	41	215	774
1187	June 5·50	27	31	139	627	22	100	775
1188	July 2·69	27	54	281	459	38	195	581
1189	July 29·90	27	53	274	506	36	184	593
1190	Aug. 26·13	28	42	230	520	36	198	619
1191	Sept. 22·39	27	37	188	519	29	146	642
1192	Oct. 19·68	27	97	554	480	74	419	578
1193	Nov. 15·98	27	128	690	553	84	458	628
1194	Dec. 13·30	28	32	174	397	23	127	469

* Expressed in millionths of the Sun's disk.
† Expressed in millionths of the Sun's hemisphere.

Table III gives for each rotation in the year 1942 the mean daily area of the whole spots (corrected for foreshortening) and the mean heliographic latitude of the spotted areas for both northern and southern hemispheres.

The mean heliographic latitude of the entire spotted area and the mean distance from the equator of all spots are also tabulated. The mean values for the year 1942 are included in Table IV.

Tables II and IV are in continuation of similar tables given in *Monthly Notices*: for the years 1874 to 1888—**49,** 381–382; 1889 to 1902—**63,** 465–466; 1901 to 1914—**76,** 402–403; 1913 to 1924—**85,** 1007–1008; 1923 to 1933—**94,** 870–871.

The rotations in Tables I and III are numbered in continuation of Carrington's series.

The chief features of this record for the year 1942 are as follows:—

(1) The continued decline towards solar minimum, the mean daily sunspot area for the year as a whole being only one-fifth that of the maximum years 1937–38 (*see* Table II).

TABLE II

Mean Daily Areas

Year	No. of Days		Projected*			Corrected for Foreshortening†		
	Photographed	Without Spots	Umbrae	Whole Spots	Faculae	Umbrae	Whole Spots	Faculae
1933	365	234	24	120	225	18	88	267
1934	365	145	27	142	297	22	119	354
1935	365	21	152	810	910	117	624	1100
1936	366	0	288	1529	2106	217	1141	2545
1937	365	0	509	2795	2856	375	2074	3505
1938	365	0	501	2706	2578	371	2019	3205
1939	365	0	404	2163	1907	295	1579	2349
1940	366	0	279	1434	1224	200	1039	1522
1941	365	8	167	915	1041	120	658	1282
1942	365	16	112	591	666	79	423	809

* Expressed in millionths of the Sun's disk.

† Expressed in millionths of the Sun's hemisphere.

The mean daily areas of sunspots from rotation to rotation (Table I), show an appreciable range, with very pronounced activity during Rotations 1183–85, and a slump in Rotation 1187 to one-tenth the earlier values. During Rotation 1188, the value for the northern spots fell to the unusually low level of two units. Probably this is a transient indication of impending solar minimum.

The mean daily values of faculae throughout the rotations in Table I are much steadier, but record the same general decrease as do the sunspots.

(2) On sixteen days, as compared with eight in the previous year, no sunspots were seen. On four of the sixteen days, no faculae were present.

(3) The northern hemisphere had a greater spotted area than the southern in the ratio of $1\frac{1}{2}:1$.

(4) The number of spot groups lasting for two days or longer was 139; 73 were in the northern hemisphere and 66 in the southern. In addition there were 50 mostly very small groups seen on one day only; 16 were in the northern hemisphere and 34 in the southern.

Five groups had an average area, during their passage across the Sun's disk, of greater than 500 millionths (corrected for foreshortening). One of these, with central meridian passage on February 28, had a mean area of 1549 millionths. This largest group of the year began on February 3 and lasted until after April 2, probably until April 27. A notable flare was associated with this spot on February 28, and a great geomagnetic storm occurred $19\frac{1}{2}$ hours later (*M.N.*, **103,** 112, 1943). With this sunspot came the first recognition of solar radiation observable on radio wave-lengths ("solar noise").

TABLE III

No. of Rotation	Rotation commenced U.T.	Spots North of the Equator: Mean Daily Area	Spots North of the Equator: Mean Heliographic Latitude	Spots South of the Equator: Mean Daily Area	Spots South of the Equator: Mean Heliographic Latitude	Mean Latitude of Entire Spotted Area	Mean Distance from Equator of all Spots
	1941		°		°	°	°
1181	Dec. 23·74	152	13·32	291	8·75	−1·19	10·31
	1942						
1182	Jan. 20·08	261	11·44	138	7·73	+4·80	10·16
1183	Feb. 16·42	903	8·01	113	11·83	+5·80	8·43
1184	Mar. 15·74	627	7·33	210	9·57	+3·08	7·90
1185	Apr. 12·04	704	11·88	345	8·33	+5·24	10·71
1186	May 9·28	113	11·70	102	5·04	+3·74	8·53
1187	June 5·50	86	7·16	14	9·15	+4·81	7·45
1188	July 2·69	2	11·33	193	4·79	−4·61	4·87
1189	July 29·90	89	9·87	95	3·51	+2·98	6·59
1190	Aug. 26·13	69	8·60	129	8·93	−2·82	8·81
1191	Sept. 22·39	11	12·00	135	9·79	−8·12	9·96
1192	Oct. 19·68	15	6·54	404	10·29	−9·71	10·16
1193	Nov. 15·98	305	9·16	154	8·13	+3·37	8·80
1194	Dec. 13·30	97	7·75	30	5·38	+4·68	7·20

TABLE IV

Year	Days Photographed	Spots North of the Equator: Mean Daily Area	Spots North of the Equator: Mean Heliographic Latitude	Spots South of the Equator: Mean Daily Area	Spots South of the Equator: Mean Heliographic Latitude	Mean Latitude of Entire Spotted Area	Mean Distance from Equator of all Spots
			°		°	°	°
1933	365	86	10·60	2	8·35	+10·23	10·56
1934	365	44	16·45	74	28·09	−11·49	23·75
1934	365 Old Cycle	19	4·10	1	4·37	+ 3·79	4·11
	365 New Cycle	26	25·44	74	28·31	−14·46	27·57
1935	365	205	22·42	419	23·72	− 8·57	23·30
1936	366	463	19·36	678	21·02	− 4·63	20·35
1937	365	1317	17·63	757	15·96	+ 5·36	17·02
1938	365	899	15·55	1120	14·17	− 0·94	14·79
1939	365	649	14·64	931	12·57	− 1·39	13·42
1940	366	499	11·65	540	10·72	+ 0·03	11·17
1941	365	427	11·31	232	8·67	+ 4·28	10·38
1942	365	252	9·32	171	8·45	+ 2·14	8·99

(5) The weighted mean latitude of all spots was 8°·99 (Table IV), i.e. 1°·4 nearer the Sun's equator than for sunspots in 1941. Latitudes of spots, lasting for two days or longer, ranged from the equator to 21°·5. On December 20 there was a one-day spot group, in latitude 30°·3, but according to the Mt. Wilson observers, who obtained its magnetic polarity later in the day, it belonged to the current cycle. Precursor spots of a new cycle usually arrive about 18 months before the frequency minimum.

Royal Observatory,
Greenwich:
1948 *November* 23.

INDEX

PAGE

Adam, M. G., Interferometric Measurements of Solar Wave-lengths and an investigation of the Einstein Gravitational Displacement 446
Addey, F., Report of his observatory (Grove Park) 78
Allen, C. W., R. v. d. R. Woolley and, The Coronal Emission Spectrum 292
Associates elected 211
Auditors of the Treasurer's accounts, Report of the Honorary, for 1947 14

Baglow, R. L., The Photometric Elements of RS Sagittarii 343
Barker, Robert, Report of his observatory (Cheshunt) 78
Bondi, C. M., Inward Integration of the Stellar Equations 324
Bondi, H., Review of Cosmology (Council report on the Progress of Astronomy) 104
Bondi, H. and T. Gold, The Steady-State Theory of the Expanding Universe 252
Bos, H. van den, Council report on double stars in 1947 121

Cambridge Observatories, Report of the proceedings of the 64
Cape of Good Hope, Royal Observatory, Report of the proceedings of the 61
Chapman, S., Solar Magnetism and the Suggested Fundamental Magnetism by Rotation ... 236
Comets : Council report on comets in 1947, *G. Merton* 124
—— On the Origin of Comets, *R. A. Lyttleton* 465
Conversazione of 1948 July 23 308
Cosmology : The Steady-State Theory of the Expanding Universe, *H. Bondi and T. Gold*... 252
—— A New Model for the Expanding Universe, *F. Hoyle* 372
—— Review of Cosmology (Council report on the Progress of Astronomy), *H. Bondi* ... 104

Das, A. K., Council report on solar activity in 1947 : Prominences 123
Dodson, Helen W., A General Study of a Prominence Field 383
Double Stars : Council Report on Double Stars in 1947, *H. van den Bos* 121
Dunsink Observatory, Report of the proceedings of the 69

Edgeworth, K. E., Some Aspects of Stellar Evolution—IV. The Mean Random Velocity of the Stars 417
Edinburgh Royal Observatory, Report of the proceedings of the 59
Errata 209, 422
Evershed, J., Report of his observatory (Ewhurst) 78
—— On an apparent change of Wave-length in Solar Iron Lines 347

Fellows deceased 8
Fellows elected 1, 2, 153, 211, 307, 353

Gascoigne, S. C. B., R. v. d. R. Woolley and, The Sun's Stellar Magnitude 491
George Darwin Lecture announced 2
—— delivered by Professor Bertil Lindblad 214
Gifts to the general funds and property of the Society 23
Giovanelli, R. G., Chromospheric Flares 163
Glasgow University Observatory, Report of the proceedings of the 66
Gold Medal : The Gold Medal of the Society awarded to Professor Bertil Lindblad for his work on the rotation of the galaxy, on the dynamics of stellar systems and on stellar luminosities 2
Gold, T., H. Bondi and, The Steady-State Theory of the Expanding Universe... 252
Greaves, W. M. H., Presentation of the Gold Medal to Professor Bertil Lindblad 212
—— The Photometry of the Continuous Spectrum (Presidential Address, 1948) 131
Greenwich, Royal Observatory, Report of the proceedings of the 54
—— Mean Areas and Heliographic Latitudes of Sunspots in the year 1940 177
—— Mean Areas and Heliographic Latitudes of Sunspots in the year 1941 420
—— Mean Areas and Heliographic Latitudes of Sunspots in the year 1942 505

PAGE

Heath, M. B. B., Report of his observatory (Kingsteignton) 79
Hey, J. S., S. J. Parsons and J. W. Phillips, Some Characteristics of Solar Radio Emissions ... 354
Holborn, F. M., Report of his observatory (Streatham) 79
Hoyle, F., A New Model for the Expanding Universe 372
Hyderabad, Nizamiah Observatory, Report of the proceedings of the 74

Institutions, with which the Society exchanges Publications 27
Investments 22

Jeffreys, Harold, The Earth's Core and the Lunar Nutation 206
—— The Origin of the Solar System (Council report on the Progress of Astronomy) ... 94
Johannesburg, Union Observatory, Report of the proceedings of the 73
Junior Members elected 153, 211, 353

Kodaikanal, Solar Physics Observatory, Report of the proceedings of the 74

Library, List of donors to the, in 1947 24
Lindblad, Bertil, The Gold Medal of the Society awarded to him for his work on the rotation of the galaxy, on the dynamics of stellar systems and on stellar luminosities... ... 2
—— On the Dynamics of Stellar Systems (George Darwin Lecture) 214
Linfoot, E. H., Some recent applications of Optics to Astronomy (Council report on the Progress of Astronomy) 81
—— On the theory of the Zonal Foucault Test 428
London, Imperial College Observatory, Report of the proceedings of the 66
London, University of, Observatory, Report of the proceedings of the 67
Lourens, J. v. B., A Very Red Star : Co.D. −62° 466 503
Lyttleton, R. A., On the Origin of Comets 465

Meetings of the Royal Astronomical Society :—Report of the proceedings of the Meeting of 1948 January 9 1
—— Report of the proceedings of the Anniversary Meeting of 1948 February 14 2
—— Report of the Annual General Meeting of the Society, 1948 3
—— Narrative account of the state and activities of the Society during the year 1948 ... 4
—— Report of the proceedings of the Meeting of 1948 March 12 153
—— Report of the proceedings of the Meeting of 1948 April 9 211
—— Report of the proceedings of the Meeting of 1948 May 14 307
—— Report of the proceedings of the Special General Meeting of 1948 May 14 307
—— Report of the proceedings of the Meeting of 1948 October 8 353
—— Report of the proceedings of the Meeting of 1948 October 29, held in Edinburgh ... 425
—— Report of the proceedings of the Meeting of 1948 November 12 425
—— Report of the proceedings of the Meeting of 1948 December 10 426
Merton, G., Council report on comets in 1947 124
Milne, E. A., Star-streaming and the Stability of Spiral Orbits in Spiral Nebulae. I.—Motion round a point-nucleus 309
—— II.—Motion in an extended distribution of Matter 316
Mount Stromlo, Commonwealth Observatory, Report of the proceedings of the 76

Newton, H. W., Council report on solar activity in 1947 : Sunspots 122

Obituary Notices :—
Guthnik, Paul 35
Strömgren, Svante Elis 37
Becker, Ludwig... 41
Hardy, Godfrey Harold 44
Holdaway, Edwin Thomas 46
Houghton, Hendon Egerton 46
MacIntyre, William 47
Maunder, Annie Scott Dill 48
Miller, John Anthony 49
Pickering, David Bedell 51
Strutt, Robert John, Lord Rayleigh 51
Wesley, Arthur Robert 53

PAGE

O'Connell, D. J. K., Orbital Elements and Apsidal Motion of the Eclipsing Binary V 526 Sagittarii 334
Officers and Council, 1948–1949, List of 152
Optics : Some recent applications of Optics to Astronomy (Council report on the Progress of Astronomy), *E. H. Linfoot* 81
—— On the theory of the Zonal Foucault Test, *E. H. Linfoot* 428
Ottawa, Dominion Observatory, Report of the proceedings of the 70
Oxford, University Observatory, Report of the proceedings of the 67

Parsons, S. J., J. S. Hey, J. W. Phillips and, Some characteristics of Solar Radio Emissions ... 354
Peek, B. M., Report of his observatory (Solihull) 79
Phillips, J. W., J. S. Hey, S. J. Parsons and, Some Characteristics of Solar Radio Emissions ... 354
Photometry : The Photometric Elements of RS Sagittarii, *R. L. Baglow* 343
—— A Photometric Light curve for μ^1 Scorpii, *D. W. N. Stibbs* 398
—— Photoelectric Photometer employing an electron counting technique, *G. G. Yates* ... 476
Planets : Observations of the Satellites of Uranus, *W. H. Steavenson* 183
—— On the Constitution of the Terrestrial Planets, *W. H. Ramsey* 406
Potter Fund, Archdeacon 24
Prasad, Chandrika, Radial Oscillations of a Particular Stellar Model 414
Presents received 1, 2, 153, 211, 307, 353
Pretoria, Radcliffe Observatory, Report of the proceedings of the 73
Progress and present state of the Society 15

Radio : Some Characteristics of Solar Radio Emissions, *J. S. Hey, S. J. Parsons and J. W. Phillips* 354
Ramsey, W. H., On the Constitution of the Terrestrial Planets 406
Richards, H. W. P. and D. H. Sadler, The application of the National Accounting Machine to the Calculation of Apparent Places of Stars 154
Riverview College Observatory, Report of the proceedings of 77

Sadler, D. H., H. W. P. Richards and, The Application of the National Accounting Machine to the Calculation of Apparent Places of Stars 154
St. Andrews, University Observatory, Report of the proceedings of the 68
Sellers, F. J., Report of his observatory (Muswell Hill) 79
Sidmouth, Norman Lockyer Observatory, Report of the proceedings of the 69
Spectroscopy and Spectrophotometry : The Photometry of the Continuous Spectrum (Presidential Address, 1948), *W. M. H. Greaves* 131
—— The Measurement of Radial Velocity from Slitless Spectra, *P. J. Treanor* 189
—— The Spectrum of ρ Cassiopeiae, 1939, *W. S. Tai and A. D. Thackeray* 271
—— The Spectrum of ρ Cassiopeiae, 1946–1947, *A. D. Thackeray* 279
—— Interferometric Measurements of Solar Wave-lengths and an investigation of the Einstein Gravitational Displacement, *M. G. Adam* 446
Stars, Double and Multiple : Council report on, in 1947, *H. van den Bos* 121
Stars, New : Observations of Novae, 1947, *W. H. Steavenson* 186
Stars : On the Dynamics of Stellar Systems (George Darwin Lecture) *Bertil Lindblad* ... 214
—— Star-streaming and the Stability of Spiral Orbits in Spiral Nebulae. I.—Motion round a point-nucleus, *E. A. Milne* 309
—— II.—Motion in an extended distribution of Matter, *E. A. Milne* 316
—— Inward Integration of the Stellar Equations, *C. M. Bondi* 324
—— Radial Oscillations of a Particular Stellar Model, *Chandrika Prasad* 414
—— Some Aspects of Stellar Evolution—IV. The Mean Random Velocity of the Stars, *K. E. Edgeworth* 417
Steavenson, W. H., Report of his observatory (Cambridge) 80
—— Observations of the Satellites of Uranus 183
—— Observations of Novae, 1947 186
Stibbs, D. W. N., A Photometric Light curve for μ^1 Scorpii 398
Stonyhurst College Observatory, Report of the proceedings of the 69
Sun : Solar Magnetism and the suggested Fundamental Magnetization by Rotation, *S. Chapman* 236
—— The Sun's Stellar Magnitude, *R. v. d. R. Woolley and S. C. B. Gascoigne* 491
Sun, Chromosphere and Prominences : Council report on solar activity in 1947 : Prominences, *A. K. Das* 123
—— Chromospheric Flares, *R. G. Giovanelli* 163
—— A General Study of a Prominence Field, *Helen W. Dodson* 383

PAGE

Sun, Corona : The Coronal Emission Spectrum, *R. d. v. R. Woolley and C. W. Allen* ... 292
Sun, Spectrum of : On an apparent change of Wave-length in Solar Iron Lines, *J. Evershed* 347
Sunspots and Faculae : Council report on solar activity in 1947 : Sunspots, *H. W. Newton* 122
—— Mean Areas and Heliographic Latitudes of Sunspots in the year, 1940, *Royal Observatory, Greenwich* 177
—— Mean Areas and Heliographic Latitudes of Sunspots in the year 1941, *Royal Observatory, Greenwich* 420
—— Mean Areas and Heliographic Latitudes of Sunspots in the year 1942, *Royal Observatory, Greenwich* 505
Sydney Observatory, Report of the proceedings of 77

Tai, W. S. and A. D. Thackeray, The Spectrum of ρ Cassiopeiae, 1939 271
Thackeray, A. D., The Spectrum of ρ Cassiopeiae 1946–1947 276
Thackeray, A. D., W. S. Tai and, The Spectrum of ρ Cassiopeiae, 1939 271
Toronto, David Dunlap Observatory, Report of the proceedings of the... 72
Trcanor, P. J., The Measurement of Radial Velocity from Slitless Spectra 189
Treasurer's Accounts for 1947 16
Trust Funds 25

Wellington, Carter Observatory, Report of the proceedings of 78
Wilkins, H. P., Report of his observatory (Barnehurst) 80
Woolley, R. v. d. R. and C. W. Allen, The Coronal Emission Spectrum 292
Woolley, R. v. d. R. and S. C. B. Gascoigne, The Sun's Stellar Magnitude 491

Yates, G. G., Photoelectric Photometer employing an electron counting technique 476

Variable Stars : The Photometric Elements of RS Sagittarii, *R. L. Baglow* 343
—— A Photometric Light curve for μ^1 Scorpii, *D. W. N. Stibbs* 398
—— Orbital Elements and Apsidal Motion of the Eclipsing Binary V 526 Sagittarii, *D. J. K. O'Connell* 334

MONTHLY NOTICES

OF THE

ROYAL ASTRONOMICAL SOCIETY

Vol. 108 No. 1 1948

ANNUAL REPORT OF THE COUNCIL

Published and Sold by the

ROYAL ASTRONOMICAL SOCIETY

BURLINGTON HOUSE

LONDON, W. 1

Price Nine Shillings

NOTICE TO AUTHORS

1. *Communications.*—Papers must be communicated to the Society by a Fellow. They should be accompanied by a summary at the *beginning* of the paper. Authors are requested to submit MSS. in duplicate, when practicable.

2. *Presentation.*—Authors are allowed considerable latitude, but they are requested to follow the general style and arrangement of *Monthly Notices.* References to literature should be given in the standard form, including a date, for printing either as footnotes or in a numbered list at the end of the paper. Each reference should give the name of the author cited, irrespectively of the occurrence of the name in the text (some latitude being permissible, however, in the case of an author referring to his own work).

3. *Notation.*—Authors should conform closely with the recommendations of Commission 3 of the International Astronomical Union (*Trans. I.A.U.*, Vol. VI, p. 345, 1938). Council has decided to adopt the I.A.U. 4-letter abbreviations for constellations where contraction is desirable (Vol. IV, p. 221, 1932).

4. *Diagrams.*—These should be drawn about twice the size required in print and prepared for direct photographic reproduction except for the lettering which should be inserted in pencil. Legends should be given in the manuscript indicating where in the text the figure should appear. Photographs are normally reproduced true to scale.

5. *Tables.*—These should be arranged so that they can be printed upright on the page.

6. *Proofs.*—Costs of alteration exceeding 5 per cent of composition must be borne by the author. Fellows are warned that such costs have risen sharply in recent years, and it is in their own and the Society's interests to seek the maximum conciseness and simplification of symbols and equations consistent with clarity.

7. *Revised Manuscripts.*—When papers are submitted in revised form it is especially requested that they be accompanied by the original MS.

Reading of Papers at Meetings

8. If a paper is to be read at a meeting it should be received by the Assistant Secretary not later than the previous Friday.

9. When submitting papers authors are requested to indicate whether they will be willing and able to read the paper at the next or some subsequent meeting, and approximately how long they would like to be allotted for speaking.

10. Postcards giving the programme of each meeting are issued some days before the meeting concerned. Fellows wishing to receive such cards whether for the Ordinary Meetings or for the Geophysical Discussions or both should notify the Assistant Secretary.

CONTENTS

PAGE

Meeting of 1948 January 9:
- Fellows elected ... 1
- Presents announced... 1

Award of the Gold Medal to Professor Bertil Lindblad ... 2

Anniversary Meeting of 1948 February 14:
- Fellows elected ... 2
- Presents announced... 2
- Address delivered by the President, Professor W. M. H. Greaves, on "The Photometry of the Continuous Spectrum" ... 2

Report of the Annual General Meeting ... 3

REPORT OF THE COUNCIL TO THE HUNDRED AND TWENTY-EIGHTH ANNUAL GENERAL MEETING OF THE SOCIETY:
- Narrative Account of the State and Activities of the Society during the Year 1947 ... 4
- Fellows deceased ... 8
- Report of the Auditors ... 14
- Table of Progress and Present State of the Society ... 15
- Treasurer's Accounts for 1947 ... 16
- Investments ... 22
- Gifts to the General Fund and Property of the Society ... 23
- Archdeacon Potter Fund ... 24
- Trust Funds... 25
- List of Institutions with which the Society exchanges Publications ... 27
- List of Public Institutions and of Persons who have contributed to the Library, etc., in 1947 ... 34

OBITUARY NOTICES:
- Paul Guthnick ... 35
- Svante Ellis Strömgren ... 37
- Ludwig Becker ... 41
- Godfrey Harold Hardy ... 44
- Edwin Thomas Holdaway ... 46
- Hendon Egerton Houghton ... 46
- William MacIntyre ... 47
- Annie Scott Dill Maunder ... 48
- John Anthony Miller ... 49
- David Bedell Pickering ... 51
- Robert John Strutt, Lord Rayleigh ... 51
- Arthur Robert Wesley ... 53

PROCEEDINGS OF OBSERVATORIES:

PAGE

Royal Observatory, Greenwich 54
Royal Observatory, Edinburgh 59
Royal Observatory, Cape of Good Hope 61
Cambridge Observatories 64
University Observatory, Glasgow 66
Imperial College Observatory, London 66
University of London Observatory, Mill Hill 67
University Observatory, Oxford 67
University Observatory, St. Andrews 68
Norman Lockyer Observatory, Sidmouth 69
Stonyhurst College Observatory 69
Dunsink Observatory 69
Dominion Observatory, Ottawa 70
David Dunlap Observatory, University of Toronto 72
Union Observatory, Johannesburg 73
Radcliffe Observatory, Pretoria 73
Nizamiah Observatory, Hyderabad 74
Solar Physics Observatory, Kodaikanal 74
Commonwealth Observatory, Mount Stromlo 76
Riverview College Observatory, N.S.W. 77
Sydney Observatory 77
Carter Observatory, Wellington, N.Z. 78
Mr F. Addey's Observatory, Grove Park 78
Mr R. Barker's Observatory, Cheshunt 78
Mr J. Evershed's Observatory, Ewhurst 78
Mr M. B. B. Heath's Observatory, Kingsteignton 79
Mr F. M. Holborn's Observatory, Streatham 79
Mr B. M. Peek's Observatory, Solihull 79
Mr F. J. Sellers' Observatory, Muswell Hill 79
Dr W. H. Steavenson's Observatory, Cambridge 80
Mr H. P. Wilkins' Observatory, Barnehurst 80

REPORTS ON THE PROGRESS OF ASTRONOMY:

Some Recent Applications of Optics to Astronomy 81
The Origin of the Solar System 94
Review of Cosmology 104
Double Stars 121
Solar Activity: Sunspots 122
Prominences 123
Comets 124
Address delivered by the President, Professor W. M. H. Greaves, on "The Photometry of the Continuous Spectrum" 131
Election of Officers and Council 152

Printed in London by Taylor & Francis Ltd., 1948 August.